THE TAILS OF TWO HISTONES: IT WAS AN OLD HISTONE, IT WAS A NEW HISTONE

By
Vuong Tran

A dissertation submitted to the Johns Hopkins University in conformity with the requirement for the degree of Doctor of Philosophy

Baltimore, Maryland

March 2014

ABSTRACT

The basis of multi-cellular systems relies on different cell types performing different roles for a properly functioning organism. However, these cells need to express different sets of genes in order to maintain their different identities while using a common genome. This phenomenon can be resolved in the context of proteins such as histones that can bind to genomic DNA and are modified post-translationally to regulate gene expression. As such, the inheritance and maintenance of distinct chromatin state may contribute to determine and maintain cell identity. Inheritance of chromatin profile after successive cell divisions is substantial for epigenetic regulation. Among all cell types, stem cells remain one of the most critical populations for maintaining homeostasis. If the ability of stem cells to maintain their identity is compromised, it will result in stem cell loss, which would eventually lead to tissue degeneration. Conversely, if that the progeny cells derived from stem cells cannot differentiate into specific cell types, but rather keep on dividing, it may lead to tumorigenesis. My thesis project aims to understand how differential histone inheritance is related to stem cell identity. I found that in the *Drosophila* male germline stem cell (GSC) system, pre-existing H3 histones are preferentially segregated to the stem cell during asymmetric germline stem cell division. Based on this finding, we propose a two-step model to explain the asymmetric histone distribution: (1) prior to mitosis, preexisting histones and newly synthesized histones are differentially distributed at two sets of sister chromatids; (2) during mitosis, the set of sister chromatids with preexisting histones are segregated to GSCs while the other set of sister chromatids with newly synthesized histones are

partitioned to the daughter cell committed for differentiation. Whether this phenomenon contributes to maintain stem cell identity and to reset chromatin structure in the other daughter cell for differentiation remains to be determined.

In addition to our findings on histone asymmetry in germline stem cell, we also explore how histone contributes to differentiating germ cell identity. Asymmetric stem cell division yields two daughter cell. Since one daughter remains a stem cell, the other daughter is the gonialblast that go on to mitotically expand into spermatogonial cysts, differentiate into spermatocytes, and consequently form functional sperms. The transitions from spermatogonia to spermatocytes and then to spermatids are regulated in a step-wise manner. Differentiation gene expression is repressed in spermatogonia. When cells transit to the spermatocyte stage genes are turned on in a coordinated manner. The Polycomb Group (PcG) protein is a class of proteins that maintain the repressed state of genes through epigenetic silencing in spermatogenesis. This is largely done through modification of histone tails. In order for differentiation to proceed, PcG function needs to be counteracted. This requires function of the testis-specific Meiotic Arrest Complex (tMAC) and the testis-specific TATA-binding protein Associated Factors (tTAFs), which antagonizes PcG repressive function. In this thesis we will examine how these complexes contribute to germ cell differentiation through regulation of the chromatin landscape.

ACKNOWLEDGEMENT

First and foremost, I would like to thank my thesis advisor Dr. Xin Chen for all her guidance and support. In addition to her advice and training, her enthusiasm for science is positively contagious. One of the most enjoyable aspects of my day is to discuss science with Xin. I cannot adequately express how her hard work, her intellect, her words of encouragement and her tenacity have continually inspired me throughout my time here. Because of everything she has done, I feel like a well-rounded scientist who can contribute with my mind as well as my hands.

I am also very fortunate to have such a wonderful group of advisors on my thesis committee. Dr. Sean Taverna has been extremely helpful with his expertise on my thesis project as well as career advice. Dr. Jie Xiao has been a blessing to this thesis project by allowing us to apply a unique approach and perspective. Dr. Mark Van Doren has been like a second thesis advisor to me. I always look forward to our joint lab meetings because he always provide the most insightful input of ongoing projects.

My time in graduate school has enriched my life in many ways, because it has given me the opportunity to meet so many wonderful people. I look forward to going to work everyday because they've all created such an enjoyable atmosphere. I would like to especially thank my lab-mates Dr. Suk Ho Eun, Dr. Qiang Gan, Dr. Jing Xie, and Dr. Zhen Shi for all their help in lab. Also, my fellow graduate students Lama Tarayrah, Lijuan Feng and especially Cindy Lim for being such wonderful colleagues and a pleasure to work with during our many long hour at the fly bench.

To all my friends, I would like to express my thanks for sharing both my successes and frustrations throughout my time here. Though there are too many to list, I would like to acknowledge a few such as Kevin Lebo, Lin Quek, Kylie Chew, Stephanie Ketchum who have kept me adequately sane and reasonably intoxicated (most of the time on both counts). The memories of our many escapades and capers we share will be forever in my heart. Though we may go our separate ways after graduate school, we will always keep in touch. I would also like to acknowledge my friends from the Edgar lab who have been very supportive and helpful even before coming to the CMDB program. Without their support I would not be here.

To my family, I love you all very much. My brother and sisters have been nothing but supportive of my endeavor. Their words of encouragement and care have made me a better person for it. Even from the other side of the country, I can feel their presence and love. Words cannot express how much my parents have to sacrifice for me to be where I am. I can never repay them for everything they've done for me throughout my life.

And last, but not least, I would like to thank my wife Zhou for all her support. My time in Baltimore would have been worthwhile because of her alone. Her diligence and thoughtfulness has been instrumental in motivating me to move forward with my career. I look forward to our future together.

TABLE OF CONTENTS

INDEX OF TABLES AND FIGURES

Chapter 1: Introduction

Chapter 2: Asymmetric histone inheritance in *Drosophila* male germline stem cells

Chapter 1

Introduction to the biology of the male *Drosophila* spermatogenesis system

Drosophila spermatogenesis

The Drosophila testis is a long tube structure containing male germ cells with the maturation progression from germline stem cells to motile sperm. The testis also contains somatic cyst cells that encase the germ cells. At the apical tip, a post-mitotic group of 10-12 cells make up a structure known as the hub, which serves as the anchor for both the germline stem cells (GSCs) and the cyst stem cells (CySCs). Asymmetric division of GSC occurs in perpendicular to the hub/GSC interface, resulting in one daughter retaining stem identity characterized by attachment to the hub (**Fig. 1-1**). The other daughter cell, the gonialblast, will go through the differentiation pathway. The single gonialblast goes through exactly four rounds of mitotic divisions to generate a 16-cell cyst, in which the cells share a cytoplasm. These stages of 2 to 16 cell cysts are termed spermatogonia. As the spermatogonial cyst continue to differentiate, the switch from mitosis to meiosis occurs and the germ cells become spermatocytes. The early spermatocyte stage is characterized as an intermediate stage where the germ cell cysts remain in meiotic pro-metaphase. This period allows the spermatocyte to become metabolically active and increase 25-fold in mass. When the spermatocytes are mature, the cyst proceeds to terminal differentiation and initiates meiotic divisions, giving rise to spermatid. These spermatids go on to become mature, functional sperm for the adult male *Drosophila*.

Mitotic cell cycle of the germline stem cells

The typical mitotic cell cycle has four distinct phases. G1 is primarily a growth phase that prepares a 2N cell for DNA replication. This is followed by DNA

synthesis in S-phase, doubling the DNA content to 4N. In G2, another growth phase following S-phase, the cell is prepared for cell division. Mitotic division follows G2, producing two 2N cells. The resulting daughter cells are 2N and begin G1 once again. While seemingly simple, the cell cycle can vary tremendously in terms of duration of overall time and each phase. Specified cells have distinctive features of the cell cycle that contribute to their function. Growth and proliferation are balanced and finely tuned by cyclins and cyclin-dependent kinase regulators (Hunter and Pines 1994).

Drosophila GSCs cell cycle has been empirically determined to be 12-16 hours. But what make the GSC cycle distinctive is the short G1 phase (~0.25 hours) and the elongated G2 (~9-12 hours) (Cheng et al 2008, Sheng and Matunis 2011, Yadlapalli et al 2011, Yamashita et al 2003, Yamashita et al 2007). While the biological significance of these features of GSC cell cycle has not been determined, it is useful to speculate on the importance of the elongated G2. Furthermore, the lineage of GSC is such that the differentiating daughter cells go on to transit-amplification, which has a shortened cell cycle compared to GSCs. After transit-amplification, germ cells switch from the mitotic to meiotic cell cycle to become spermatocytes.

Asymmetric cell division of germline stem cells

Stem cells are unique in their capacity to both self-renew and give rise to many differentiated cell types. Adult stem cells in biological systems have been identified in tissues such as blood, intestine, muscle, skin, and the germline. Normal activities of adult

stem cells are required for homeostasis and tissue regeneration. The mis-regulation of stem cell fate or the malfunction of the resulting daughter cell derivatives can cause diseases such as diabetes, muscular dystrophy, neurodegenerative disease, infertility, and many forms of cancer (Morrison and Kimble 2006, Rando et al 2006, Rossi et al 2008). Many adult stem cells use asymmetric cell division is a strategy for self-renewal and differentiation that result in tissue homeostasis [(Inaba et al 2012, Knoblich et al 2008, Morrison and Kimble 2006) reviews on ACD]. The *Drosophila* male and female GSCs are among the most well-characterized adult stem cell systems in terms of physiological locations, micro-environments (i.e. niches), cellular morphology, genetic interactions, and the signaling pathways that maintain their stem cell identities (Fuller and Spradling 2007, Morrison and Spradling 2008, review). Male GSCs undergo asymmetric cell divisions. Both intrinsic factors and extrinsic cues contribute to the success of asymmetric divisions of the male GSCs (Fuller and Spradling 2007, Yamashita and Fuller 2005). One particular example includes the extrinsic Unpaired (Upd) ligand for the JAK-STAT signaling pathway. Upd is released from the aforementioned hub cells located at the tip of the testis to which the GSCs make physical contact by adherence junctions. This in turns activates JAK-STAT signaling required for GSC maintenance through maintaining CySC identities (Kiger et al 2001, Leather and Dinardo 2008, Leatherman and Dinardo 2010, Tulina and Matunis 2001) (**Fig. 1-2**). The roles of intrinsic factors in ACD are also characterized in male GSCs. One example is the centrosome. Male GSCs retain the mother centrosome that is anchored by microtubules at the GSC-hub interface, while the newly synthesized daughter centrosome migrates to the opposite end of GSC to be segregated to gonialblast (**Fig. 1-3**). This asymmetric

segregation of centrosomes serves as an important intrinsic mechanism to set up proper spindle orientation for ACD of male GSCs (Yamashita et al 2003, Yamashita et al 2007. Interestingly, the ability of centrosomes to asymmetrically segregate decline as the flies age, which results in reduced dividing abilities of GSCs (Cheng et al 2008). These findings lead to a "spindle checkpoint" hypothesis, which proposes that various cellular components prevent mis-oriented spindle formation in the presence of mis-oriented centrosomes, as an important intrinsic mechanism to ensure ACD (Cheng et al 2008, Inaba et al 2010, Roth et al 2012, Yuan et al 2012).

Histone and epigenetics

Histones play a critical role in the eukaryotic nucleus. DNAs are wrapped around a core octamer histone protein complex to compact and organize the genome. Each unit of histone octamer plus associated DNA is called a nucleosome, the basic unit of chromatin structure. Within each nucleosome, histone octamer consists of two subunits each of H2A, H2B, H3 and H4. H3 and H4 form a stable tetramer to which two H2A-H2B dimers dock (**Fig. 1-4).** In addition, each histone protein has N-terminal tails that can be post-translationally modified. These modifications serve many purposes ranging from determination of chromatin state to recruitment of complexes such as transcription factors and chromatin-modifying enzymes to regulate gene expression. Indeed, the epigenetic information contained in histone tail is significant and known in the field as the "histone code." The histone code is synonymous epigenetics because histones, like DNA, can be inherited, and the marks they carry can maintain potential gene regulatory function that is carried on to the daughter cells. Epigenetic mechanisms that alter

chromatin structure while preserving primary DNA sequences contribute significantly to "cellular memory", which maintains a particular cell state through many cell divisions (Jacobs and van Lohuizen 2002, Ringrose and Paro 2004, Turner 2002). There is more evidence supporting the hypothesis that extensive post-translational modifications of histones have profound impact on regulating gene expression (Berger et al 2007, Fischle et al 2003, Jenuwein and Allis 2001, Schreiber and Bernstein 2002, Turner et al 2002). Thus, it is possible that stem cells have a chromatin structure distinct from their differentiated cells, which may maintain their unique molecular characteristics (Eun et al 2010, Jaenisch and Young 2008, Jenuwein and Allis 2001). One of the most well-characterized epigenetic mechanism is DNA methylation, which allows regulation whose inheritance is best understood due to its semi-conservative propagation (Bonasio et al 2010, Martin and Zhang 2007. Similarly, repressive histone modifications such as H3K9me3 have also been shown to remain associated with chromatin during mitosis (Fischle et al 2005), which is probably important for faithful inheritance of heterochromatin structure (Irvine et al 2006, Motamedi et al 2004). However, it still remains unclear whether and how the histone modification patterns could be inherited or re-established asymmetrically between stem cells and their differentiating daughter cells.

Replication-dependent vs. replication-independent histone deposition

The bulk of canonical histones are synthesized and incorporated during DNA replication when the entire genome duplicates. During this process, it is commonly accepted that H3 and H4 are incorporated as a tetramer, while H2A and H2B are incorporated as two dimers (Jackson and Chalkley 1981a, b, Russev and

Hancock1981, Annunziato et al 1982; Xu et al 2010). Replication-dependent histone deposition is a highly regulated process and requires an orchestrated series of events, including disruption and recycling of preexisting octamers, as well as deposition of newly synthesized histones at the replication fork (Corpet and Almouzni 2009). Abnormal nucleosome assembly and deposition could cause failure in genome stability and increased sensitivity to DNA damage, which may lead to tumorigenesis and other diseases. This process must be coordinated very efficiently to assemble chromatin right after the passage of replication fork (Gasser et al 1996, Guilbaud et al 2011, Smith and Whitehouse 2012). Incorporation of newly synthesized histones is facilitated by chromatin remodeling complexes (Saha et al 2006), histone chaperones (De Koning et al 2007), and histone-modifying enzymes (Corpet and Almouzni 2009). Chromatin remodelers have ATPase activity, which can slide nucleosome and facilitate disruption of preexisting nucleosome in preparation for replication-coupled reformation. Newly synthesized histones first undergo specific modifications at their N termini; for example, lysine 56 of H3 and lysine 5 and 12 of H4 are acetylated (Ai and Parthun 2004, Masumoto et al 2005). The acetylation marks of H3 and H4 allow their binding to histone chaperones CAF-1, ASF-1, and Rtt106 to facilitate H3–H4 assembly and deposition (Verreault et al 1996; Rechtet al 2006, Chen et al 2008, Li et al 2008). Histone chaperones coordinate deposition of newly assembled histones through direct interaction with proliferating cell nuclear antigen (PCNA), a processivity factor for DNA polymerase, at the replication fork (Shibahara and Stillman 1999, Moggs et al 2000). After deposition, the acetylated histone modifications are removed by HDAC (Ruiz-

Carrillo et al 1975, Jackson et al 1976). In addition to acetylation, histone lysine methylations may also play important roles during epigenetic inheritance. For example, increasing evidence indicates that "cellular memory" of Homeobox gene expression is maintained by a balance between the repressive H3K27me3 and active H3K4me3 marks generated by the polycomb group (PcG) and the trithorax group (TrxG) complexes, respectively (Ringrose and Paro 2004, Hansen and Helin 2009, Zhu and Reinberg 2011). Interestingly, PcG remains at the DNA replication forks in vitro (Francis 2009a, b, Francis et al 2009). Interactions between two different PcG complexes through dimerization can prevent their dissociation from chromatin during DNA replication (Lengsfeld et al 2012, Lo et al 2012). A recent in vivo study examined histone methylation marks in S phase cells from Drosophila embryos (Petruk et al 2012). Consistent with the in vitro work, this study shows that both PcG and TrxG proteins bind to newly synthesized DNA at their response elements and associate with PCNA. However, neither H3K4me3 nor H3K27me3 was detected at replication forks in S phase cells. Instead, unmodified H3 was found to be in close proximity to PCNA and newly synthesized DNA. These data suggest that histone modifying enzymes reestablish histone methylation patterns after the passage of replication fork. Despite increasing knowledge on incorporation of newly synthesized histones during DNA replication, our understanding about whether and how preexisting histones are recycled at replication forks is limited. Transmission of histone modification information from mother cell to two daughter cells is critical for reliable inheritance. On the other hand, resetting this information may be important when the two daughter cells must distinguish from each other

during ACD of adult stem cells or different fate choices during lineage specification.

Increasing evidence indicates that histone variants influence epigenetic inheritance via a transcription-coupled mechanism (Henikoff et al 2004a, b). However, in contrast to canonical histones, deposition of the histone variants is replication-independent. One of the best characterized histone turnovers during transcription is the replacement of canonical H3 with the H3.3 variant (Ahmad and Henikoff 2002b, Schwartz and Ahmad 2005). This replacement is more frequent at gene regulatory regions such as TrxG and PcG response elements, actively transcribed coding sequences, and replication origins (Mito et al 2007, Deal et al 2010). This process requires histone chaperones, such as HirA (Ray-Gallet et al 2002), Daxx, and Atrx (Drane et al 2010, Goldberg et al 2010), as well as chromatin remodeling complexes (Konev et al 2007). H3.3 can potentially transmit either active or repressive chromatin state to maintain the epigenetic memory of gene expression during mitosis or meiosis (Szenker et al 2011). In addition to H3.3, other histone variants play distinct roles in a variety of different cellular processes (Kamakaka and Biggins 2005). Among them, CENPA is an H3 variant found specifically at the centromere region, which is also deposited in a replication independent manner (Ahmad and Henikoff 2002a). CENP-A may play a critical role in differentially labeling the two sister chromatids for asymmetric epigenetic inheritance, which will be discussed later.

Chromatin-dependent regulation of transcription in differentiating germ cells

During *Drosophila* spermatogenesis, germline stem cells (GSCs) asymmetrically divide into a gonialblast that mitotically amplify to give rise to spermatogonia. At the 16-cell cyst, spermatogonia differentiate into spermatocytes. During this process differentiation genes that are transcriptionally silent in spermatogonia are activated in an orchestrated manner. The spermatocyte serves as an intermediate stage when differentiation genes are transcribed necessary for terminal differentiation into spermatids. Previous studies have characterized spermatocyte transit into terminally differentiated spermatids (Chen et al 2011, Chen et al 2005). Although these assays were performed using representative differentiation genes rather than a genome-wide basis, but they suggests that the manner of regulation is done in part through changes in the chromatin structure on a genome-wide scale, mediated by active and repressive marks on histone tails. Furthermore, the establishment of the chromatin state that prepares differentiation genes for transcription is most likely coordinated by regulation of Polycomb group protein activity.

The Polycomb group protein (PcG) potentially plays a role in stem cell maintenance through modifications of the chromatin state (Boyer et al 2006). PcG genes are highly conserved from flies to mammals (Schwartz et al 2010). There are two known PcG families, the Polycomb Repressive Complex 1 and 2 (PRC1 and PRC2). PRC2 function is necessary for maintenance of germline stem cells (GSC) in the *Drosophila* germline. PRC2 serves as an epigenetic "writer" by methylating histone H3 at lysine 27 to generate the H3K27me3 repressive mark (Cao et al 2002) **(Fig 1-5A**). One model for repression suggests that PRC1 recognizes and binds to

the H3K27me3 repressive mark. PRC1 act as a "reader" to prevent transcription initiation and/or elongation of differentiation genes (Fischle et al 2003, Min et al 2003) **(Fig. 1-5B)**. In contrast, the modified histone H3K4me3 serves as an active mark to recruit factors necessary for gene transcription. This active mark is most likely established through the activity of Trithorax (TrxG) group proteins (Byrd et al 2003). It is likely that PRC1 and PRC2 activities need to be counteracted and active marks need to be placed in order for differentiation genes to be expressed. The replacement of the repressive H3K27me3 mark by the active H3K4me3 mark at the differentiation genes presents a complex relationship between chromatin structure and gene expression that still remains unclear. PRC2 is enriched only in undifferentiated germ cells and down-regulated when cells transit into the differentiating spermatocyte stage (**Fig. 1-6).** Removal of PRC2 and its repressive marks along with establishment of the H3K4me3 activation mark could be important for progression to terminal differentiation. Although H3K4me3 activation marks oppose gene repression, its presence alone may not be sufficient to turn on gene expression (Cui et al 2009, Akkers et al 2009). Differentiation genes in early spermatocytes are not transcribed because the repressive marks established by PRC2 remains to recruit PRC1 to occupy and repress regions for transcription initiation and/or elongation (Wang et al 2004). Only when PcG activity is gone and the H3K27me3 mark removed will terminal differentiation genes be expressed. If this is the case, then regulation of this switch will have to be done through antagonizing both PRC1 and PRC2 function. It is possible that two classes of genes that counteract repressive PcG function necessary for terminal differentiation.

These classes form two separate complexes known as the *Drosophila* testis-specific Meiotic Arrest Complex (tMAC) and the testis-specific TBP-Associated Factor (tTAF). They may act independently or cooperatively to counter PcG function in a genome-wide manner to change the chromatin state, marking loci for activation and gene transcription (**Fig. 1-7).** It is likely that these two complexes directly antagonize PcG activity to de-repress differentiation genes as the germ cell transition from the mitosis to meiotic cell cycle.

The *Drosophila* testis-specific Meiotic Arrest Complex (tMAC) is a class of genes necessary for terminal differentiation during spermatogenesis. The tMAC contains at least four subunits: Always Early (Aly), Matotopetli (Topi), Mip40 and Cookie Monster (Comr) (Beall et al 2007, Lin et al 1996). Loss of function in any of these genes result in meiotic arrest at the spermatocyte stage, preventing both meiotic cell cycle progression and terminal differentiation of spermatocytes into spermatids (Lin et al 1996, White-Cooper et al 1998). Experimental data implicates tMAC as a transcriptional regulator due to homology and shared subunits to the MIP/dREAM complex (Beall et al 2007). The testis-specific TATA-binding protein Associated Factor (tTAF) is the other class of factors also involved in terminal differentiation in the germline lineage. There are 5 known testes-specific TAFs: Cannonball (Can), No Hitter (Nht), TAF12L (Rye), Meiosis Arrest (Mia), and Spermatocyte Arrest (Sa) (Hiller et al 2001). In the germ cell lineage, the *Drosophila* tTAF binds to the general transcription factor known as $TF_{II}D$ to initiate robust transcription (Hiller et al 2004). Like tMAC, mutation of any subunits would also result in arrest at the spermatocyte stage (Hiller et al 2001). While the TATA

binding protein (TBP) complex can support basal transcription of genes, they need tTAF to activate transcription to a sufficient level to initiate differentiation (Pugh et al 1990, Dynlacht et al 1991, Zhou et al 1992). Even though the molecular functions of tMAC and tTAF are different, their shared mutant phenotype suggests they are in the same pathway. In tMAC mutants, tTAF does not properly localize to differentiation gene promoter, suggesting that tMAC is needed to recruit tTAF to the promoter of differentiation genes. Loss of tMAC function also results in mis-localization of PRC1 complex in late stage spermatocytes, indicating its potential role in PcG inactivation through sequestration (Chen et al, 2011). Whether tMAC and tTAF work together in the same complex to cooperatively act against PcG complex is still unclear. However, it is interesting to note that the transcription machinery of tMAC mutants, including RNA Polymerase II, is still recruited to the promoter with little or no transcription activity, indicating a "poised" status (Chen et al 2011). This suggests that transcriptional machinery is waiting for tMAC and tTAF function to turn on.

Further examination into the role of tTAF in the context of PcG regulation reveals an additional role. tTAF potentially act against PcG repressive function by binding itself to PRC1 and sequesters it to the nucleolus (Chen et al 2005). This may expose the chromatin to TrxG protein recruitment to lay down H3K4me3 active marks to initiate transcription (Francis et al 2004). Whether this antagonistic function of tTAF is independent remains unclear. If tMAC and tTAF does antagonize the function of PcG on a genome-wide scale, then loss-of-function in both tMAC and tTAF should cause distinct changes to active and repressive marks as well as RNA

polymerase II binding. These changes will lead to reduced expression of differentiation genes in spermatocyte during transit to spermatids.

FIGURES AND TABLES

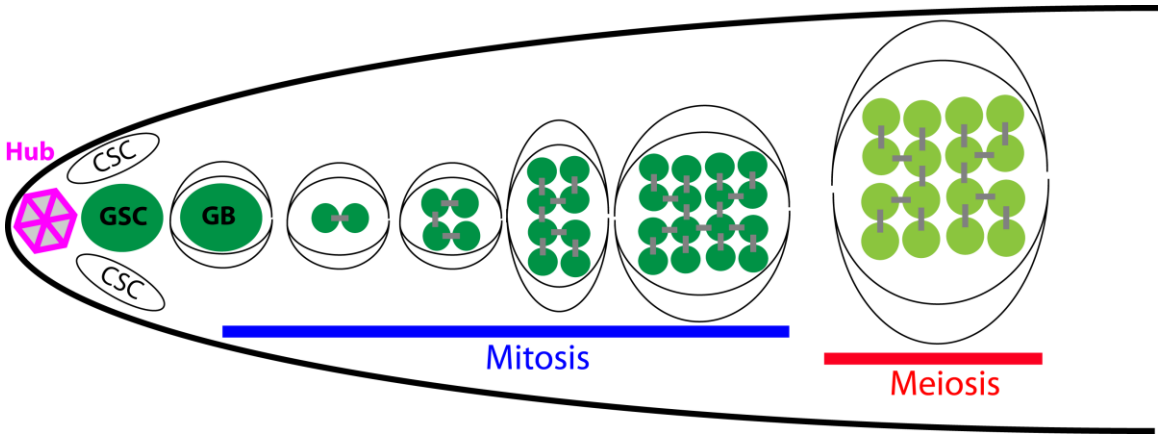

Figure 1. *Drosophila* Spermatogenesis. The hub is located at the apical tip of the testis. Cyst stem cells (CSC) and germline stem cell (GSC) makes contact with the hub. For simplicity, the lineage of only one GSC is represented in this diagram.

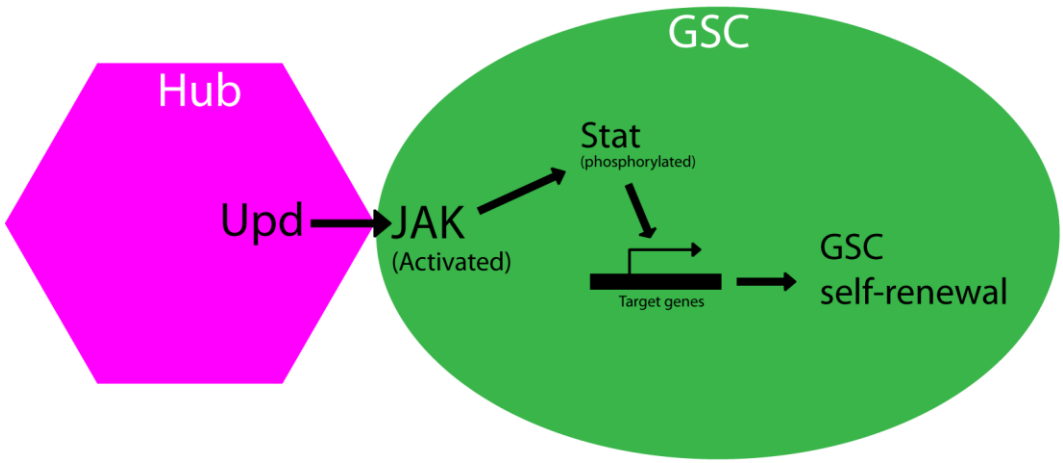

Figure 1-2. Extrinsic JAK-STAT signaling contributes to GSC cell identity. Upd ligand is secreted from the hub. Binding of unpaired ligand activates the JAK (Hopscotch) to phosphorylate STAT (Stat92E), which activates gene transcription in the GSC.

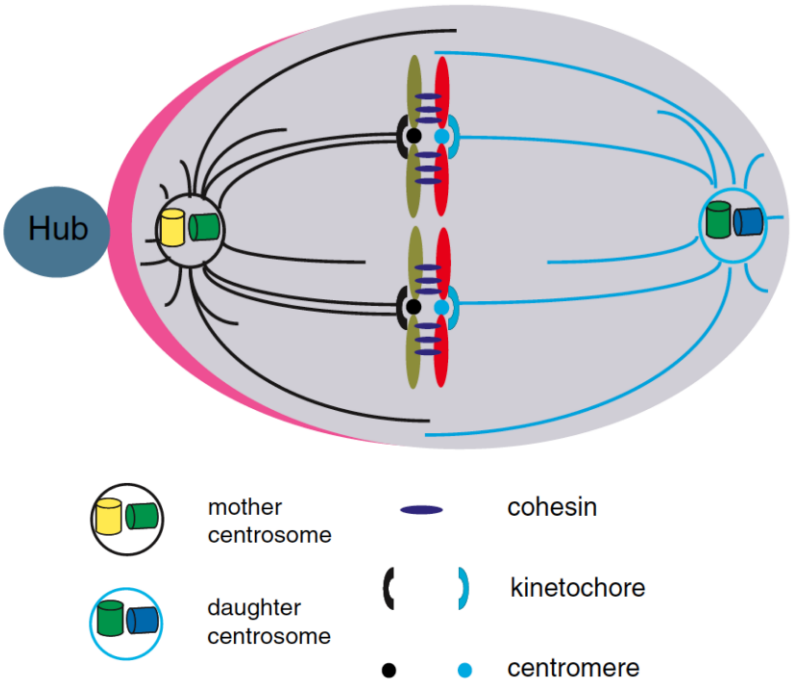

Figure 1-3. The mother centrosome is preferentially retained in the GSC during asymmetric division. The mother centrosome is anchored to the GSC side and serves as an intrinsic mechanism for spindle formation. Mother centrosome is retained through successive GSC division.

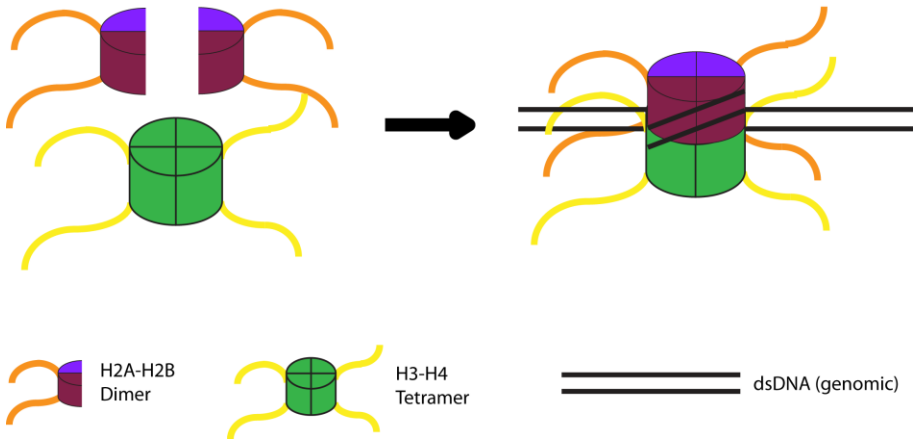

Figure 1-4. Nucleosome assembly of canonical core histone octamer. H3-H4 exist as a stable tetramer and serves as a scaffold H2A-H2B dimers to bind for DNA wrapping to form a nucleosome. N-terminal tails are exposed as substrate for modification and recruitment of various factors.

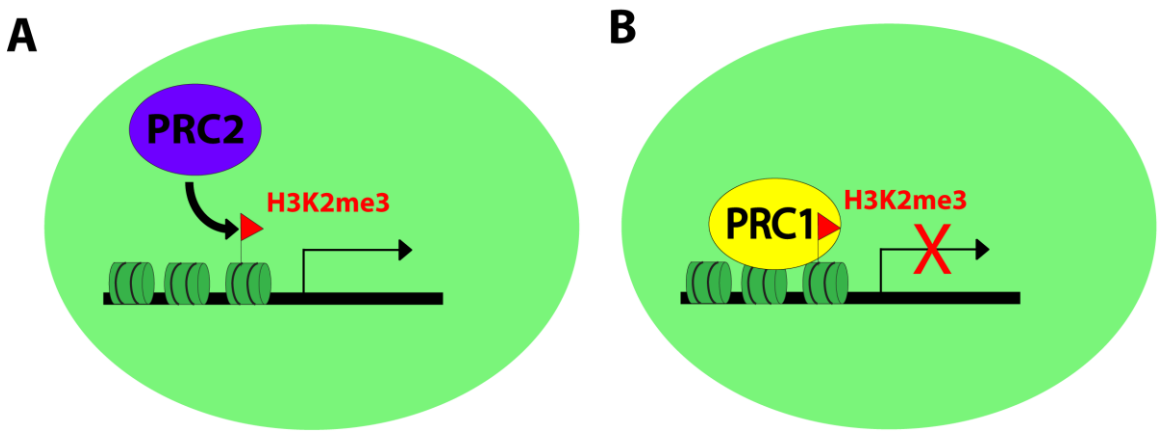

Figure 1-5. Polycomb Group Complex as Epigenetic "writer" and "reader." PRC1 and PRC2 work together to repress gene expression. A) PRC2 has methyl-transferase activity to establish trimethyl mark on lysine 27 on the H3 histone subunit (H3K27me3) B) PRC1 recognize the H3K27me3 mark, binds and prevents gene transcription.

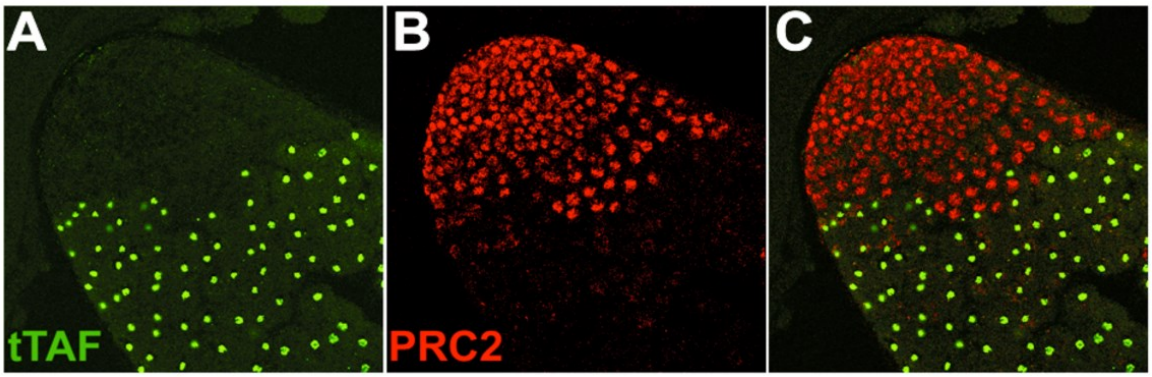

Figure 1-6. PRC2 protein is absent in differentiating cells. A) Sa, a subunit of tTAF (green), marks differentiating cells. B) E(z), a subunit of PRC2 (red), is present in early undifferentiated germ cell. C) PRC2 is absent in differentiated germ cells.

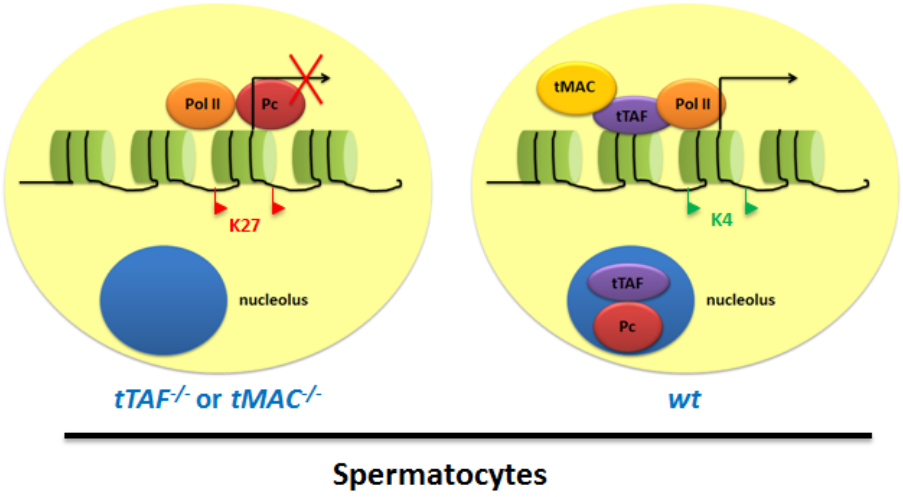

Figure 1-7. tTAF and tMAC antagonize PcG activity to activate transcription of genes. A proposed diagram of the potential chromatin state in spermatocytes mutant for tMAC (*aly*) or tTAF (*can*) compared to wild-type (wt) spermatocytes. K27 = H3K27me3, K4 = H3K4me3.

Chapter 2

Asymmetric histone inheritance in *Drosophila* male germline stem cells

INTRODUCTION

A long-standing question is whether and how stem cells maintain their epigenetic information. Epigenetic information can be defined as any DNA-associated factors that determine gene expression without altering the primary DNA sequences. And epigenetic changes are inheritable after successive cell divisions (Ringrose et al 2004, Jacobs et al 2002, Turner et al 2002). It is the epigenetic information that directs cells with the identical genome to become distinct cell types by turning on different sets of genes in multicellular organisms. How cells with the identical genetic code decide which genes they should express in a spatiotemporally specific manner remains one of the biggest questions in modern biology. Stem cells have the remarkable ability to both self-renew and generate daughter cells that enter differentiation (Knoblich et al 2008). Epigenetic mechanisms have been reported to regulate stem cell activity in multiple lineages, leading to a hypothesis that stem cells have a unique chromatin structure to maintain their identity (Eun et al 2010, Jaenisch et l 2008, Buszczak et al 2006). However, except for DNA methylation little is known about the molecular mechanisms of epigenetic inheritance (Martin et al 2007, Bonasio et al 2010). However, DNA methyl-transferase activity is almost negligible in adult flies (Richards et al 2002, Lyko et al 2000, Hung et al 1999, Lyko et al 2000). To date, there has been little direct *in vivo* evidence demonstrating whether and how stem cells retain their epigenetic memory. Therefore, histone modifications likely represent the major source of epigenetic information in flies. In this chapter we demonstrate that during the asymmetric division of *Drosophila* male germline stem cell (GSC), preexisting histones are selectively segregated to the GSC whereas newly

synthesized histones incorporated during DNA replication are enriched in the differentiating daughter cell. The asymmetric histone inheritance occurs in GSCs but not in symmetrically dividing spermatogonia cells. Furthermore, if GSCs are genetically manipulated to divide symmetrically, the asymmetric histone inheritance mode is lost. In contrast to canonical histones, the histone variant H3.3 does not exhibit this asymmetry during GSC divisions. This provides the first direct evidence that stem cells retain preexisting canonical histones during asymmetric cell divisions.

MATERIALS AND METHODS

Identifying the lineage of daughters in the germline stem cell division

The *Drosophila* male GSCs are well characterized in terms of their physiological location, microenvironment (i.e. niche), and cellular structures (Fuller et al 2007, Losick et al 2011) (**Fig. 2-1A**). Male GSCs are identified precisely by their distinct anatomical positions and morphological features. A GSC usually divides asymmetrically to give rise to a self-renewed GSC and another daughter cell gonialblast (GB) that undergoes differentiation. Therefore, GSCs can be examined at single-cell resolution for a direct comparison of two daughter cells from one GSC division. We define the GSC as any cells directly adjacent to the hub structure. The testis hub is immunofluorescence-labeled using the FasIII marker. Since there are 10-12 GSCs attached to each hub, it is difficult to identify the GSC-GB division pair. To address this issue, we use α-spectrin antibody to label the spectrosome, a structure that keeps the GSC and GB attached to each other subsequent to mitotic division **(Figure 2-1B).**

Switchable dual-color system facilitates distinction of pre-existing histone versus newly synthesized histones

Histones are one of the major carriers of epigenetic information (Kourarides et al 2007). To address how histones are inherited during the GSC asymmetric division, we developed a switchable dual-color method to differentially label "old" vs. "new" histones **(Fig. 2-2)**. This method employs both spatial (by Gal4; UAS system) and temporal (by heat shock induction) controls to switch labeled histones from green

[Green Fluorescent Protein (GFP)] to red [monomeric Kusabira-Orange (mKO)]. Heat shock treatment induces an irreversible DNA recombination to shut down expression of GFP-labeled old histones and initiate expression of mKO-labeled new histones. If the old histones are inherited non-selectively, the GFP will initially exhibit equal distribution in the GSC and GB, and will be gradually replaced by the mKO (**Fig. 2-3A**). However, if the old histones are preferentially retained in the GSCs and potentially contribute to GSC-specific chromatin structure, the GFP will be retained specifically in the GSCs (**Fig.2-3B**). During DNA replication-dependent canonical histone deposition, histones H3 and H4 are incorporated as a tetramer, and histones H2A and H2B are incorporated as dimers (Xu et al 2010, Jackson et al 1981, Jackson et al 1981, Russev et al 1981, Annunziato et al 1982). Therefore, we generated independent transgenic strains for H3 and H2B, respectively. On the other hand, histone variants are incorporated into chromatin in a transcription-coupled, but DNA replication-independent manner (Tagami et al 2004, Ahmad et al 2002). Therefore, the histone variant H3.3 was used as a control for canonical histones.

To avoid potential complications caused by heat shock-induced DNA recombination on either one or both chromosomes in GSCs, each of the three transgenes (H3, H2B and H3.3) was integrated as a single copy and analyzed in heterozygous flies. Examination of testes with transgenes revealed nuclear GFP but little mKO signal before heat shock. After heat shock, mKO signals were detectable. Different GSCs undergo mitosis asynchronously, and an average cell cycle length of GSCs is approximately 12 to 16 hours. Among all GSCs, 75-77% are in G2 phase,

21% are in S phase, less than 2% are in mitosis, and G1 phase GSCs are almost negligible (Cheng et al 2008, Sheng et al 2011, Yamashita et al 2003, Yadlapalli et al 2011, Yamashita et al 2007). Moreover, the GSC and GB arising from an asymmetric division remain connected after mitosis by a cellular structure known as the spectrosome, when they undergo the next G1 and S phases synchronously (Sheng et al 2011, Yadlapalli et al 2001).

Heat shock scheme

In order prevent the random flipase-induced recombination of the UAS-FRT-Histone-GFP-FRT-Histone-mKO, the flies are raised at 18C. Adult flies at 3-5 days after eclosion is heat shock in a 37C water bath for 2 hours. The heat shock should most likely occur within the 9 hours of G2, according to the empirically determined GSC cell cycle. Therefore, selection testes analyzed at 4-6 hours after heat shock should only have GSC divide in the first S-phase while testes analyzed at 16-20 hours after heat shock should have GSC mostly in the second S-phase.

Quantification of fluorescence signal

The quantification of pre-existing (GFP) and newly synthesized (mKO) histones cannot be done relative to one another since GFP and mKO are two different molecules with variable intensity. We determined that the optimal comparison would be to compare GFP and mKO separately, but the comparison of each fluorescence molecule should be done between the GSC and the GB in order to identify the distribution of pre-existing and newly synthesized histones. This is done by selecting the middle image in the confocal stack of both the GSC and the GB

(often the region with the largest area) for analysis. Using ImageJ software, the region of interest is selected from the DAPI stain overlay of the image. The average fluorescence of each signal (GFP and mKO) is recorded and subtracted by the average signal of the background of the tissue. Calculations are determined by relative value of each fluorescence molecule between the pairs of cell determined to be GSC-GB daughters of the same lineage. Calculations for GB-GB daughter cells are also done. Raw values are indicated in **Tables 1 and 2**.

RESULTS

Pre-existing histones are asymmetrically segregated and retained in GSC

To examine the distribution of old vs. new histones in GSC and GB after one round of DNA replication-dependent histone deposition, testes were studied 16 to 20 hours after heat shock. Based on the cell cycle length of GSCs, these GSC-GB pairs were from GSCs that switched from *histone-GFP* to *histone-mKO* genetic code during their G2 phase, underwent the first mitosis followed by G1, S, G2 phase and the second mitosis **(Fig. 2-4A**). GSC-GB pairs connected by spectrosomes were examined (**Fig. 2-5A, arrow**). With this time frame, both old histones and new histones were detectable in GSCs at the second G2 phase (**Fig. 2-4B, Table 1**), because new histones had been synthesized and incorporated during the first S phase. For histone H3, the pre-existing histones, indicated by GFP signal, was detected primarily in the GSC, but not in the GB. By contrast, the mKO signals were present in both the GSC and the GB, with a relatively higher level in the GB (**Fig. 2-5A, Table 1**) The asymmetric inheritance mode of histone H3 was specific for GSC divisions, because both the GFP and the mKO signals were equally distributed in spermatogonial cells derived from a symmetric division of the GB, in the same testes (**Fig. 2-5B**). Quantification of fluorescence intensity revealed that the old H3 (GFP-labeled) signal was ~5.7-fold more enriched in the GSC compared to the GB, while new H3 (mKO-labeled) signal was ~1.6-fold more enriched in the GB compared to the GSC (H3 GSC/GB data in **Fig.2-6, Table 1**). By contrast, this differential distribution of old vs. new histone was not detected for symmetrically dividing

spermatogonial cells (H3 SG1/SG2 data in **Fig.2-6, Table 1**: H3-GFP ratio in SG1/SG2= 1.09; H3-mKO ratio in SG1/SG2= 1.02).

Next, to examine the histone inheritance mode during the first GSC division, GSCs were recovered for 4 to 6 hours following heat shock (**Fig. 2-7**). Interestingly, an asymmetric inheritance mode was also found in the GSC-GB pairs with the H3 transgene (**Fig.2-8A**). By contrast, symmetric inheritance mode was observed dividing spermatogonial cells with the H3 transgene (**Fig. 2-8B**). Quantification of fluorescence intensity revealed that the old H3-GFP signal was ~13-fold more enriched in the GSC compared to the GB, while the new H3-mKO signal was ~2.4-fold more enriched in the GB compared to the GSC (H3 GSC/GB data in **Fig.2-9**, **Table 2**). By contrast, there was no differential distribution of the old vs. new histone for the symmetrically dividing spermatogonial cells (H3 SG1/SG2 data in **Fig.2-9, Table 2**: H3-GFP ratio in SG1/SG2=1.07; H3-mKO ratio in SG1/SG2=1.06). Although asymmetric histone inheritance was detected in post-mitotic GSC-GB pairs, examination of the mitotic GSC at this stage did not show any asymmetric distribution. This is consistent with the fact that in the first cell cycle, heat shock should occur in G2, after S-phase, so replication-dependent histone deposition does not happen. However, this suggests that there is a differential rate of histone turnover between the GSC-GB pair where the GB has a higher turnover rate. Since heat shock has occurred, only H3-mKO histone should be expressed. The discrepancy between what we see in **Fig. 2-8A** and **Fig. 2-10** is due to the GB incorporating newly synthesized histones faster than the GSC. We propose that this turnover mechanism in the GB may be necessary mechanism for the GB to reset the

chromatin for differentiation. These data suggest that the primary mechanism for asymmetric segregation relies on replication-dependent histone incorporation prior to mitosis. However, replication-independent turnover of histone contributes to incorporation of the newly synthesized histones either masks or enhances the readout of the GSC-GB pairs.

Asymmetrical segregation of canonical histones occurs exclusively in the GSC in a replication-dependent manner

In contrast to the asymmetric inheritance pattern for the canonical histone H3, the histone variant H3.3 did not show this asymmetry during GSC divisions in the second or the first cell cycle (**Fig. 2-11A and 2-11B, respectively).** Quantification of GFP and mKO signals indicates nearly equal ratios between the GSC and GB (H3.3 GSC/GB data in **Fig. 2-6 and 2-9**, **Tables 1 and 2**: H3.3-GFP ratio in the second cycle GSC/GB = 1.03; H3.3-mKO ratio in GSC/GB= 1.03, and H3.3-GFP ratio in the first cycle GSC/GB =1.00; H3.3-mKO ratio in GSC/GB =1.02). The symmetry of the histone variant H3.3 suggest that the asymmetric inheritance mode is specific for canonical histone H3.

Active asymmetric patterning does not occur for H2B canonical histone

The dual-switch transgene for the canonical histone H2B was similarly analyzed as the H3 and H3.3. However, the result is more ambiguous than expected. Initially, the patterns of pre-existing and newly synthesized histones seem to be asymmetrically segregated, similar to the pattern of H3 after the first division (**Fig. 2-12A**). However, the expression of fluorescent signal is weak and unreliable, this is

due to the insertion of the transgene. Once another transgene of the same construct is generated where the expression of H2B-GFP/H2B-mKO is strong, the histone patterning shows a symmetric patterning (**Fig. 2-12B**). Furthermore, analysis of the H2B-expressing transgene in mitotic GSC indicates no obvious segregation between pre-existing (GFP) and newly synthesized (mKO) histones (**Fig. 2-12C**) as observed in the H3 patterning (**Fig. 2-13 and 2-14**). These results, when taken into context with the results for the H3 asymmetric histone distribution patterning in the first cell cycle provides a consistent picture. The asymmetric patterning of H2B in the first cell cycle is most likely due to the differential turnover between the GSC and GB. But when expression of H2B-GFP/mKO is improved, the asymmetric pattern is diminished. This is indeed supported by the metaphase data showing no clear segregation before mitosis.

Asymmetric canonical histone deposition is established before mitosis

Because mitotic GSCs are less than 2%, all analysis above were based on post-mitotic GSC-GB pairs. To further examine the histone segregation pattern during mitosis, we screened for mitotic GSCs. The morphology of mitotic cells can be characterized as small and condensed DAPI staining less than 5μm. Indeed, old histones were mainly associated with the chromatids segregated to the GSC-side at metaphase and anaphase stages of GSC division (**Fig. 2-13**). Furthermore, live-imaging experiments were performed to improve the probability of capture mitotic cells. The results yield more GSCs undergoing anaphase and telophase (**Fig. 2-14**). These results suggest that pre-existing histones are preloaded selectively onto one

sister chromatid. This sister chromatid are enriched with epigenetic marks, capable of being selected by the spindle machinery of the GSC to be retained in successive divisions.

Loss of GSC asymmetric division leads to loss of histone asymmetric division

The phenomenon of asymmetric cell divisions of GSCs is found to be lost under certain conditions, such as ectopic activation of the key JAK-STAT (Janus kinase and signal transducer and activator of transcription) signaling pathway in the niche (Kiger et al 2001, Tulina et al 2001, Leatherman et al 2008). When the assay is performed accompanied by the overexpression of the JAK-STAT ligand *unpaired* (OE-*upd*), the result is overpopulation of GSCs, where all early germ cells have JAK-STAT signaling (Kiger et al 2001, Tulina et al 2001). Consistent with the loss of asymmetry in expanded GSCs, the asymmetric inheritance mode of the histone H3 was not observed in OE-*upd* testes 16-20 hour after heat shock (**Fig. 2-15**). These results suggest that the asymmetric histone inheritance pattern is dependent on GSC asymmetric divisions. This is due to the fact that JAK-STAT overexpression produces two daughter cells with similar molecular features. Hence, proper JAK-STAT expression in the hub may be necessary to maintain asymmetric cell division, and ultimate asymmetric histone segregation.

DISCUSSION

In order to understand all the histone patterning for the various histone species, we must begin by tracing the precise timeline of each event (**Fig. 2-16**). First, we look at the H3 canonical histone patterning. Before heat shock the GSC should only be expressing H3-GFP, but after heat shock the GSC is genetically expressing H3-mKO. We presume the GSC were heat shock in G2 for two reasons: GSCs spend most of their time in G2, and our selection of S-phase cells relative to the timing of the cell cycle. At 4-6 hours after heat shock (first cell cycle), we observe asymmetrical histone patterning. However, at this time, the newly synthesized histone generated after heat shock (mKO) could not have been deposited into the chromosome via the replication-dependent mechanism since the new histones have not gone through a previous S-phase. Hence, we conclude that the asymmetric histone segregation is established only through the differential turnover between the GSC and GB. We see similar results between the H3 and H2B for the first cell cycle, but not the histone variant H3.3. We believe that this due to the fact that H3.3 is constitutive expressed and turned over in a replication-independent manner. Thus, we propose that asymmetric patterning in the first cell cycle is caused by a passive mechanism caused by the differential turnover between the GSC and GB. This proposed mechanism is relevant because it is possible that the GB, a daughter that proceeds to the differentiation lineage, need to reset its chromatin content to remove the epigenetic marks for stem cell identity. While we acknowledge this proposed mechanism, it is another aspect of not wholly relevant to the epigenetics of adult stem cell systems.

Next we look at the second cell cycle (16-20 hours) after the color switch. We go to the same heat shock conditions, but we let the GSC proceed through the first S-phase. As the GSC finishes the first S-phase, the newly synthesized histones (mKO) are the only histones available to be deposited into the chromatin. As a result, the GSC in G2 should have both GFP and mKO (**Fig. 2-4B**). More importantly, we propose that the histone deposition may asymmetric to one set of sister chromatid. As the cell proceeds from G2 to mitosis, the asymmetric deposition can already be observed (**Fig. 2-13 and 2-14**). This patterning readout is asymmetric between the GSC and GB as is from the first cell cycle (**Fig. 2-5A and Figure 2-8A**). But the mechanism that establishes this pattern is different. The asymmetric pattern in the second cell cycle is determined by some unknown mechanism before mitosis. This is the more compelling mechanism we wish to explore further. In essence, the patterning of S-phase as a readout may be unreliable due to various other mechanisms that either masks or enhances the asymmetric histone patterning. However, the mitotic data of the pre-existing and newly synthesized histones are unquestionable. In future experiments, our data collection and analysis would rely heavily on mitotic data rather than S-phase GSC-GB pairs.

In contrast to the H3 canonical histone data, H2B histone deposition does not seem to share the same mechanism and patterning. This may seem counter-intuitive since they are both subunits in the same histone octamer. This discrepancy can be addressed when we consider the biochemical characteristics of H3 versus H2B. First, H3 can form a stable tetramer with H4. Furthermore, the H3-H4 tetramer itself have DNA-binding properties (Eickbush and Moudrianakis 1978),

H2B-H2B dimer does not share the same ability. In fact, H2A-H2B dimer is shown to bind loosely to the H3-H4 tetramer and it is the wrapping of genomic DNA around the octamer that prevents H2A-H2B from easily dissociating from the octamer and is thought to be randomly distributed during replication-dependent deposition (Gruss et al 1993, Jackson 1987 and 1990). Secondly, the comparison of the N-terminal tail of H3 versus H2B indicates H3 contain trimethylation at lysine 4 and 27 (H3K4me3 and H3K27me3), which are well-characterized marks for activation and repression of genes (Byrd et al 2003, Cao et al 2002). In comparison, the known marks on H2B do not seem to have the same extent for gene regulation. These evidence suggests that perhaps it is not necessary for GSCs to retain the H2A-H2B dimer in order to retain epigenetic information necessary to maintain stem cell identity.

The results of asymmetric histone patterning in GSC provide compelling evidence in the role of epigenetic factors contributing to adult stem cell identity. It is a critical first step toward identifying more detailed mechanisms of pre-existing histone retention in GSC asymmetric division. These findings in the well-characterized GSC model system will help understanding how epigenetic information could be maintained by stem cells. Although, the turnover of histones in these cells would suggest that the retention of histones are not permanent. They are not immortal histones. It is possible that retention of histone serve as a stop-gap to minimize that loss of too many old histones containing important marks. As the chromatin modifying enzymes come in, the new histones would have these important marks re-established.

While we will continue to use these dual-switch systems to further characterize the underlying mechanism, we must be aware of the inherent caveats. First, the transgene is constitutive expressed, unlike the endogenous canonical histone that are only synthesized in bulk shortly before S-phase. Secondly, the histones we generated are tagged with large fluorescent molecules. Therefore, we should approach these results with due caution.

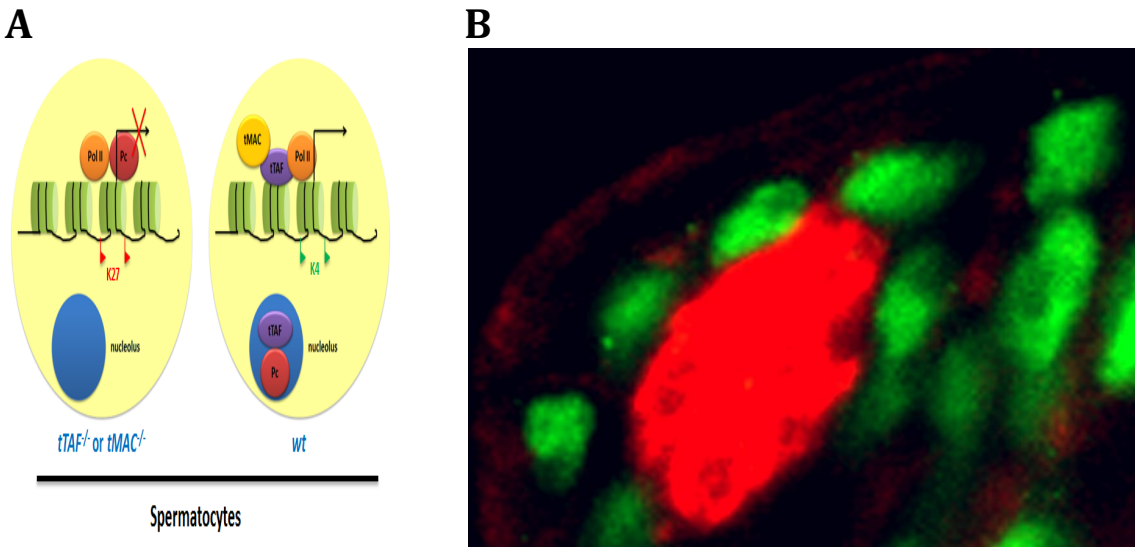

Figure 2-1: The *Drosophila* testis is a well-characterized system in terms of structure and molecular markers (**A**) A diagram of the GSC niche. HUB- hub cells, CySC- cyst progenitor/somatic stem cell. (**B**) Immunofluorescent image of the niche: HUB (anti-Fas III, red, asterisk), GSC-GB pair expressing H3-GFP (green) connected by a spectrosome (anti-a-Spectrin, red, arrow).

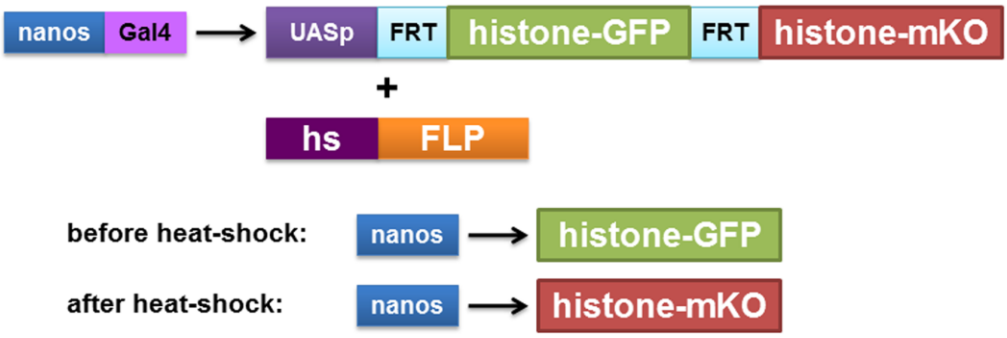

Figure 2-2: The *UASp-FRT-histone-GFP-PolyA-FRT-histone-mKO-PolyA* transgene. UAS: upstream activating sequence; FRT: FLP (flippase) recombination target; histone: H3, H2B, or histone variant H3.3. *nanos-Gal4*: a germline-specific

driver. *hs-FLP*: the yeast FLP recombinase controlled by the heat shock (*hs*) promoter.

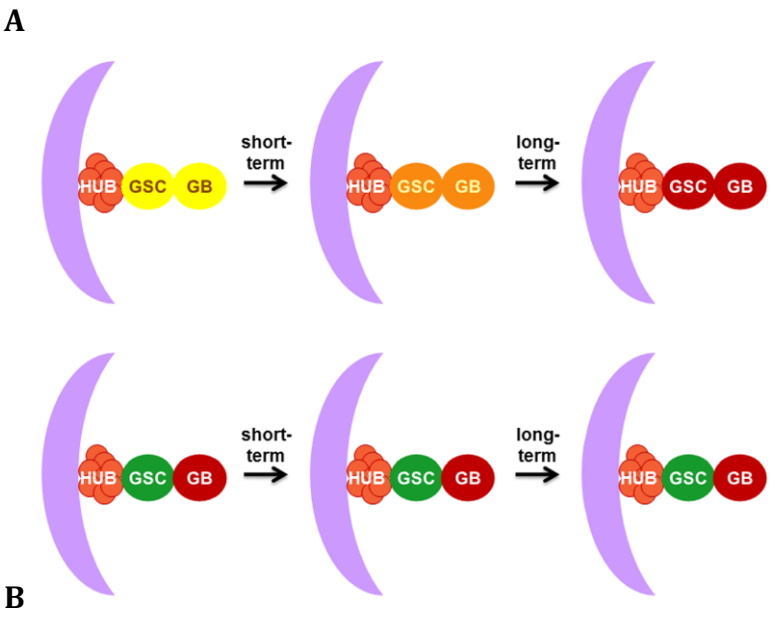

Figure 2-3: **Potential patterning of histone distribution after heat shock.** Two extreme potential results: for simplicity, only one GSC-GB pair is shown, and each entire cell is colored according to histone fluorescence. A) Histones have random segregation and remain evenly distributed in both daughter cells. After multiple cell cycle, pre-existing histone is lost since they are no longer produced. B) Histones are selectively segregated, with pre-existing histone remaining in the GSC. This results in pre-existing histones perdurance, however, pre-existing histones should not remain indefinitely.

A

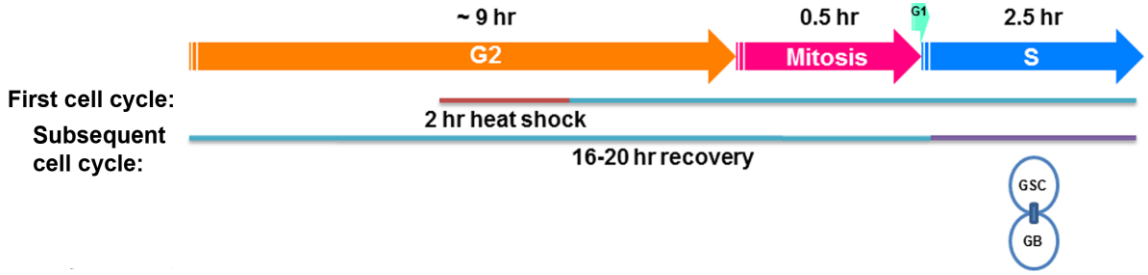

B

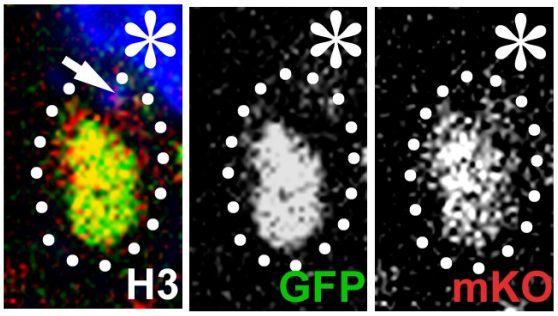

Figure 2-4: Heat shock regimen for analysis of histone segregation in the second post-mitotic GSC-GB pair. A) After 16-20 hours after heat shock the GSC should go through one full cell cycle and proceed with the second cycle. By this time, the cells of interest should have the GSC-GB attachment indicated by the spectrosome. **B)** After heat shock, GSC in G2 have both pre-existing and newly synthesized histones.

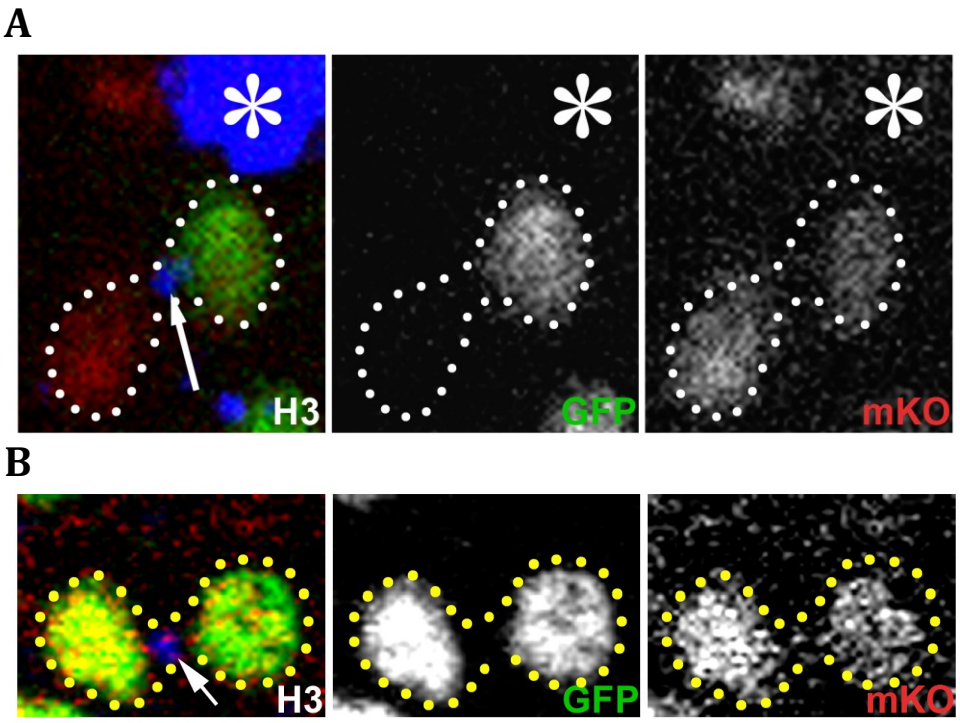

Figure 2-5: H3 is asymmetrically segregated during the second GSC division after heat shock. GSC is located adjacent to the hub labeled with FasIII (blue). Spectrosome determines the two daughter cells from the same division (blue). Pre-existing histone is labeled with GFP (green) and newly synthesized histones is labeled with mKO (red) **A)** Pre-existing H3 is inherited asymmetrically in GSC vs. GB **B)** Spermatogonia have symmetrically distributed histones for both species

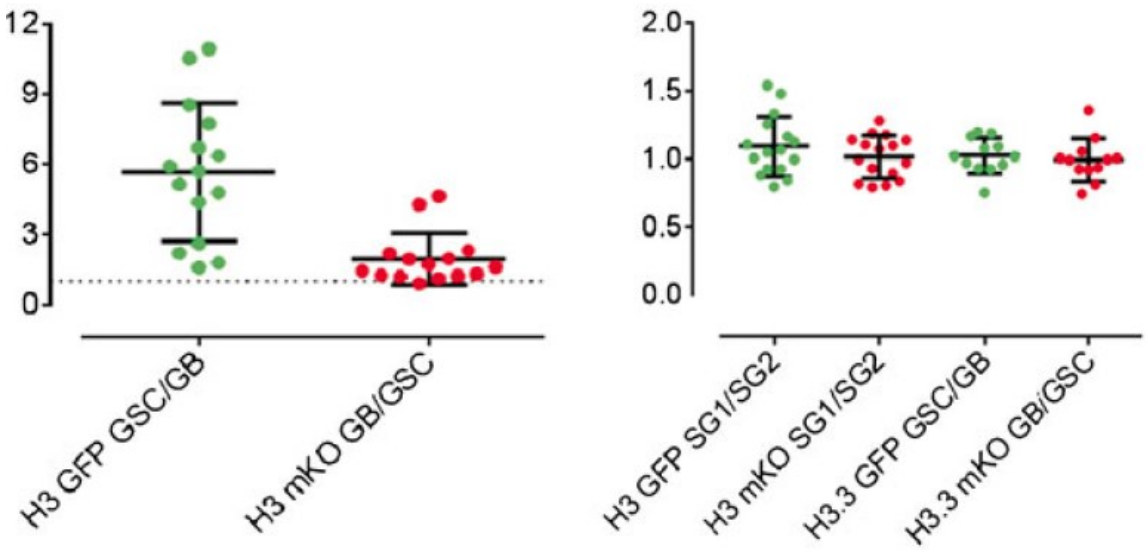

Figure 2-6: Quantification of GFP and mKO fluorescence intensity ratio for the second cell cycle (Table 1). H3 GSC/GB GFP ratio > 1 (* $P<10^{-5}$), GSC/GB mKO ratio < 1 (* $P<10^{-5}$), N=15. H3 two-cell spermatogonial (SG) SG1/SG2 GFP ratio (# P=0.103) and mKO ratio (# P=0.684) insignificantly different from 1, N=16. H3.3 GSC/GB GFP ratio (# P=0.513) and mKO ratio (# P=0.532) insignificantly different from 1, N=12. Error bars: S.E. P-value: one-sample t-test.

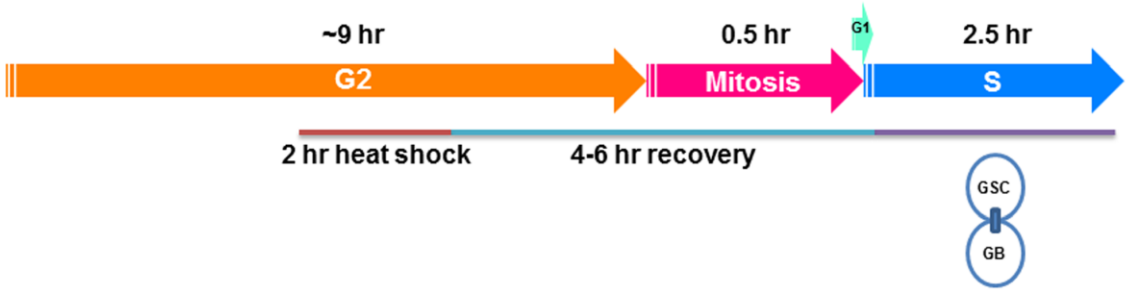

Figure 2-7: Heat shock regimen for analysis of histone segregation in the first post-mitotic GSC-GB pair. After 4-6 hours after heat shock, selection for the post-mitotic GSC-GB pair should place the time of heat shock within G2. The cells of interest should have the GSC-GB attachment indicated by the spectrosome.

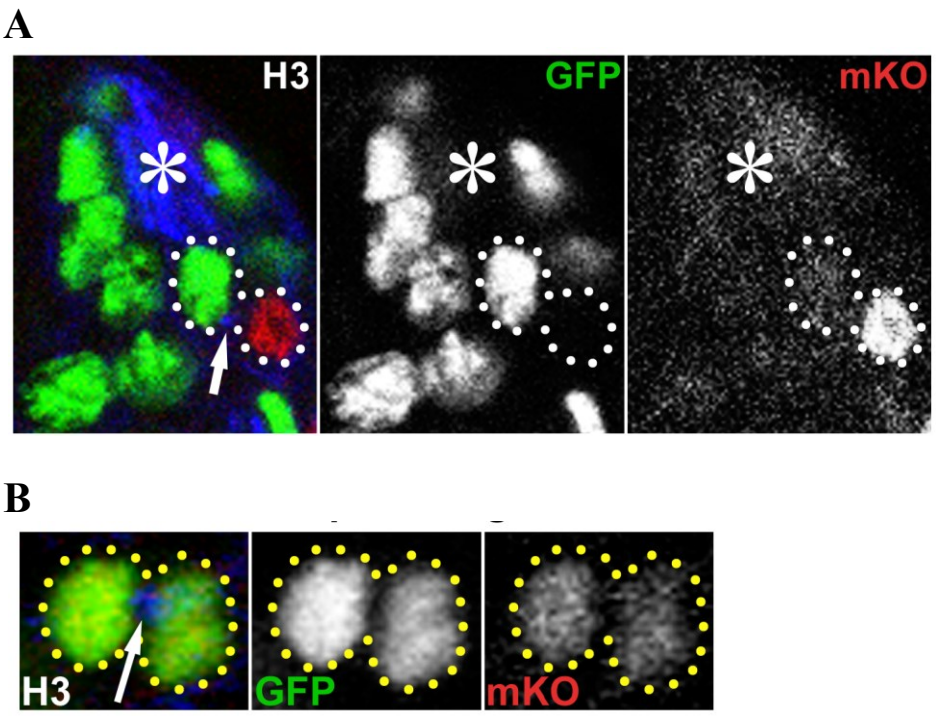

Figure 2-8: H3 is asymmetrically segregated during the first GSC division after heat shock. GSC is located adjacent to the hub labeled with FasIII (blue). Spectrosome determines the two daughter cells from the same division (blue). Pre-existing histone is labeled with GFP (green) and newly synthesized histones is labeled with mKO (red) Spectrosome determines the two daughter cells from the same division (blue). **A)** Pre-existing histone is labeled with GFP (green) and newly synthesized histones is labeled with mKO (red) H3 is inherited asymmetrically in GSC vs. GB. **B)** Spermatogonia have symmetrically distributed histones for both GFP and mKO.

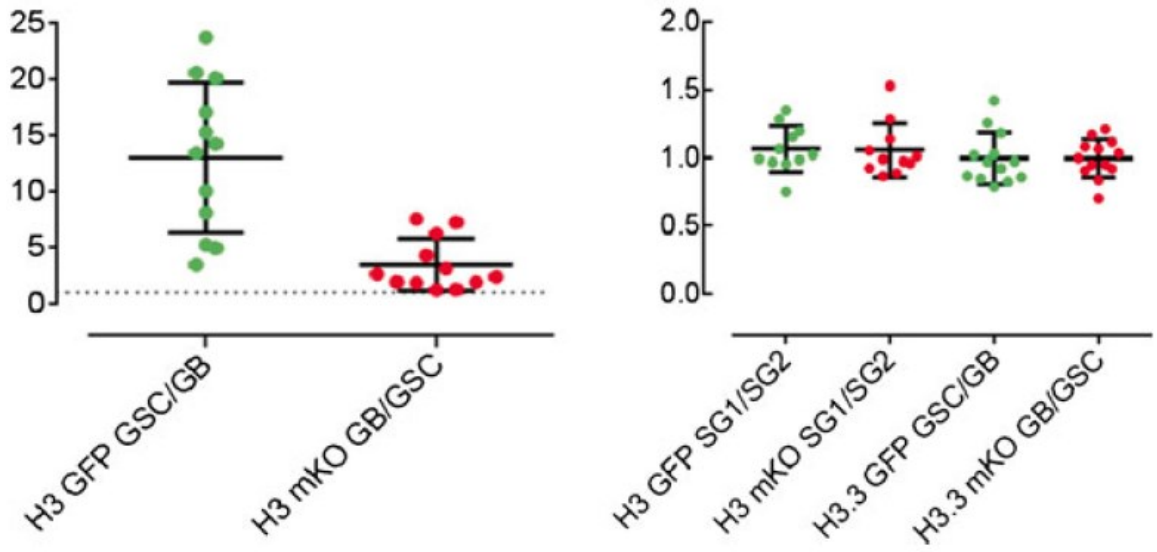

Figure 2-9: Quantification of GFP and mKO fluorescence intensity ratio for the first cell cycle (Table 2). Quantification of GFP and mKO fluorescence intensity ratio (Table S4). H3 GSC/GB GFP ratio > 1 (* $P< 10^{-5}$), GSC/GB mKO ratio < 1 (* $P< 10^{-5}$), N=12. H3 two-cell spermatogonial (SG) SG1/SG2 GFP ratio (# P=0.225) and mKO ratio (# P=0.365) insignificantly different from 1, N=11. H3.3 GSC/GB GFP ratio (# P=0.970) and mKO ratio (# P=0.594) insignificantly different from 1, N=13. Error bars: S.E. P-value: one-sample t-test.

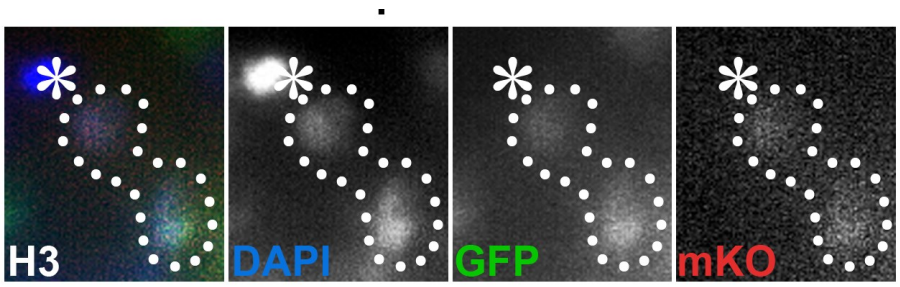

Figure 2-10: GSC captured in telophase in the first cell cycle. Pre-existing histone is labeled with GFP and newly synthesized histones is labeled with mKO. Asterisk: HUB. GSC is outlined.

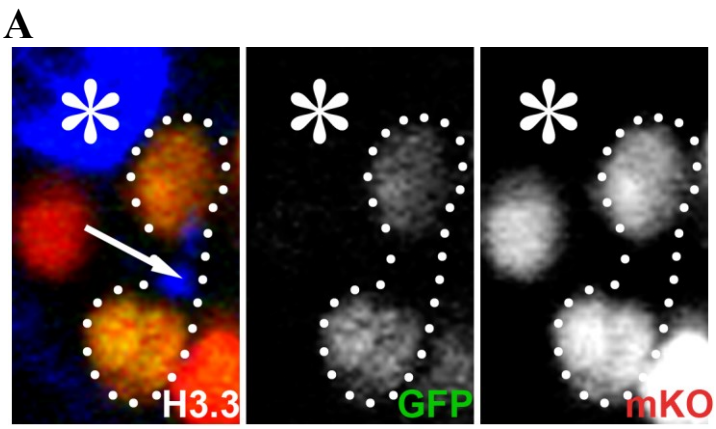

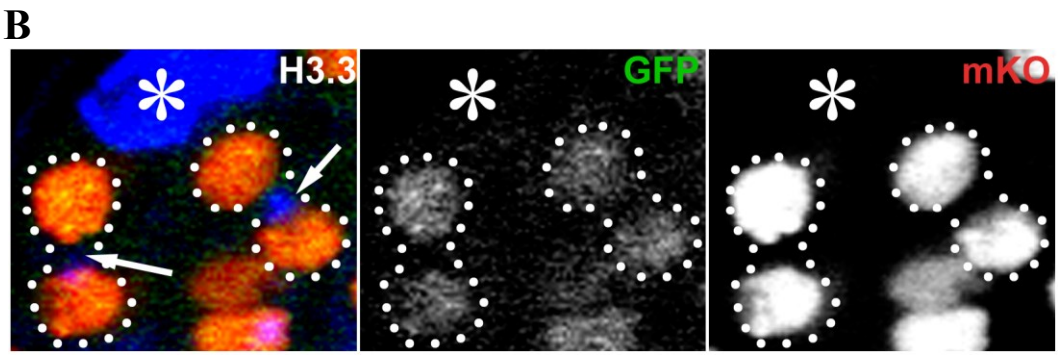

Figure 2-11: H3.3 Histone variant is symmetrically segregated in both the second and first cell cycles after heat shock color switch. GSC is located adjacent to the hub labeled with FasIII (blue). Spectrosome determines the two daughter cells from the same division (blue). Pre-existing histone is labeled with GFP (green) and newly synthesized histones is labeled with mKO (red) Spectrosome (arrows) determines the two daughter cells from the same division (blue) **A)** GSC-GB pair in the second cell cycle **B)** GSC-GB pair in the first cell cycle.

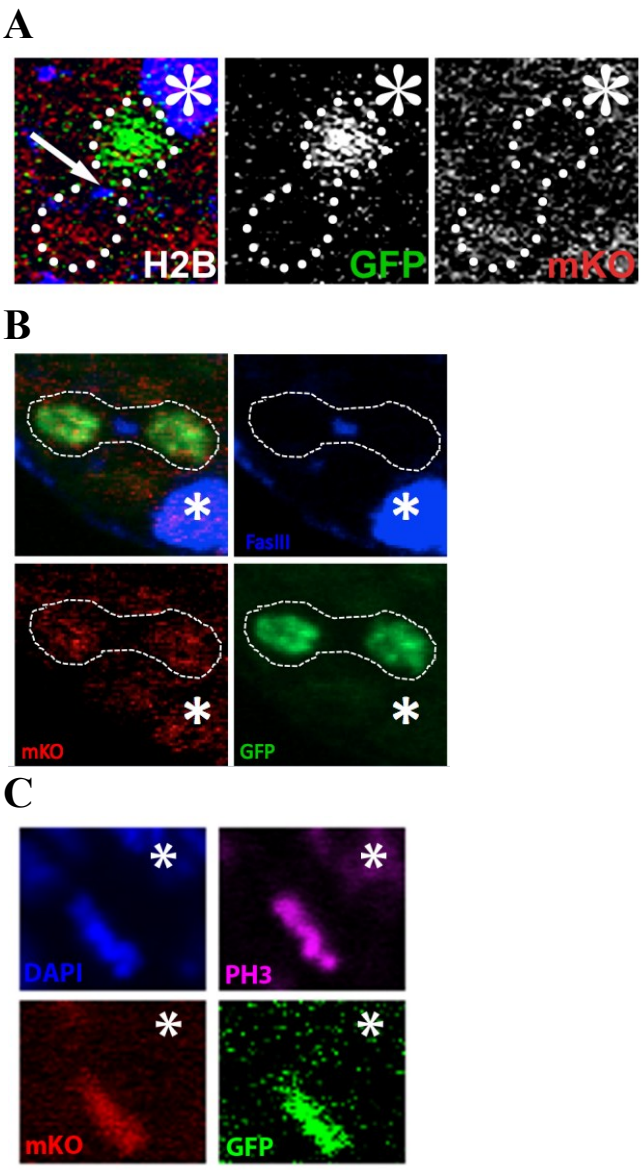

Figure 2-12: Distribution of histone H2B have ambiguous distribution. But does not seem to have segregation before mitosis. Asterisk (*) indicates the hub. **A)** Asymmetric segregation of H2B in the first cell cycle. GSC-GB is identified by the spectrosome (arrow). **B)** Symmetric distribution of H2B histone between the GSC and GB. Spectrosome indicates the dividing pair (arrow). **C)** PH3 marker and DAPI morphology indicates GSC cell in metaphase. Pre-existing and newly synthesized histones overlap almost completely.

A

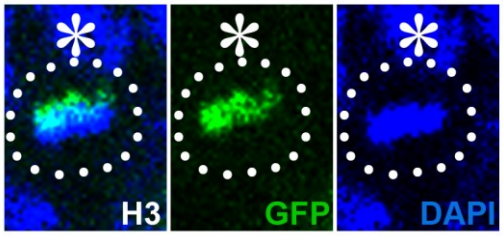

B

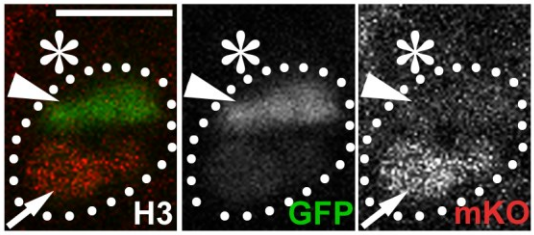

Figure 2-13: GSCs in mitosis indicate asymmetric histone segregation is established well before cell division. Asterisk (*) indicates hub region. **A)** metaphase GSC cell 16-20 hours after heat shock induction. **B)** anaphase GSC cell 16-20 hours after heat shock induction. Pre-existing histone (wedge) is oriented near the hub side while newly synthesized histone (arrow) is oriented away from the hub.

A

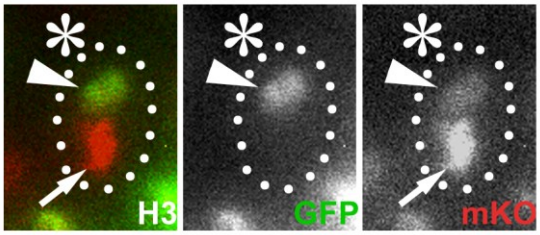

B

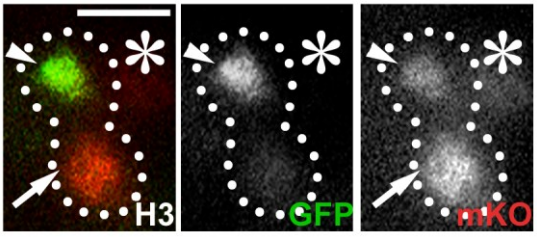

Figure 2-14: Live-imaging captures GSCs in mitosis with asymmetric histone segregation. Asterisk (*) indicates hub region. **A)** anaphase GSC cell 16-20 hours after heat shock induction. **B)** telophase GSC cell 16-20 hours after heat shock induction. Pre-existing histone (wedge) is oriented near the hub side while newly synthesized histone (arrow) is oriented away from the hub.

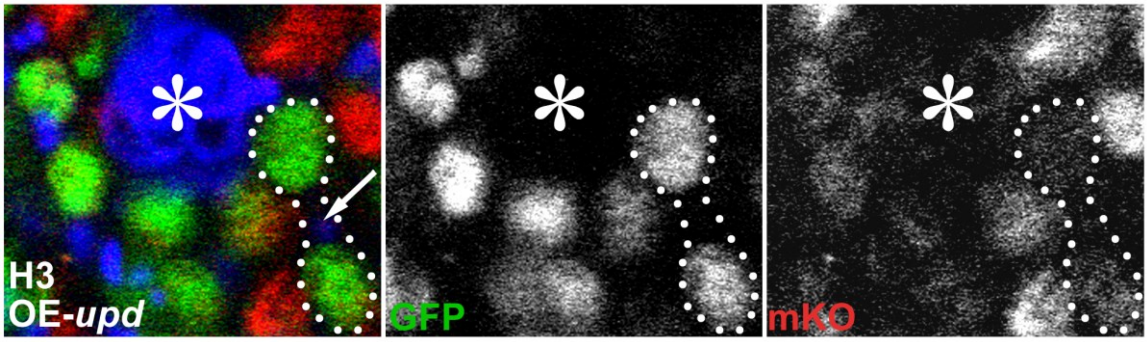

Figure 2-15: Loss of asymmetric H3 inheritance upon overexpression of *upd*. Hub is indicated by an asterisk (*). Symmetric distribution of pre-existing H3-GFP and newly synthesized H3-mKO in the two daughter cells from a GSC division in *nanos-Gal4*; *UAS-upd* background of UAS-FRT-H3-GFP-FRT-H3-mKO male testis.

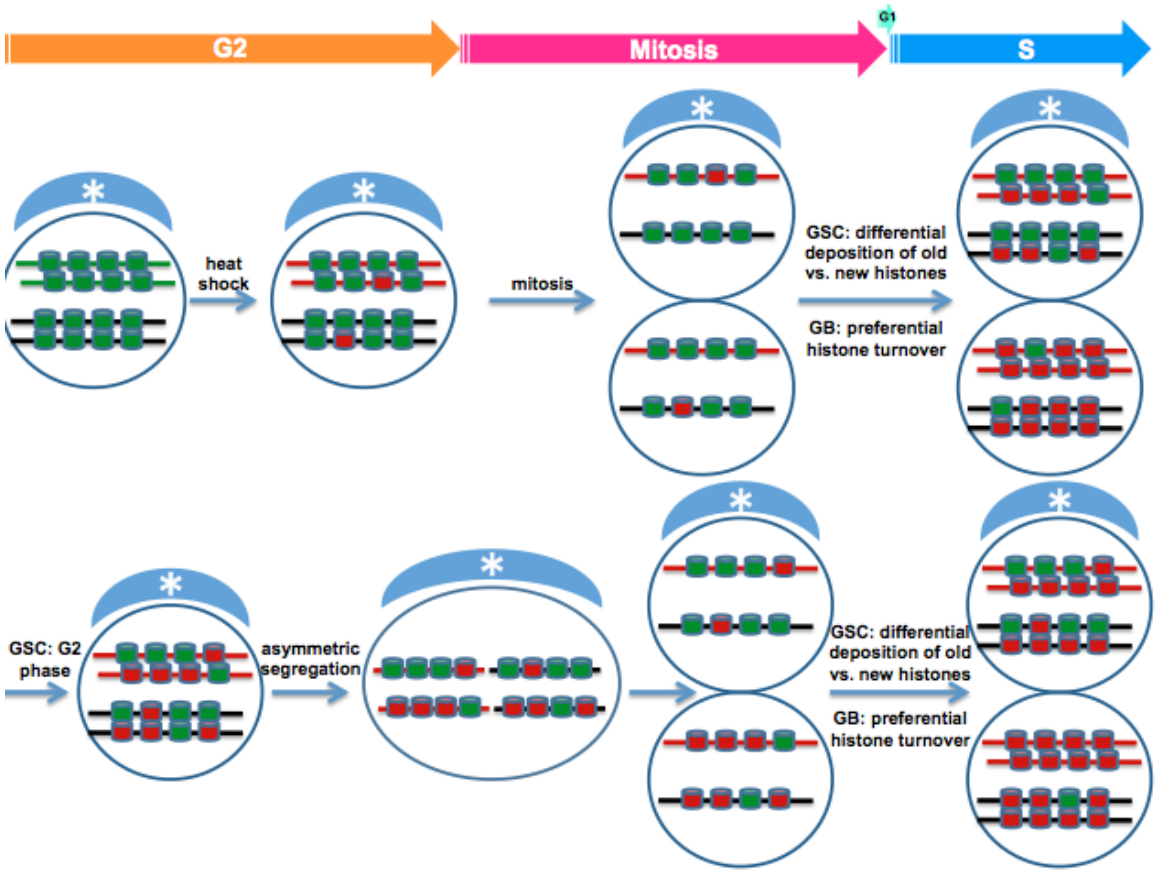

Figure 2-16: A model delineating the patterning of histone segregation in the first and second cell cycle subsequent to heat shock. Data interpretation in the context of GSC cell cycle: each line represents one sister chromatid. Black line = chromosome without transgene; green line = chromosome with transgene (Fig. 2-2) before heat-shock; red line = chromosome with transgene after heat-shock. Green cylinder = nucleosome containing histone-GFP, red cylinder = nucleosome with histone-mKO (canonical histones). Histone turnover in a replication-independent manner (Dion et al, 2007) should not occur globally. For simplicity, nucleosomes with both histone-GFP and histone-mKO, or free histones, are not discussed here.

Table 1: Raw data in 16-20hr chasing experiments after heat shock treatment.

								
#	H3 GSC-GB pair		H3 two-cell gonial		H3 G2 phase		H3.3 GSC-GB pair	
1	GSC	1500.099	Cell 1	1397.613	GSC	1401.806	GSC	285.215
		291.183		330.821				1014.544
	GB	142.511	Cell 2	1387.796		454.398	GB	264.673
		466.943		301.563				825.591
2	GSC	1529.681	Cell 1	1418.267	GSC	1265.373	GSC	196.707
		136.623		417.317				676.726
	GB	319.211	Cell 2	1355.055		409.654	GB	260.726
		585.575		446.387				918.63
3	GSC	435.249	Cell 1	188.7	GSC	517.538	GSC	283.127
		287.555		40.685				770.667
	GB	129.322	Cell 2	236.416		288.972	GB	291.394
		386.614		51.116				724.056
4	GSC	865.323	Cell 1	1151.203	GSC	393.291	GSC	255.564
		365.887		728.587				740.029
	GB	111.639	Cell 2	917.165		714.193	GB	250.216
		851.825		614.398				745.186
5	GSC	942.64	Cell	880.966	GSC	1152.725	GSC	2062.419

	C	535.296	1	861.091				1289.867
	GB	140.525 913.644	Cell 2	595.153 733.017		671.884	GB	2026.555 1190.467
6	GSC GB	928.09 416.658 168.942 897.531	Cell 1 Cell 2	664.26 747.059 622.782 657.118	GSC	1262.267 679.617	GSC GB	912.084 3428.707 782.29 3184.586
7	GSC GB	312.252 248.17 28.58 323.363	Cell 1 Cell 2	480.14 623.93 360.393 566.118	GSC	535.575 93.178	GSC GB	952.056 3772.343 1019.955 3755.15
8	GSC GB	121.038 145.349 23.446 129.898	Cell 1 Cell 2	157.33 171.068 135.381 150.069	GSC	276.904 218.829	GSC GB	3128.038 2667.677 3258.834 2810.174
9	GSC GB	158.333 119.02 48.848 141.182	Cell 1 Cell 2	516.145 359.614 335.694 280.728	GSC	39.134 250.698	GSC GB	1040.175 3812.473 956.841 3833.674
10	GSC GB	180.352 192.303 81.708 891.491	Cell 1 Cell 2	437.637 305.594 396.481 340.233	GSC	649.452 200.867	GSC GB	893.77 3391.099 962.749 3912.301
11	GSC GB	1517.473 703.033 177.875	Cell 1 Cell	729.995 364.953 648.624	GSC	206.963 169.836	GSC GB	946.844 3703.863 798.391

		842.059	2	366.977				3673.802
	GSC	365.388	Cell 1	990.755		238.279	GSC	1013.492
		376.23		281.937				3214.758
	GB	230.469	Cell 2	1171.972			GB	846.325
12		739.583		349.169	GSC	195.984		2395.879
	GSC	621.364	Cell 1	213.948				
		421.954		188.766		1103.981		
	GB	141.598	Cell 2	242.074				
13		519.144		230.611	GSC	686.025		
	GSC	405.951	Cell 1	520.058				
		379.202		404.64		1021.287		
	GB	239.143	Cell 2	560.002				
14		377.236		416.185	GSC	372.79		
			Cell 1	1189.539				
				541.433		287.769		
			Cell 2	1193.312				
15				505.559	GSC	582.587		
			Cell 1	1001.169				
				390.725		196.403		
			Cell 2	1078.839				
16				465.487	GSC	82.243		

Table 1: Fluorescence intensity of H3 GFP and mKO in GSC vs. GB, H3 GFP and mKO in spermatogonia pair, H3 GFP and mKO in G2 GSCs, and H3.3 GFP and mKO in GSC vs. GB, 16-20 hours after heat shock (second cell cycle). Green highlighted data are GFP signal, pink highlighted data are mKO signal. ImageJ.

Table 2: Raw data in 4-6hr chasing experiments after heat shock treatment.

#		H3 GSC-GB pair		H3 two-cell gonial		H3 G2 phase		H3.3 GSC-GB pair
		2224.035		619.872				97.941
	GSC	158.255	Cell 1	771.852		1739.536	GSC	2206.255
		130.344		458.859				112.722
1	GB	416.013	Cell 2	734.225	GSC	99.933	GB	2578.891
		2483.218		123.883				815.022
	GSC	359.261	Cell 1	3012.525		2880.902	GSC	3124.291
		123.707		96.526				960.713
2	GB	1538.096	Cell 2	2651.048	GSC	327.19	GB	3780.433
		61.378		420.982				976.13
	GSC	12.819	Cell 1	861.173		632.338	GSC	3793.243
		2.588		559.676				826.487
3	GB	30.512	Cell 2	870.169	GSC	435.945	GB	3453.721
		1507.757		1111.096				936.795
	GSC	272.196	Cell 1	788.81		1928.43	GSC	3913.044
		98.831		928.897				1133.497
4	GB	843.043	Cell 2	810.529	GSC	245.314	GB	4038.758
		290.853		3524.34				924.133
	GSC	104.439	Cell 1	698.885		955.023	GSC	3698.133
5	GB	55.963	Cell 2	3317.38	GSC	79.693	GB	950.278

		131.534		457.829				3929.375
		524.237		2035.577				1931.467
	GSC	64.787	Cell 1	88.119		1071.436	GSC	1247.392
		80.529		1766.823				1896.342
6	GB	225.956	Cell 2	68.511	GSC	69.562	GB	1186.402
		701.129		2448.66				3089.152
	GSC	82.682	Cell 1	237.496		789.924	GSC	2589.167
		86.618		2469.899				3337.602
7	GB	159.093	Cell 2	234.81	GSC	68.229	GB	2877.842
		932.499		2727.286				3483.646
	GSC	107.458	Cell 1	202.021		729.871	GSC	2161.199
		69.637		2817.974				3389.671
8	GB	133.159	Cell 2	210.216	GSC	95.088	GB	2057.182
		2725.749		3007.404				893.532
	GSC	651.351	Cell 1	323.327		2018.215	GSC	3390.044
		791.951		2940.333				920.61
9	GB	1192.171	Cell 2	349.009	GSC	638.479	GB	3659.989
		2191.801		3535.573				1012.585
	GSC	513.333	Cell 1	512.304		2145.188	GSC	4068.886
		565.407		3586.377				1175.963
10	GB	846.212	Cell 2	588.952	GSC	749.946	GB	4064.611
				2781.275				2547.362
			Cell 1	243.681		2287.577	GSC	3051.526
				2906.644				3224.452
11			Cell 2	274	GSC	102.398	GB	2818.903
								639.407
12							GSC	3329.088

		449.305
	GB	2341.38
		631.352
	GSC	3288.112
		502.314
13	GB	2757.68

Table 2: Fluorescence intensity of H3 GFP and mKO in GSC vs. GB, H3 GFP and mKO in spermatogonia pair, H3 GFP and mKO in G2 GSCs, and H3.3 GFP and mKO in GSC vs. GB, 16-20 hours after heat shock (first cell cycle). Green highlighted data are GFP signal, pink highlighted data are mKO signal. Quantified by ImageJ software.

Chapter 3

Exploring the mechanism for maintaining asymmetric histone segregation in *Drosophila* male germline stem cell

INTRODUCTION

The phenomenon of asymmetric histone segregation provides a compelling glimpse into stem cell biology. It seems inevitable that these results put forth many more questions that need to be answered. There numerous criteria that need to be addressed in order to achieve histone segregation. The first and most inescapable issue is how the cell distinguishes pre-existing versus newly synthesized histones. Afterward, how the mechanism of recognition uses these cues to deposit histones in an asymmetric manner is unknown. Exactly when does this mechanism act is also up for debate. And lastly, it is critical to ask the question of how the mitotic machinery distinguishes these different histones to properly segregate them resulting in proper asymmetry. It is obvious that the degree or organization required for successful segregation is astounding. Even though the biochemistry of histone structure, folding and modifications is extremely well-characterized in the past decades, the model for histone incorporation and histone dynamics in a functioning is surprisingly unknown. In this chapter, we attempt to de-construct the components for the asymmetric histone segregation and establish a working model. Furthermore, we attempt to use new tools and observations to address these pressing questions.

Potential mechanisms contributing to asymmetric histone distribution

The finding of differential segregation of preexisting versus newly synthesized H3 during ACD of GSCs suggests coordinated molecular and cellular events in GSCs. There are two main mechanism that need to take place in order to result in histone asymmetry. First, prior to mitosis, preexisting H3 and newly synthesized H3 have already differentially distributed to the two sets of sister chromatids. Second, during mitosis, the molecular machinery needs to distinguish the set of sister chromatids carrying preexisting H3 from the other set of sisters enriched with newly synthesized H3, followed by partitioning them toward GSCs and GBs, respectively. Here, we will propose and discuss several models to explain this intriguing observation.

The "silent sister chromatid" or "strand-specific imprinting and selective chromatid segregation" (SSIS) model

One explanation of the epigenetic inheritance of stem cells is the "silent sister chromatids" hypothesis (Lansdorp 2007), which holds that sister chromatids carry different epigenetic marks at the centromeric region or at specific genomic loci in stem or progenitor cells. Conceivably there are two different epigenetic marks based on their distinct locations and functions: Nonequivalent centromeric epigenetic marks are required for nonrandom chromatid segregation, while different epigenetic marks at gene-enriched genomic loci regulate differential gene expression. In contrast to self-renewing cells, which selectively inherit chromatids with active expression of "stemness" genes, differentiated daughter cells inherit the chromatids silent for "stemness" genes. Similar to the "silent sister

chromatids" hypothesis, the strand-specific imprinting and selective chromatid segregation (SSIS) model also proposes that epigenetically distinct sister chromatids cosegregate (Klar 1994, 2007. Evidence supporting these two similar models came from experiments that can distinguish sister chromatids. For example, in one study, a genetic manipulation was introduced specifically to mouse chromosome 7, which showed biased sister chromatid segregation pattern in a cell type-specific manner (Armakolas and Klar 2006). Recently, a CO-FISH (chromosome orientation fluorescence in situ hybridization) method was used to distinguish sister chromatids using unidirectional probes specific for centromeric or telomeric repeats and test for silent sister chromatid hypothesis (Falconer et al 2010). Using this method, it was shown that in a subpopulation of adult skeletal stem cells, all sister chromatids segregate asymmetrically with a bias for the parental DNA strand containing ones retained in the stem cells (Rocheteau et al 2012). More recent work in Drosophila male GSC demonstrated that sex chromosomes (X and Y chromosomes), but not autosomes, have biased sister chromatid segregation (Yadlapalli and Yamashita 2013). In all these models discussed above, both centromeres and centrosomes are hypothesized to be asymmetric to achieve the asymmetric segregation pattern (Lansdorp 2007, Lew et al 2008, Tajbakhsh and Gonzalez 2009). Asymmetric centromeres may be established through leading versus lagging strand difference if replication of the centromeric region is biased toward a unidirectional movement of the replication fork, which has been shown in Escherichia coli (White et al 2008). However, no evidence has shown unidirectional movement of replication fork in eukaryotic cells. Alternatively,

asymmetric centromeres may be at the epigenetic level by their unique chromatin structure (Vagnarelli et al 2008, Malik and Henikoff 2009, Verdaasdonk and Bloom 2011). Asymmetric centrosome segregation has been reported in Drosophila male GSCs (Yamashita et al 2007), neuroblasts (Rebollo et al 2007, and mouse neural progenitor cells (Wang et al 2009). To test if asymmetric inheritance of centrosome may be utilized for biased segregation of DNA strands, BrdU was used to label newly synthesized DNA strands in asymmetrically dividing male GSCs; however, the results exhibit random segregation (Yadlapalli et al 2011). Interestingly, in the same system, mutations in a centrosome component Cnn resulted in randomized centrosome segregation (Yamashita et al 2007), as well as randomized sex chromosome segregation (Yadlapalli and Yamashita 2013. However, it remains unclear whether randomized centrosome is the causal reason for the loss of asymmetric sex chromosome segregation. Therefore, the connection between asymmetric centrosome segregation and biased DNA strand or sister chromatid inheritance will await future studies [(Tajbakhsh and Gonzalez 2009) and (Yamashita 2013)].

Replication-dependent differential H3 deposition onto sister chromatids in S-phase GSCs.

As discussed earlier, DNA replication is a highly regulated process, which requires a high degree of cooperation among DNA synthesis, histone synthesis, and incorporation. Because parental H3–H4 tetramer does not dissociate during replication (Seal 1975) and H3 and H4 carry the majority of the known histone modifications (Bannister and Kouzarides 2011), it is possible that H3 and H4 are

responsible for transmitting most of the epigenetic information. On the other hand, H2A–H2B dimer readily dissociates from the octamer at replication forks; therefore, they may not be the major players. This model is supported by the earlier results in Chapter 2 (**Fig. 2-12B and 2-12C**), where H2B does not seem to be asymmetrically segregated, especially at mitosis. While our finding is congruent with the model, the issue of how the H3-H4 tetramers are retained onto one single sister chromatid is yet to be answered.

If the mechanism being used by GSC is indeed replication-dependent, then the most intuitive mechanism to distinguish the sister strands is the leading versus lagging strand at the replication fork. However, there are some problems with this model. Since eukaryotic cells have multiple replication forks during S-phase, the next question is how all replication forks coordinate the deposition of pre-existing histone onto one sister and newly synthesized histones onto the other sister. Furthermore, because a replication fork is bi-directional, histone loading cannot depend on the difference between leading and lagging strands. It has been reported recently that the two sister chromatids of either X or Y chromosome are segregated asymmetrically during GSC division (Yadlapalli et al 2011b, Yadlapalli and Yamashita 2013). However, this asymmetry of sister chromatid segregation does not apply to autosomes (Yadlapalli and Yamashita 2013), suggesting that the preferential partitioning of old H3 into GSCs is not completely dependent on DNA strand difference. We hypothesize that it is epigenetic difference that distinguishes the two sister chromatids during the first S phase after genetic switch, which could be different histone modifications. For example, the H3K27me3 mark generated by

PcG could be recognized by the chromodomain of polycomb protein. Because polycomb group proteins can dimerize (Min et al 2003, Lengsfeld et al 2012, Lo et al 2012) and directly interact with PCNA at the replication fork (Petruk et al 2012), it is possible that, through dimerization, polycomb coordinates preferential retention of preexisting H3–H4 tetramers carrying the H3K27me3 mark onto one sister chromatid at the replication fork (**Fig. 3-1**). Epigenetic marks on preexisting histones may contribute to maintain unique gene expression pattern in stem cells. Although H3K27me3 was not detected at replication forks in Drosophila embryos, it is possible that this phenomenon is different in stem cells because embryonic cells have a fast cell cycle and undergo symmetric cell divisions.

Replication-independent differential H3 turnover at sister chromatids in G2 phase GSCs

Another model that may contribute to this asymmetric histone distribution pattern relies on replication-independent histone turnover. In this model, old and new H3 are incorporated randomly onto sister chromatids during S phase. However, during the subsequent elongated G2 phase (**Fig. 3-2A**), new histones replace old ones in a sister chromatid-specific manner (**Fig. 3B**). As discussed previously, nucleosomes undergo dynamic turnover at actively transcribed regions or regulatory elements, and either histone variants such as H3.3 (Mito et al 2007, Deal et al 2010) or newly synthesized H3 (Dion et al 2007) could replace preexisting H3. In this context, it is possible that sister chromatids have different chromatin states, leading to higher transcriptional activity and faster histone turnover of one sister chromatid compared with another one. This difference could then result in differential

distribution of old versus new histones toward the end of G2 phase. This active replacement mechanism is especially appealing since the Drosophila male GSC spend most time in G2 phase[9–10 hr out of a 12-hr cycle (Yamashita et al 2003, 2007, Cheng et al 2008, Sheng and Matunis 2011, Yadlapalli et al 2011a)]. The prolonged G2 may give the chromatin remodeler sufficient time to establish sister chromatid asymmetry through regulation of histone turnover. We observed a higher ratio of preexisting H3 in GSC compared with GB in the first cell cycle compared with the second one (**Fig. 2-5A and 2-11A**), suggesting that random incorporation of preexisting histones onto the two sister chromatids during S phase, followed by sister chromatid-specific turnover in G2 phase, could be involved. Asymmetric chromatin states between homologous chromosomes have been shown for X inactivation, which requires long noncoding RNAs, such as Xist, to silence one X chromosome in female mammalian cells (Borsani et al 1991). Although it is unclear how different chromatin states between two sister chromatids are determined, one possible mechanism is through noncoding RNAs (Bernstein and Allis 2005, Tajbakhsh and Gonzalez 2009, Bonasio et al 2010, Rinn and Chang 2012). For example, one sister chromatid could transcribe a Xist-like non-coding RNA, which could then recruit PcG to generate the H3K27me3 mark to spread the silencing effect (Zhao et al 2008). Subsequently, different transcriptional activity between two sister chromatids could be established, and the sister chromatid without PcG-mediated repression would be more transcriptionally active, resulting in a higher rate of histone turnover. In addition to long non-coding RNAs, RNAi machinery that normally produces small non-coding RNAs has also been shown to

establish heterochromatin in fission yeast, suggesting an intimate interplay between noncoding RNAs and chromatin structure (Bayne et al 2010). Another example of different chromatin states between homologous chromosomes comes from studies of allelic exclusion, which result in one active allele and one silent allele. This could happen at the transcriptional level such as imprinting due to differential DNA methylation (Ferguson-Smith 2011) or at the post-transcriptional level, which results in removal of protein product of one allele (Mostoslavsky et al 2004).

The differential S-phase deposition model and G2-phase turnover model are not mutually exclusive. It is also possible that the asymmetry between two sister chromatids are established at some, but not all, genomic regions during S phase. For example, it was hypothesized that different nucleosomal density exists at particular gene loci due to asymmetric distribution of PCNA and histone chaperones between leading and lagging strands (Shibahara and Stillman 1999). Different nucleosomal density can lead to differential gene expression (Nakano et al 2011) or directly affect histone-modifying enzymes, such as PcG activity (Yuan et al 2012b). Such an asymmetry could be subsequently expanded to the major, if not entire, chromosomal region during G2 phase, which would lead to a genome-wide epigenetic difference between two sets of sister chromatids prior to mitosis. Future studies to determine the timing and to identify such epigenetic differences between sister chromatids will undoubtedly shed light on the cellular and molecular mechanisms underlying asymmetric histone inheritance during ACD of Drosophila male GSCs.

Mitotic machinery asymmetrically segregates sister chromatids in M phase GSCs

If preexisting H3 and newly synthesized H3 are differentially distributed at two sets of sister chromatids prior to mitosis, the next question is how they are recognized by the mitotic machinery in GSC (**Fig. 3-3**). According to the silent sister chromatid hypothesis, different epigenetic marks at centromeric region of the sister chromatids could establish their attachment to a polarized mitotic spindle.

In Drosophila S2 cells, CENP-A homolog called CID is recruited to centromeric region at metaphase (Mellone et al 2011), which is interspersed with nucleosomes containing canonical H3 (Blower et al 2002). In Drosophila embryos, CENP-A is found to be incorporated into centromeres at anaphase (Schuh et al 2007). However, the timing of CENP-A incorporation in male GSCs is unknown. If it happens at metaphase in a sister chromatid-specific manner, it may contribute to the asymmetric segregation of H3 in male GSCs. In addition to CENP-A, centromeric chromatin has a unique histone modification pattern, which may be responsible for their specific functions during mitosis (Sullivan and Karpen 2004, Vagnarelli et al 2008). For example, the H3K4me2 mark at centromeric region is required for kinetochore assembly at centromeres (Sullivan and Karpen 2004, Bergmann et al 2011). Kinetochore is the protein structure on chromatids whereby the spindle fibers attach to pull sister chromatids apart. Kinetochore facilitates interaction between centromeric chromatin and dynamic microtubules. Components of the yeast kinetochore were reported to divide asymmetrically (Thorpe et al 2009). However, it is unclear whether asymmetric kinetochores also

exist in higher eukaryotes. Interestingly, kinetochore-associated kinesin-7 was reported to regulate sequential congression of chromosomes to the equator in mammalian cells, which may allow temporal difference for mitotic spindle to anchor different sister chromatids (Kapoor et al 2006). In Drosophila male GSCs, the mother centrosome was reported to have higher microtubule-organizing center activity (Yamashita et al 2007). It is possible that microtubules emanating from the mother centrosome anchor preexisting H3-enriched sister chromatids, possibly through regulation by asymmetric kinetochore, CENP-A, or other epigenetic marks at the centromeric region (**Fig. 3-3**). Remarkably, a recent study in male GSCs revealed that sister chromatids from homologous autosome co-segregate even though there is no strand preference (Yadlapalli and Yamashita 2013). If the asymmetry between preexisting and newly synthesized H3 on sister chromatids has already been established prior to mitosis (**Figs. 3-2 and 3-3**), co-segregation of sister chromatids from homologous autosomes (~80 % of genome) could greatly facilitate the asymmetric segregation of H3 during mitosis. Motor proteins like Dynein may also contribute to asymmetric chromatid segregation (Armakolas and Klar 2007).

MATERIALS AND METHODS

Proximity ligation assay (PLA)

The biology of the *Drosophila* male germline limits the use of biochemical tools. Since there are only 10-12 GSCs per testis, it is not feasible to obtain enough starting material for immunoprecipitation or binding assays. To address this issue, we are using proximity ligation assay (PLA) as a viable alternative to biochemistry. PLA takes advantage of the pre-existing immunohistochemistry assays to identify potential interaction between two known substrate. Using primary antibodies against substrate 1 and substrate 2, the PLA kit (CAT #) uses secondary antibody PLA probes to target the primary antibody. The secondary antibody is conjugated to a specific sequence of oligonucleotide. If the secondary antibodies are close enough in proximity [~40 nm (Fredriksson et al 2002)] then the oligonucleotide should ligate and a color-metric rolling circle amplification assay will indicate this close proximity between two substrates.

Bessel beam microscopy

Using confocal microscopy, we were able to make the initial observations in Chapter 2. However, the quality of confocal microscopy is limited in terms of resolution and signal to noise ratio. The ideal method would allow us to capture the dynamics of histone patterning in GSC. One of the methods we choose to explore is Bessel beam microscopy system. This microscopy system is a fast, sensitive method to generate a clean 3 dimensional image of thick tissues, especially in live samples (Pastrana, 2013, Planchon et al 2011). Through collaboration with Eric Betzig's lab,

we are able to generate relevant data to address our questions. *Drosophila* testes are fixed, stained and whole-mounted onto the Bessel system for imaging. The Bessel beam can image stacks of ~200 sections at 0.4 microns in the z dimension. This allows us to view GSCs at a much higher resolution than in previous experiments.

Photoactivated Localization Microscopy (PALM)

Although the Bessel plane super-resolution microscopy is fast and efficient, it is still limited by the physics of fluorescence molecules. Any form of fluorescence microscopy has a lower limit of half the wavelength of the fluorescence channel. We chose to use an additional super-resolution method to address our question. Photoactivated localization microscopy (PALM) can achieve resolution as small as 25 nanometers using fluorescence microscopy (Betzig et al 2006). The underlying principle of this method addresses the issue of fluorescent wavelengths being greater than the size of the actual fluorescence molecules. By excitation of only a small subset of these fluorescence molecules, the fluorescence concentration will be low. By isolating each of these fluorescence with a known minimal size, processing each molecule based on the point-spread-function of each one, the actual localization of each molecule can be achieved. By taking streams of multiple exposures of the same image, we can obtain thousands of fluorescent molecule to process and compile into a single image. Our collaboration with Jie Xiao's lab allows us to achieve this level of resolution of histone localization in GSCs, especially during S-phase. Processing of the image can be seen in **Fig. 3-9.** While the system

previously described in Chapter 2 uses GFP and mKO in the dual color switch, PALM requires fluorescent molecules that can be permanently switch off in order for successful processing and resolving the <50-nanometer resolution. So, we use photoactivated DronPA and mCherry as alternatives to GFP and mKO, respectively. The UAS-FRT-H3-DronPA-FRT-H3-mCherry is similarly crossed to the hsflp; nos-GAL4 to achieve the same spatial and temporal controls.

RESULTS

Proximity ligation assay suggests pre-existing histone is retained in the replication fork

Replication-dependent histone deposition is a highly regulated process and requires an orchestrated series of events, including disruption and recycling of preexisting histone octamers, as well as deposition of newly synthesized histones at the replication fork (Corpet and Almouzni 2009). Incorporation of newly synthesized histones is facilitated by chromatin remodeling complexes (Saha et al 2006), histone chaperones such as ASF1 and CAF-1 (De Koning et al 2007), and histone-modifying enzymes (Corpet and Almouzni 2009). However, despite increasing knowledge on incorporation of newly synthesized histones during DNA replication, our understanding about whether and how preexisting histones are recycled at replication forks is limited. We hypothesize that preexisting histones are not completely released at the replication fork, enabling a quick and efficient re-incorporation. Therefore we used PLA as an initial screen method to examine potential interactions between candidate DNA replication machinery components (or other proteins known to be at replication fork) and different histones. Because preexisting histones presumably carry important post-translational modifications, we investigated potential interactions between candidate replication fork-associated proteins and modified histones. During replication, DNA helicase MCM2 is required to unwind double-strand DNA and remove histones from the nucleosomal structure temporarily. Recent *in vitro* biochemical assays have shown that facilitates chromatin transcription (FACT) complex components binds to both

DNA helicase and histones (Foltman et al 2013), which may provide a bridge to retain preexisting histones at the replication forks (**Fig. 3-2B**). In addition, it was shown that PcG remains at the DNA replication forks *in vitro* (Francis et al 2009, Francis 2009, Francis 2009) and interactions between two different PcG complexes through dimerization can prevent their dissociation from chromatin during DNA replication (Lengsfeld et al 2012, Lo et al 2012, Fig. 3-1). A recent *in vivo* study showed that PcG binds to newly synthesized DNA at their response elements and associates with PCNA in *Drosophila* embryos(Petruk et al 2012). Therefore, FACT and PcG complex components are most likely to contribute to retaining preexisting histones at close proximity to replication fork. It is also known that histone chaperones, such as ASF1 and CAF1, interact with both newly synthesized histones and the PCNA processivity factor for DNA polymerase. Therefore these histone chaperones may coordinate deposition of newly synthesized histones with preexisting histones at the replication fork.

Assuming that the replication-dependent model is viable, regardless of what the exact mechanism for retention of pre-existing histone is, the end result should be that these histones remain sequestered by the replication fork. Previous PLA experiments in *Drosophila* show that modified histones are not retained during replication of embryos (Petruk et al 2012). This is probably due to the fact that the cell cycle happens too quickly in early embryos. However, when the same PLA assays are applied to *Drosophila* testis, we see that pre-existing histones potentially interacts with PCNA, a component of the replication machinery (**Fig. 3-4**). In this PLA experiment, H3K27me3 is representative of pre-existing histone, since newly

synthesized histones being incorporated into the replication fork should not carry this mark. This result suggests that it is likely that pre-existing histones are retained in the replication fork. While this is not in direct support of the replication-dependent asymmetric histone segregation model, it also does not contradict it.

Bessel beam microscopy supports the replication-dependent asymmetric histone segregation model

According to the replication-dependent histone deposition model, the bulk of canonical histone is deposited during S-phase. In accordance to this model, histone segregation should be visible during S-phase. In order to address this claim, we used Bessel beam microscopy to visualize the GSC carrying the same transgene for H3 dual-switch of GFP and mKO as described previously in Chapter 2. Using the same criteria to identify GSC, we observe asymmetrically segregated histone, with pre-existing histones being retained in the GSC (**Fig. 3-5**). Use of the Bessel beam resolution reveals the sub-nuclear patterning of the replicating GSC. Our initial observations saw that these cells have puncta patterns for both pre-existing (GFP) and newly synthesized pattern (mKO). We propose that these puncta are newly replicated regions. More importantly, the pattern between puncta of pre-existing and newly synthesized histones do not overlap. This is critical, because if these two histone species are randomly segregated between the two replicated strands of sister chromatids, then there should be a high degree of overlap between GFP and mKO because the two sister strands should carry both types of histones. This segregation of histone signal in replicating GSCs are not indicative of replication

fork, but rather a representation of newly synthesized regions. Since histone segregation patterning is clearly seen during S-phase, this evidence is in support of the replication-dependent histone segregation model. In addition to our observations of S-phase GSCs, we also looked at S-phase gonialblast (GB) with similar puncta signaling (**Fig 3-6**). Patterning of histones in GB show a higher degree of overlap between pre-existing and newly synthesized histones. This suggests that the replication-dependent segregation model may not apply to differentiating cell and is exclusive reserved for GSCs. Furthermore, when we observe the patterning of non-canonical H3.3 the puncta are not as obvious and we do not see the same patterning of segregation (**Fig 3-7**). This is probably due to the fact that H3.3 itself is not typically incorporated during DNA replication. These results show support the replication-dependent replication model.

Indeed the Bessel plane microscopy system is effective in resolving the finer structures, allowing for easy identification of histone patterning in various cell cycle stages. Even during the metaphase stage of mitosis, clear separation of condensed sister chromatids containing separated pre-existing and newly synthesized histones can be seen (**Fig**. **3-8**). Despite the clear signaling from the Bessel plane system, it is still necessary to definitively determine the replication-dependent histone deposition. Since the lower limit of Bessel resolution is 250-300 nm, we cannot directly resolve a true replication fork using this system, because the average diameter of replication forks in eukaryotic cells is approximately 150 - 400 nm (Leonhardt et al 1992, Leonhardt et al 2000, Murti et al 1996, Cseresnyes et al 2009.)

Photoactivated localization microscopy supports the replication-dependent asymmetric histone segregation model

In order to further explore the findings of the Bessel plane system, it is necessary to achieve better super-resolution. We turn to PALM microscopy for further analysis. Our finding showed that both transgenes were expressed and that H3-Dronpa and H3-PAmcherry could be clearly visualized at a resolution of ~40 nm (**Fig. 3-10)**. Interestingly, the punctate structure previously observed with the Bessel beam microscope was recapitulated. Furthermore, the H3-Dronpa and H3-PAmcherry signals were adjacent but not overlapping, consistent with our hypothesis. While these results are promising, there are a few caveats. First, we could only determine a cell to be GSCs due to the morphology and location at the testis tip. Second, we cannot definitively say that this GSC is undergoing S-phase due to the α–spectrin marker as we've done in previous experiments. This is due to the sensitivity of the PALM system limiting the use of additional fluorescent marker staining. Despite these setbacks, the PALM offers two critical pieces of evidence in support of our hypothesis. First, the recapitulation of the Bessel plan system results reduces the possibility of artifacts inherent in each system of microscopy. Second, the uses of the GFP/mKO versus the DronPA/mCherry tags eliminate the possibility of artifacts inherent in the fluorescent molecules.

Pre-existing and newly synthesized histones are transiently phosphorylated during mitosis in a processive manner to facilitate proper asymmetric sister

chromosome segregation

At this point, we have gathered evidence of histones asymmetric segregation establishment prior to mitosis, specifically in during S-phase. Even so, this segregation still requires proper recognition and sorting of sister chromatids in order to sequester the same of sisters with pre-existing histone to be retained in GSCs and the other set of sisters containing newly synthesized histones to be segregated to the GB. We speculate his mechanism would most likely rely on the fact that pre-existing histone contains specific modification that newly synthesized histones do not have. But the end result would be different identities for different sister chromatid sets. More importantly, this differential parity between sisters should manifest during mitosis, where spindle attachment to sister chromatids are regulated. Different histone modifications at centromeric region of sister chromatids could establish their differential attachment to a polarized mitotic spindle, as hypothesized by the "silent sister chromatid" hypothesis (Landsdorp 2007). It is known that the phosphorylated histone at threonine 3 (H3T3P) is enriched at centromeres of mitotic chromosomes (Wang et al 2010, Inaba et al 2011, Kelly et al 2010). And asymmetric centrosome segregation has been reported in *Drosophila* male GSCs (Yamashita et al 2007), which may contribute to a polarized mitotic spindle. Interestingly, we found that pre-existing histone H3 (GFP) and newly synthesized histone (mKO) signals were already differentially localized in prometaphase GSC (**Fig. 3-11**). At the same time, the H3T3P signal is strongly associated with H3-GFP during chromosomal compaction (**Fig. 3-11**). We analyze these metaphase cells based on DNA morphology of DAPI staining and PH3 antibody

staining. And even more compelling, we also observe that H3T3P signal also associates with H3-mKO but not after condensation (**Fig. 3-12**). In fact, H3T3P signal does not associate with H3-mKO signal until after condensation of H3-GFP-enriched chromatids. By contrast, such a temporal order of H3T3P was not observed in mitotic GB or spermatogonial cells, which undergo symmetric cell divisions **(Fig. 3-13)**. Moreover, the pre-existing and newly synthesized histones are not have differentially localized as is in the GSCs. Based on these results, we propose that the H3T3P mark could distinguish sister chromatids enriched with either preexisting or newly synthesized H3 and regulate their condensation in a temporally-controlled manner exclusively in the male GSCs.

DISCUSSION

The primary purpose of this chapter is to propose viable models to explain the phenomenon of asymmetric histone segregation discovered in Chapter 2. Although the nature of histone folding, modification, are incorporation are known, there are large gaps in the literature about histone regulation, especially in histone dynamics. Given what is known in the mechanism of histone dynamics, it is possible to propose two viable models: a replication-dependent asymmetric histone segregation and a replication independent model that relies on differential turnover between a set of two sister chromatids. Furthermore, the aftermath of this asymmetric segregation still relies on proper mitotic segregation of the two sisters to achieve the proper patterning in the GSC we observed in S-phase. By using what is known in the literature, we can make reasonable conjecture on what is happening.

In addition to proposing viable working models, we also attempt to perform experiments to test these models. The results obtained from the Bessel beam and the PALM systems appear to support the replication-dependent asymmetric histone segregation model. Although we do not have any evidence to support replication-independent model, this does not necessarily invalidate it. It will take more time and different sets of biological tools to full explore this model. Furthermore, the two models are not necessarily mutually exclusive. In fact, the replication-dependent model may not establish complete histone asymmetry, but rather partial asymmetry. And it is also likely that they work in tandem to achieve an asymmetric histone pattern. Regarding the mitotic mechanism that contributes to the asymmetric histone segregation, we have very convincing evidence that differential

phosphorylation very important. But by this time in the cell cycle, we propose that the asymmetry is already establish and the mitotic machinery is merely following these established epigenetic cues. Yet, this piece of evidence is critical because it supports the asymmetry of these histones without any possible artifacts.

While the evidence in this chapter is only preliminary, it opens up the possibility of an active epigenetic mechanism that contributes to stem cell identity. And solving this mechanism will change the current paradigm in the fields of histone epigenetic, stem cell biology and DNA replication. Even more important, unpublished evidence in the lab suggests that loss of this segregation mechanism may adversely effect both germline stem cell identity and the differentiating germ cells.

FIGURES AND TABLES

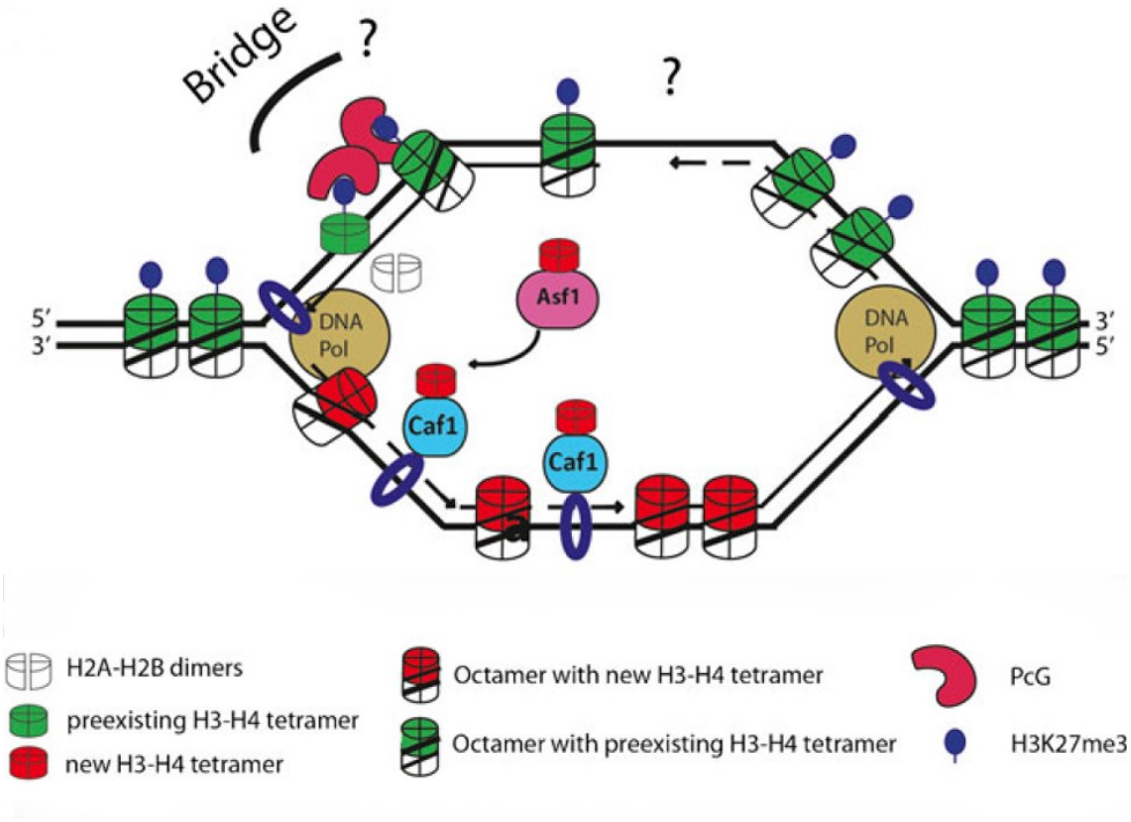

Figure 3-1. Replication-dependent histone deposition model. H3–H4 tetramers are retained and loaded in a chromatid-specific manner at the replication fork. PcG binds specifically to old histone H3 that carries the H3K27me3 mark. PcG–PcG dimerization could bridge two H3–H4 tetramers to ensure their incorporation into the same sister chromatid. For simplicity, only one H3K27me3-Pc-Pc- H3K27me3 is shown here

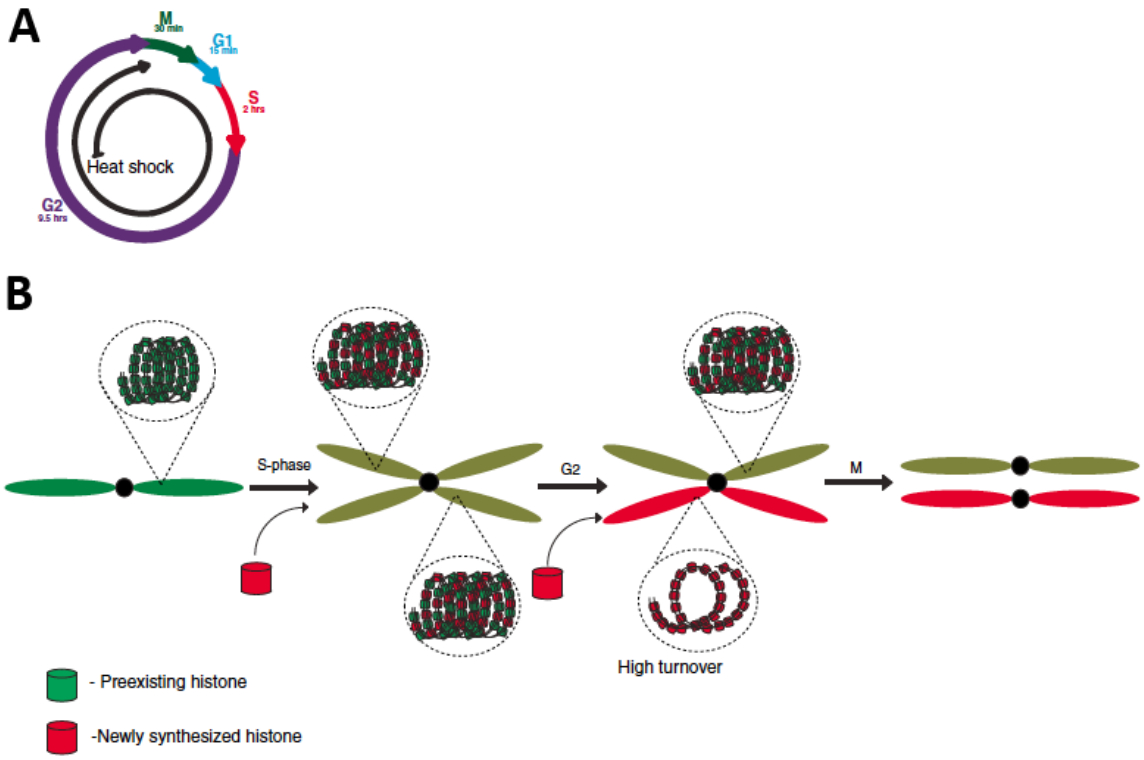

Figure 3-2. Replication-independent histone turnover model.

A) Cell cycle information: The second G2 phase after genetic switch is discussed here. B) Asymmetry between sister chromatids could be established in G2 phase, when one sister has a higher turnover of old H3 and allows more incorporation of newly synthesized H3. For simplicity, only one pair of sister chromatids are shown.

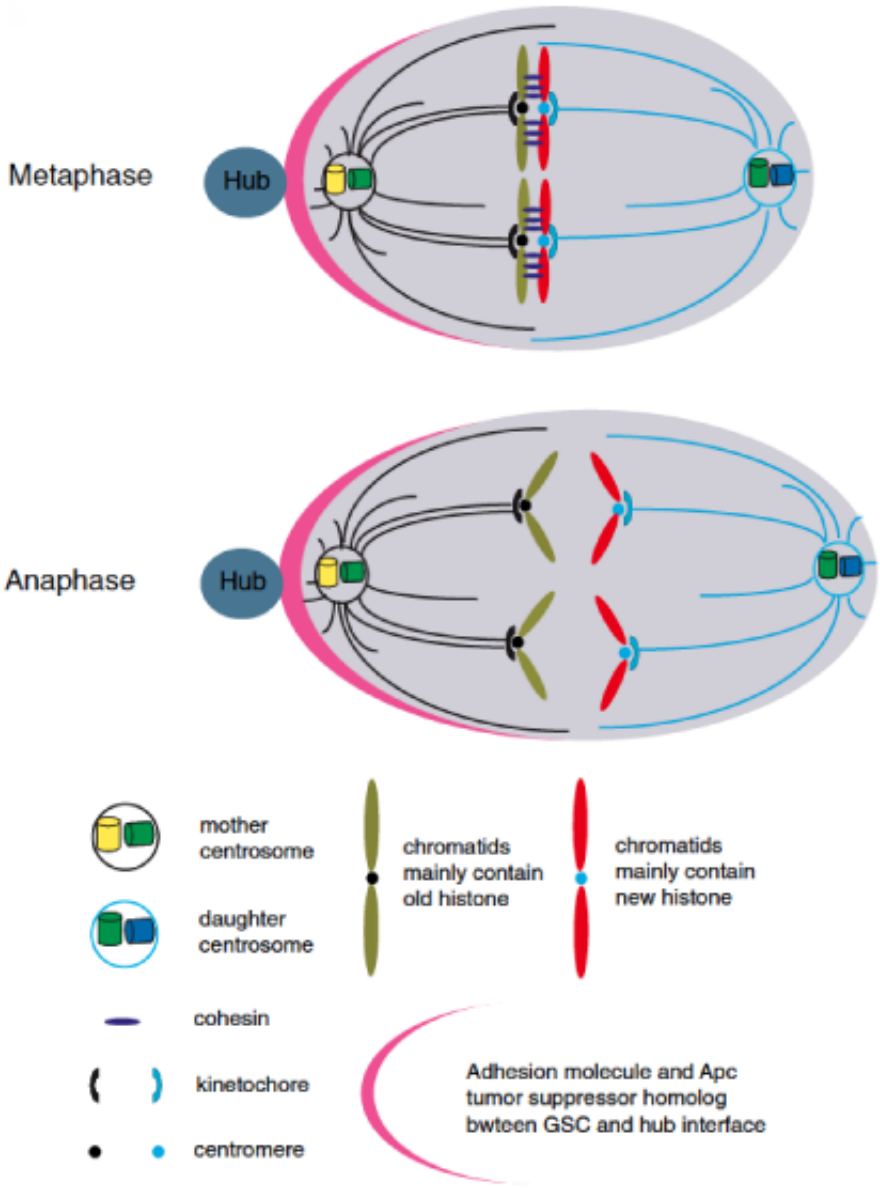

Figure 3-3. Asymmetric segregation of sister chromatids carrying different sets of histones. At metaphase, microtubules from mother centrosome attach to sister chromatids enriched with old H3 through unknown epigenetic marks at the centromeric region and, possibly, the asymmetric kinetochore structure. Two pairs of sister chromatids from homologous autosomes are shown here. Co-segregation of sister chromatids from homologous autosomes greatly facilitates asymmetric H3 segregation in anaphase GSCs

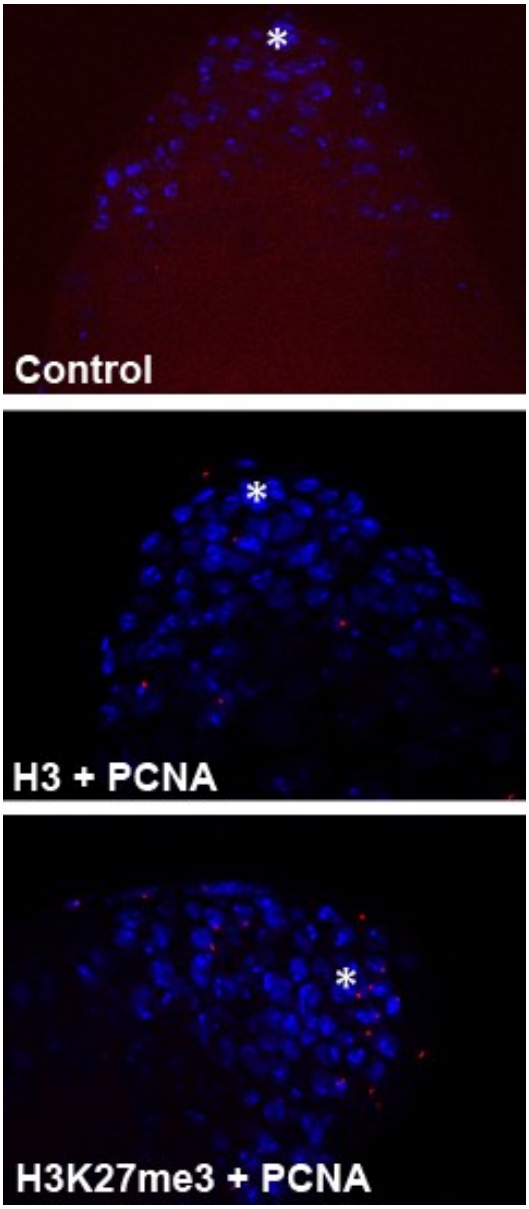

Figure 3-4. Proximity ligation assay (PLA) indicates 'pre-existing' histones potentially interacts with replication machinery. Control = no primary antibody, H3+PCNA = using H3 (rabbit) and PCNA (mouse) primary antibody, H3K27me3+PCNA = using H3K27me3 (rabbit) and PCNA (mouse) primary antibody**.** Blue = DAPI DNA dye, Red = PLA color reaction, indicating ligation and amplification between two substrates.

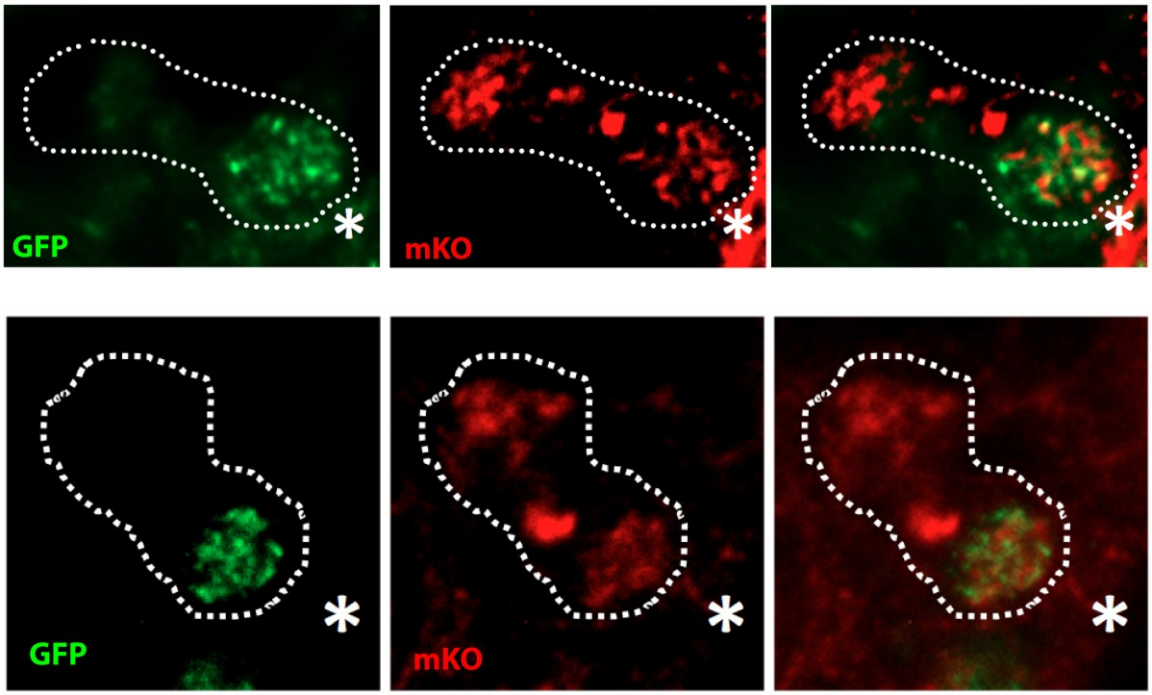

Figure 3-5. : A snapshot of S-phase GSC captured using Bessel beam microscope showed punctate H3-GFP (green) and H3-mKO (red). Asterisk: hub region. Highlighted pairs delineate GSC and GB, with GSCs adjacent to the hub.

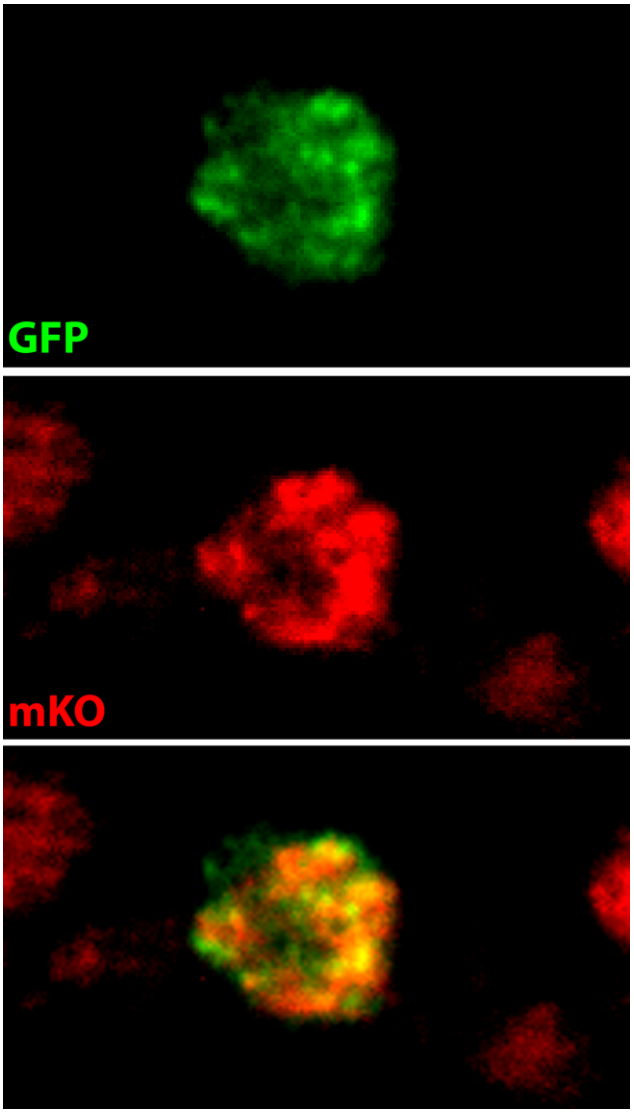

Figure 3-6. A snapshot of gonialblast (GB) germ cell undergoing S-phase using the Bessel beam system. Morphology of GB undergoing S-phase is indicated by both GFP and mKO puncta (punctas are newly replicated regions). This GB demonstrates a high degree of overlap of GFP and mKO of newly replicated regions.

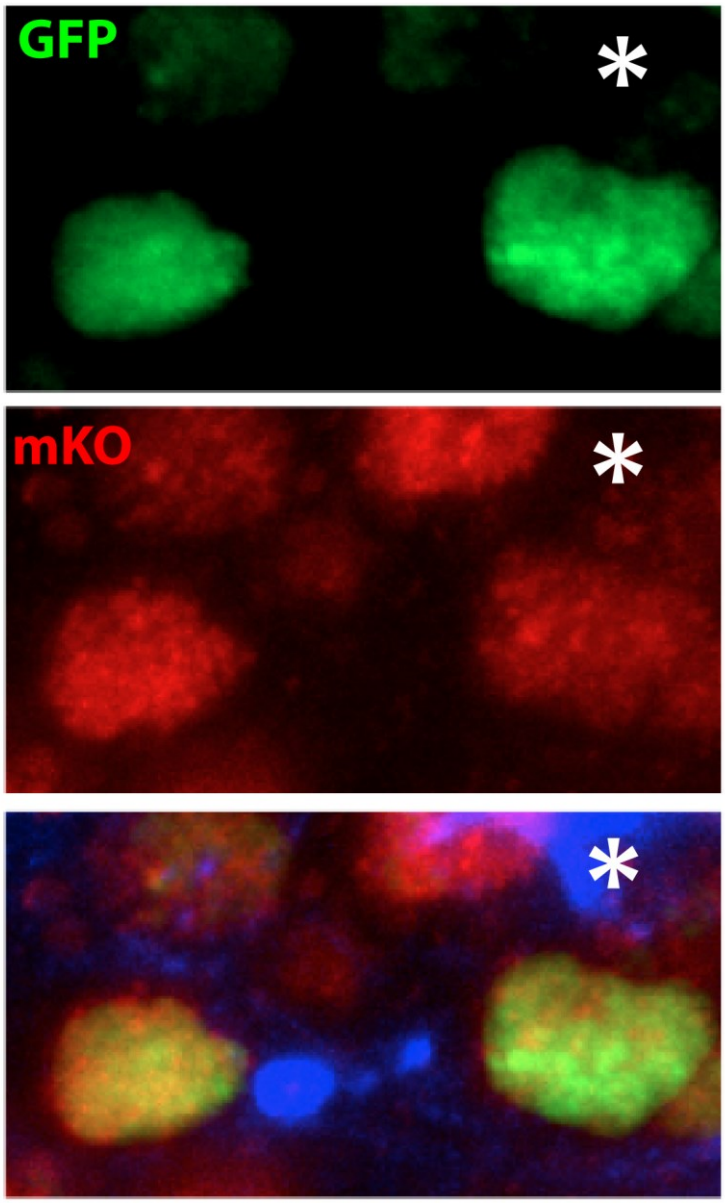

Figure 3-7. A snapshot of S-phase GSC captured using Bessel beam microscope showed punctate H3.3-GFP (green) and H3.3-mKO (red). Spectrosome and hub is indicated in blue**.** Asterisk: hub region. Highlighted pairs delineate GSC and GB, with GSCs adjacent to the hub. Puncta are not as clearly present due to the replication-independent incorporation nature of H3.3 histone variant.

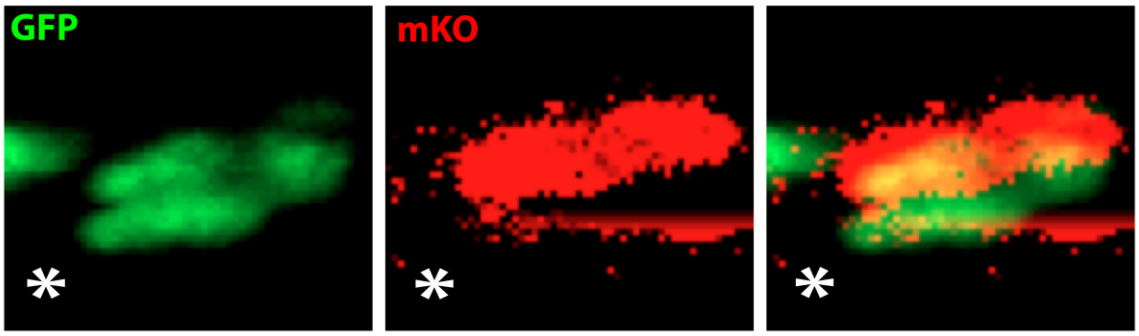

Figure 3-8. Bessel beam system identifies GSC in metaphase. DNA condensation is clearly shown with sister chromatid pairs aligned during metaphase. Differential localization of pre-existing histone (GFP) and newly synthesized histones (mKO) are clearly seen.

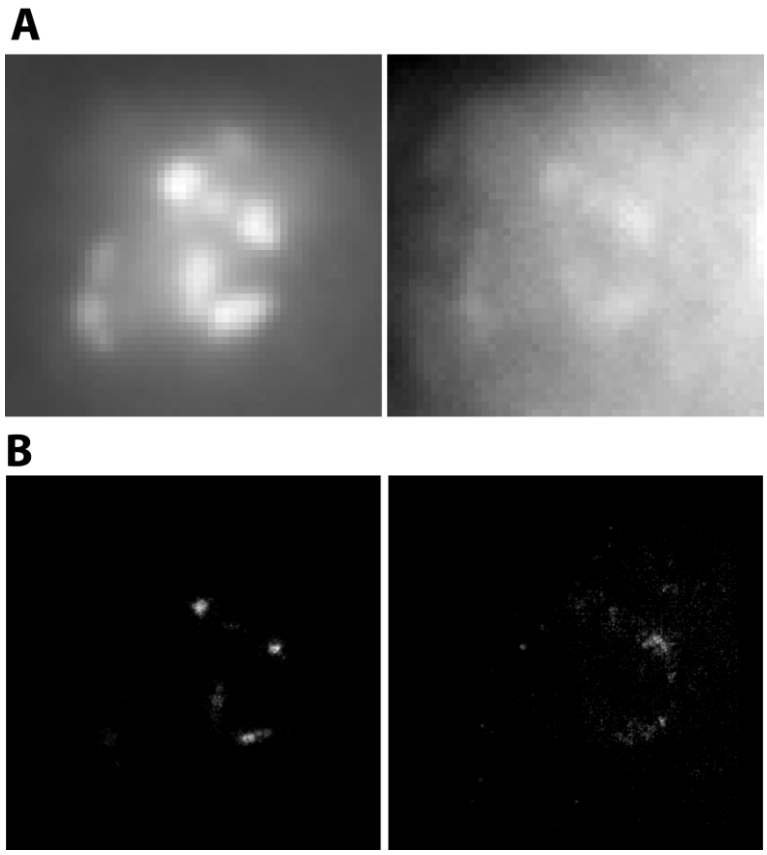

Figure 3-9. Raw data obtained from PALM processing yields true localization of pre-existing histone (H3-DronPA, left) and newly synthesized histone (H3-PAmCherry, right) A) compilation of PALM streaming before processing B) compilation of PALM after processing.

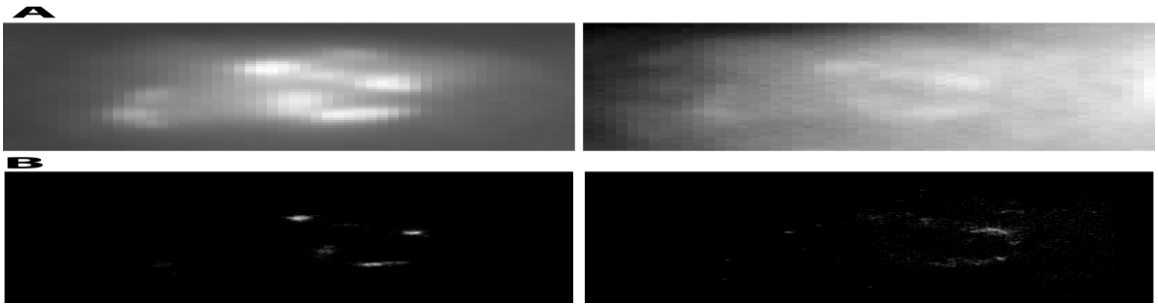

Figure 3-10. Pre-existing and newly synthesized histones show segregation as early as S-phase. An image of H3-Dronpa (green) and H3-PAmcherry (red) visualized using PALM**.** Outlined is a GSC nucleus, ens: ensemble images, compiled from PALM stream**. "**PALM, zoom" image (far right) is isolated from highlighted region of PALM (middle right). (Single GSC is isolated from larger PALM image streams).

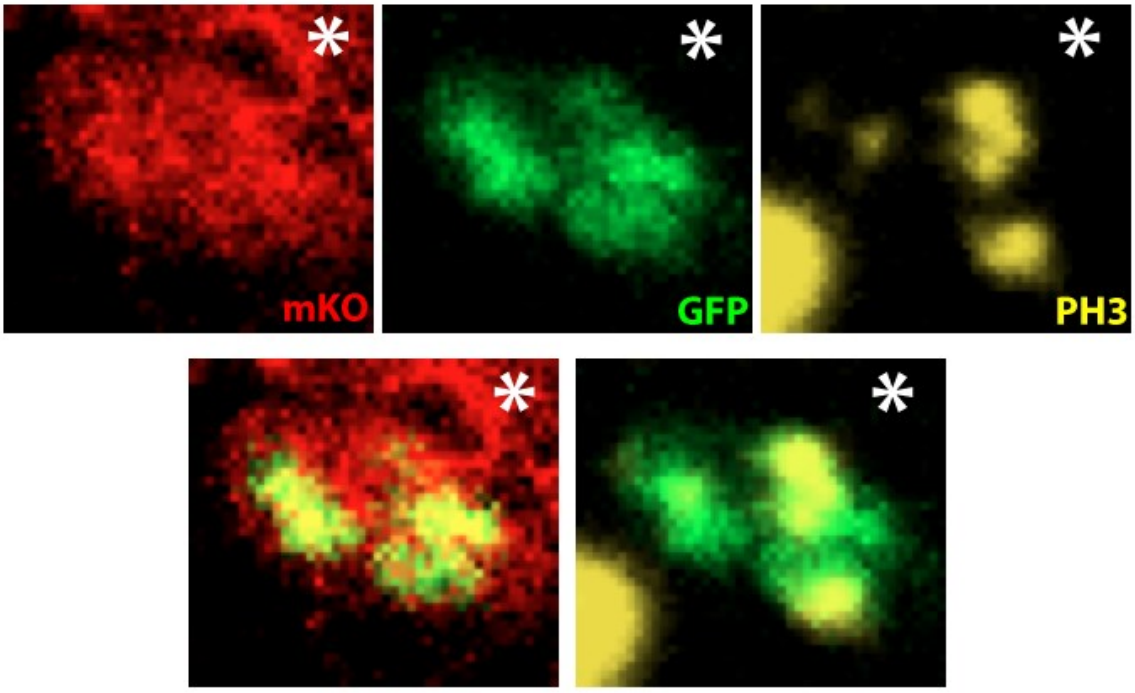

Figure 3-11. Prometaphase GSC indicates differential localization of pre-existing histone (GFP) and newly synthesized histone (mKO) with phosphorylation preferentially localized to pre-existing histone. Asterisk indicates hub. Pre-existing histone show signs of condensation, overlapped by phosphorylation at H3 threonine 3 (PH3). Newly synthesized histones do not show signs of condensation.

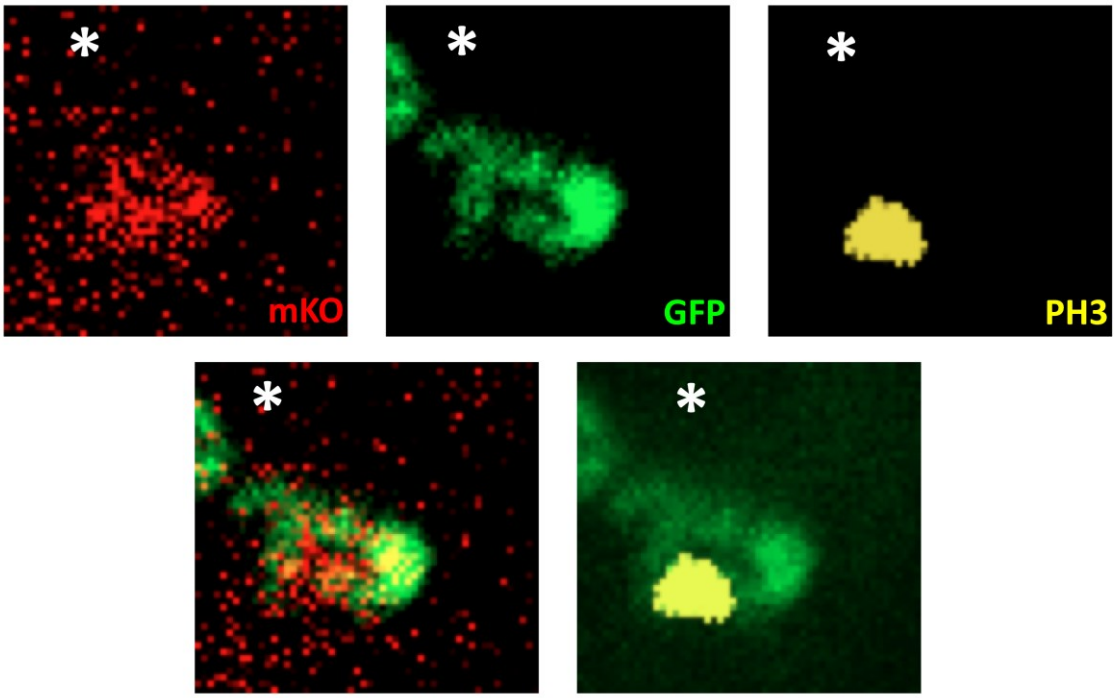

Figure 3-12. Prometaphase GSC indicates differential localization of pre-existing histone (GFP) and newly synthesized histone (mKO) with phosphorylation preferentially localized to newly synthesized histone. Asterisk indicates hub. Pre-existing histone show signs of condensation, but phosphorylation at H3 threonine 3 (PH3) signal is overlapped by mKO. Newly synthesized histones do not show signs of condensation yet.

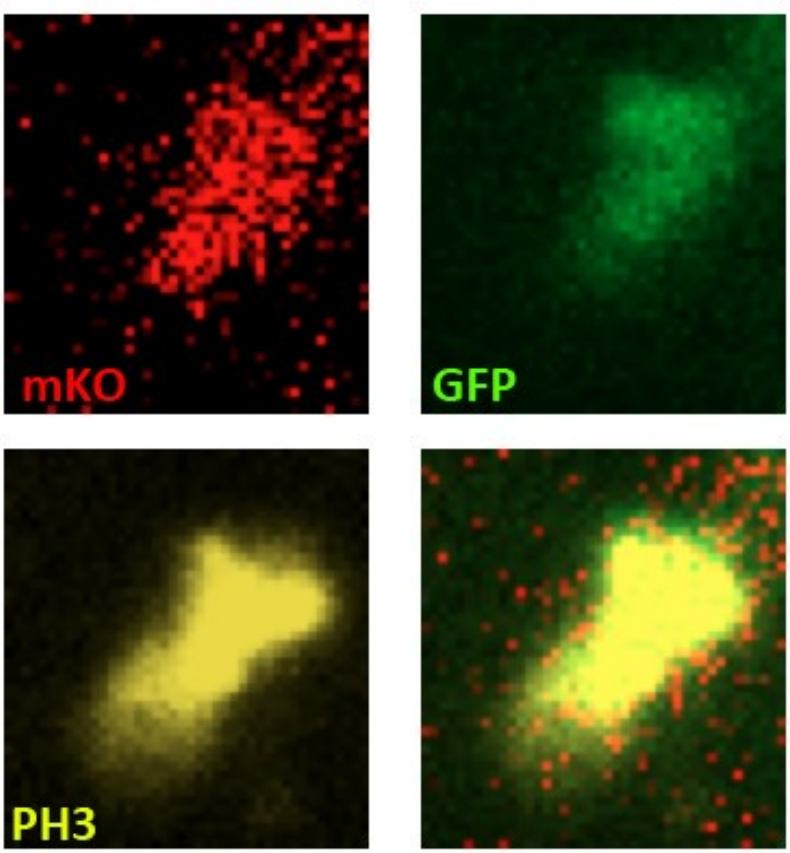

Figure 3-13. Prometaphase gonialblast (GB) indicates completely co-localized signals between pre-existing histone (GFP) and newly synthesized histone (mKO). Phosphorylation at H3 threonine 3 (PH3) is not preferential between pre-existing and newly synthesized histone.

Chapter 4

Epigenome analysis of differentiating germ cells at distinct stages of *Drosophila* spermatogenesis

INTRODUCTION

In earlier Chapters 2 and 3, we demonstrate how histones are retained in GSCs, which is presumed to be critical for maintenance of stem cell identity. This is because pre-existing histones carry the necessary marks to regulate gene expression. In this chapter, we will explore how specific histone modifications marks are organized and regulated in order to maintain and change cell identity in the later stages of *Drosophila* male germ cell development. As previously noted, the germline stem cells asymmetrically divide to self-renew and give rise to gonialblasts. The gonialblasts mitotically divide into spermatogonia. After four rounds of mitotic divisions, the 16-cell spermatogonial cysts then transition into meiotic prophase spermatocytes, after which they undergo meiotic division and terminally differentiate to become functional sperm. During the transition from spermatogonia to spermatocyte and subsequent differentiation into spermatids, the *Drosophila* male germ cells exhibit dramatic changes in gene expression. By turning off one set of genes such as those required for mitosis and turning on another set of genes required for both meiosis and other sperm-specific genes, the germ cells can terminally differentiate and form a morphologically and functionally developed sperm. Mis-regulation of the pattern of gene-expression cascade could result in dysfunctional sperm, which causes sterility or uncontrolled proliferation leading to oncogenesis (Clarke and Fuller 2006, Rando 2006).

The Polycomb Group (PcG) protein is a class of proteins that maintain the repressed state of genes through epigenetic silencing in spermatogenesis (Delino et

al 2004). This is largely done through modification of histone tails (Cao et al 2002). In order for differentiation to proceed, PcG function needs to be counteracted. This requires function of the testis-specific Meiotic Arrest Complex (tMAC) (Beall et al 2007) and the testis-specific TATA-binding protein Associated Factors (tTAFs) (Hiller et al 2001), which antagonizes PcG repressive function. The specific molecular detail is provided in the Introduction Chapter 1. In addition, active marks on histone tails need to be established. This is likely done through Trithorax Group (TrxG) protein (Byrd et al 2003), though the mechanism is not fully characterized. The regulation of the switch of these opposing marks and how this regulation epigenetically affect gene expression during cellular differentiation in an adult stem cell lineage poses an intriguing topic. Indeed, the transitions from spermatogonia to spermatocytes and then to spermatids are regulated in a step-wise manner. The following model demonstrates a step-by-step sequence of events (**Fig. 1)**. When spermatogonia transit to spermatocytes, the epigenetic "writer" PRC2 activity is down-regulated independently. This is followed by tMAC and tTAF antagonism of Polycomb repressive activity. In the spermatocyte stage, tTAF has been shown to bind to promoters of differentiation genes to reduce Polycomb binding and repression. The binding of tTAF may also promote accumulation of H3K4me3 and reduce H3K27me3 repressive marks (Chen et al 2005). The function of tTAF maybe dependent on tMAC for location to the nucleus. In fact, tTAF can bind and localize PRC1 to the nucleolus. This function is impaired in tMAC mutant, suggesting that these two complexes may function cooperatively.

In this chapter, we use a genome-wide approach by generating ChIP-seq (Mardis et al 2009) profiles of these stages in conjunction with gene expression (obtained from RNA-seq data from Cindy Lim, unpublished) to determine how the effects of the chromatin landscape contributes to coordinated gene regulation, especially in the context of chromatin regulating complexes such as tMAC and tTAF. In order to achieve the level of precision in chromatin landscape, we use newly adapted techniques of purifying germ cell at specific stages and perform ChIP-seq using small cell numbers. This is critical in two ways. First it allows us to look at very pure cell samples that do not include other cell types with chromatins that may mask any pattern we need to see. Second, the purified cells are harvested *in vivo*, and thus, will more accurate reflect the biological effects of chromatin landscape in a differentiating germ cell.

MATERIALS AND METHODS

Purifying germ cells at specific stages

The protocol in this section is developed especially for isolating specific stages in *Drosophila* germline cell development. To achieve this, we use a combination of stage-specific expression of CD8 protein in germ cells. Stage-specific germ cells are isolated by binding to beads conjugate to CD8 antibodies. After dissection, larval testes are rupture and washed. Beads are applied to bind to stage-specific cells. The mixture is subsequently washed, removing any cells that do not bind **(Fig. 4-2A and 4-2B)**.

To isolate spermatogonia, gonia-specific promoter *Bag of marbles* (*bam*) expressing Gal4 is used to express UAS-CD8. The coding sequence for the CD8 protein is isolated from mouse transcript. When the *bam*-Gal4 transgene is combined to the UAS-CD8 strain, the Gal4 will bind to the Upstream Activating Sequence (UAS) to express CD8 on the spermatogonial membrane. Since CD8 is a stable protein, spermatogonia that develop into spermatocyte will retain the CD8 membrane protein, resulting in a mixed sample that will include spermatocytes also. To prevent this, the bam-Gal4/UAS-CD8 transgenes are expressed in *bam* trans-heterozygous mutant background. Since wildtype function of Bam is required for spermatogonia transition to spermatocytes, and mutant alleles will result in differentiation arrest at the spermatogonial stage (Milne et al 2002, Wang et al 2009). Consequently, the entire *bam* mutant testes will have no spermatocytes and are enriched with spermatogonia (**Fig. 4-2C and 4-2D**).

Isolation of spermatocytes requires use of the spermatocyte-specific promoter *sa* gene. We have generated a sa-CD8 and have confirmed that CD8 is expressed in spermatocytes and spermatids. In order to prevent spermatids from co-purifying with spermatocytes, larval testes are used since spermatids have not developed in this early stage. In order to achieve consistency between the spermatogonia and spermatocyte samples, we also isolate spermatogonia cells from larval testes.

Validation of germ cell purification

To achieve consistency for data analyses, tissues from larval testes are used to purify spermatogonia and spermatocytes. Using larval testes has additional advantages such as excluding elongating sperms and muscle cells that non-specifically bind to Dynabeads. The successfully purified samples validated through quantitative reverse-transcript PCR (qRT-PCR) of known transcripts of molecular features in each different stage.

Using RNA-seq data obtain from stage-specific single cyst (unpublished data), we are able to determine the specific transcripts in each cell stage. Primers are designed for subsequent validation using qRT-PCR. In the case of the spermatogonia sample, we observe an enrichment of spermatogonia-specific genes (**Fig. 4-3).** In addition, these samples do not have enrichment in somatic transcripts (**Fig. 4-4**) These results indicate that the spermatogonia samples do not contain any contaminations of extraneous cells for use in the Chromatin immunoprecipitation (ChIP).

Similarly, qRT-PCR of purified spermatocyte samples yielded enriched spermatocyte-specific transcripts (**Fig. 4-5**). Indeed, somatic cell-specific transcript such as *eya*, are depleted (**Fig. 4-6**). In addition, we have harvested purified spermatocytes from the tTAF and tMAC mutants using the trans-heterozygous mutants for *can* and *aly* genes, respectively. The arrest phenotypes of these genes are very useful for profiling that chromatin landscape as early spermatocytes. Overall, the enrich of only spermatocyte-specific genes indicates the samples obtained from our purification protocol is sufficient for ChIP analysis.

ChIP-seq of purified germ cells

Given the small samples of starting material, it is necessary to perform ChIP experiments using the MAGnify kit for ChIP of small cell samples. The system uses magnetic beads to precipitate DNA at high efficiency. This is necessary to obtain a sufficient amount of genomic DNA. The genomic DNA will be amplified by adaptor attachment followed by PCR to prepare for high-throughput sequencing. Sequence data will be mapped to the *Drosophila* genome to detect enrichment of each modified histone at the promoter of individual genes (Gan et al 2010). Quantification of modified histones enrichment of each gene will be done relative the transcription start site (TSS). For both modified histones H3 trimethylation at lysine 27 (H3K27me3) and histone H3 trimethylation at lysine 4 (H3K4me3), detection of enrichment will be done from the TSS to +500 bp downstream. By quantifying the degree of enrichment of each modified histone species relative to

the TSS, we can determine if each gene locus is marked for activation through H3K4me3 (Byrd et al 2003) or repression through H3K27m3 (Cao et al 2002).

High throughput sequencing is done in our collaborator Dr. Keji Zhao's laboratory at the NIH. The sequencing results are mapped to the *Drosophila* transcriptome. Normalization is done first by normalizing to the length of transcripts followed by the entire sequencing reads, which yields a digital number of each detectable transcript, which is Reads Per kb transcript per Million reads (RPKM). Using these values we compare expression of each gene as well as the entire transcriptome between spermatogonia and spermatocytes. Genes that are turned on as spermatogonia differentiate into spermatocytes will be classified as "differentiation" genes. In contrast, genes that are high in spermatogonia and low in spermatocytes are classified as undifferentiated cell-enriched genes.

RESULTS

H3K27me3 ChIP-seq is consistent with chromatin profile

The transition from spermatocytes to terminally differentiated spermatids is characterized by morphological changes as well as meiotic progression, which is critical for proper haploid sperm formation. Concurrently, differentiation genes need to be expressed in spermatocytes to enter meiosis and terminal differentiation. In spermatogonia, differentiation genes are enriched in H3K27me3 and PcG. As spermatogonia transit to spermatocytes, PcG activity is counteracted and the repressive marks are removed to allow differentiation genes to be expressed and terminal differentiation to proceed. It is likely that tMAC and tTAF complexes antagonizes PcG function to de-repress differentiation genes for transit from spermatocyte to spermatids.

It is clear that while the staging of spermatogonia to spermatocyte is far more complex than their morphological features. We can actually classify the spermatocytes as early and later stages in development. As a result, we performed ChIP-seq on early stages spermatocytes using tMAC (*aly* mutants) and tTAF (*can* mutants to compare with the later stage wildtype spermatocytes. The initial ChIP-seq results are mapped to the *Drosophila* genome. In order to validate that the H3K27me3 ChIP, we aligned the ChIP profiles of gene relative to the transcription start site (tss). Next, we classify all the *Drosophila* genes into four groups according to their level of their expression: high, medium, low and silent expression. The enrichment of H3K27me3 around the tss is averaged for each gene group and

plotted. Since H3K27me3 is a repressive mark, we should expect high enrichment of would correlate to gene groups of low or silent expression. Correspondingly, genes with high expression would have low H3K27me3 enrichment. This is indeed the case when we plot for H3K27me3 ChIP of tMAC (*aly*) (**Fig. 4-7A**), tTAF (*can*) (**Fig. 4-7B**) and wildtype (**Fig. 4-7C**) spermatocytes to the gene expression. All three samples have distinct correlation of H3K27me3 as a repressive mark for gene expression. This gives us a high level of confidence in the efficacy of our ChIP-seq using small cell samples. Although, the robustness between these samples vary. Wildtype spermatocyte is more obvious than tMAC and tTAF mutant. This is due to the fact that ChIP-seq results for each sample vary in terms of total read numbers. Wildtype spermatocyte H3K27me3 ChIP has ~9 million reads while tMAC and tTAF only contain 1.7 and 3 million reads, respectively. Nevertheless, the results from the H3K27me3 ChIP are sufficient for analysis of chromatin profile in these stages of spermatocyte development.

Tracking chromatin landscape changes in developing spermatocytes in a temporal manner

Using the H3K27me3 data, we compare expression of each gene relative to the H3K27me enrichment for tMAC, tTAF and wildtype spermatocytes **(Fig. 4-8)** . The gene expression data is obtained by RNA-sequencing of single cell cysts (Cindy Lim, unpublished data). The accompanying scatter plots indicate each dot as a single gene. More importantly, we indicate genes classified as differentiation genes in

green. A differentiation gene is defined by its absence (<10 RPKM) in the 16-cell spermatogonial cyst and presence (>10 RPKM) in 16-cell spermatocyte cyst. The plot for H3K27me3 (y-axis) vs. the expression data (x-axis) for tMAC (*aly*) (**Fig. 4-8A**), tTAF (*can*) (**Fig. 4-8B**) and wildtype (**Fig. 4-8C**) spermatocytes are representative of a temporal chromatin state from early spermatocyte to late spermatocyte. Since tMAC (*aly*) and tTAF (*can*) mutants do not proceed to terminally differentiation into spermatid, they are at the ideal stage of early spermatocyte.

Based on comparison temporal stages, we can clearly see that differentiation genes expression (indicated in green) is gradually increased at the cell progress from tMAC mutant (386 differentiation genes active) to tTAF mutant (793 differentiation genes active) and finally to wildtype spermatocytes (1,149 differentiation genes active). This trend provides convincing evidence that the gene expression profile of each stage is molecularly distinct. If tMAC and tTAF do indeed act cooperatively antagonize polycomb activity, then the expression profile would be more similar. In fact, the distribution of differentiation genes in tTAF mutant seems to be an intermediate between tMAC and wildtype spermatocyte. Additionally, the H3K27me3 also supports the distinction of tMAC and tTAF function. In tMAC mutant, 294 differentiation genes have high H3K27me3 enrichment, whereas tTAF mutants have 218 differentiation genes with high H3K27me enrichment. At this point, it should be noted that differentiation genes of spermatocytes is also highly enrich in H3K27me3. This seems to be counter-intuitive, since high gene expression should have low H3K27me3 enrichment.

However, we propose that this high enrichment is caused by the fact that purified wildtype spermatocytes also contains early stages as well as later stages, because purification does not distinguish these stages. Therefore, the H3K27me3 profile of the spermatocyte is a mixture and reflects both population where early cells would have high H3K27me3 and late cells would have low H3K27me3.

In addition to looking at the overall gene population, we also track individual genes. Putative targets PcG such as *Don Juan (Dj)* and *MST87F* are tracked and labeled on the plot of all three stages (**Fig. 4-8**). It appears that these genes decrease in H3K27me3 enrichment as they increase in transcript when spermatocytes transit from early stages (*aly* and *can* mutants) to later stages. This is a strong validation of the changes these genes go through from early to later stage spermatocytes (Chen et al 2011). More importantly, the pure sample provides allows for observation of more intermediate enrichment of H3K27me3 enrichment.

tMAC and tTAF does not antagonize global PRC2 function, but rather a subset of differentiation genes

In order to look closer at tMAC and tTAF function, it is necessary to compare the data of each mutant spermatocyte samples from the previous section. By plotting the H3K27me3 ChIP data in both the tMAC and tTAF mutant against wildtype spermatocytes (**Fig. 4-9**), we can see that the enrichments of H3K27me3 in early spermatocytes (tMAC and tTAF mutants) do not decrease as the germ cells shift to the later stage (wildtype spermatocytes). In the quadrant with high

H3K27me3 enrichment for both tMAC vs. wildtype and tTAF vs. wildtype, we see that there are 884 and 993 genes, respectively. From this preliminary analysis, we can see that neither tMAC nor tTAF antagonize PRC2 activity in a global manner. Were that the case, then we would expect a high number of genes with high H3K27me3 enrichment in tMAC and tTAF mutants to have low enrichment of the same marks in wildtype spermatocytes (**Fig. 4-9A and 4-9B**, upper left quadrant). Additionally, genes that are low H3K27me3 enrichment in the mutants would be high in wildtype spermatocytes (**Fig. 4-9A and 4-9B**, lower right quadrant). This is however not the case. Instead, we see relatively even enrichment of H3K27me3 marks.

To look closer at the role of tMAC and tTAF, we use gene cluster analysis to group the expression data obtained from single cysts and the H3K27me3 data from ChIP-seq (**Fig. 4-10**) One of the criteria we chose in our cluster analyses is for genes with low expression in tMAC and tTAF, but high expression in wildtype spermatocytes. Additionally, these genes should have high enrichment H3K27me3 mark in the tMAC and tTAF mutant, but low enrichment in wildtype spermatocytes. We posit that these gene cluster would potentially be the direct targets of tMAC and tTAF. Purportedly, the absence of tMAC or tTAF complex in these respective mutants would prevent these complexes from antagonizing PRC2 activity. As a result, H3K27me3 enrichment remains high and these target genes would not be expressed. But in the wildtype spermatocytes, the very same genes would have functional tMAC and tTAF, which would counter PRC2 function and remove the H3K27me3 marks, resulting in expressions of said genes. By looking through the

cluster analysis, we can see that in the tMAC mutant, 170 genes fit this criteria. Similarly, the tTAF mutant has 110 genes in the same cluster. These results suggest that perhaps the role of both tMAC and tTAF are not global. Instead the complexes act on a small subset of genes that are upstream of gene targets responsible for terminal differentiation into spermatid. Furthermore, the 170 genes in tMAC and the 110 genes in tTAF clusters share only 50 genes. This further supports the evidence that tMAC and tTAF do not act cooperatively to antagonize PRC2 function, at least not completely. Also, the gene expression data suggests that tMAC mutant spermatocytes arrest at an earlier stage than tTAF. This is due to the fact that tMAC have less differentiation genes turned on than tTAF. This data is also contrary to the tMAC/tTAF cooperative function.

DISCUSSION

The main purpose of this chapter is to view the function cell development from a molecular perspective. Too often do we base our classification of cell based on a morphological basis or a single molecular marker. The tMAC and tTAF function is the best example of this, because we cannot distinguish the differences between the mutants of these two complexes based purely on morphology, merely that they arrest in early spermatocyte development. As a result, the view of what a functional cell is narrowed. By profiling the molecular aspects of cell development through gene expression and chromatin landscape, we provide a new paradigm of how the field should view developmental biology. In fact, cell development is a gradual process, not a step-by-step process.

The best contribution of the work in this chapter to the field is a technical aspect. ChIP-seq has been done numerous times before, but the majority has been done in cell culture due to the uniformity of the tissue. The major advantage is the tissue culture is not *in vivo.* Alternatively, ChIP-seq has also been done on tissues harvested from an organism, but the cell population of the starting material is often heterogeneous and includes populations of unwanted cells. By doing ChIP-seq from freshly purified and harvested material, we can eliminate both these obstacles in the same experiment.

Although the results in this chapter are not complete, it has already given glimpse into how a cell behaves and greater resolution than any other tools available. More importantly, much can be built upon from the existing data.

H3K4me3 and RNA Pol II ChIP-seq will provide even better resolution on the molecular aspects of cell development. And the tools developed in this chapter are applicable to many other multi-cellular systems. Indeed this is only the beginning of a new way to use molecular genetics to address important questions in developmental biology.

FIGURES AND TABLES

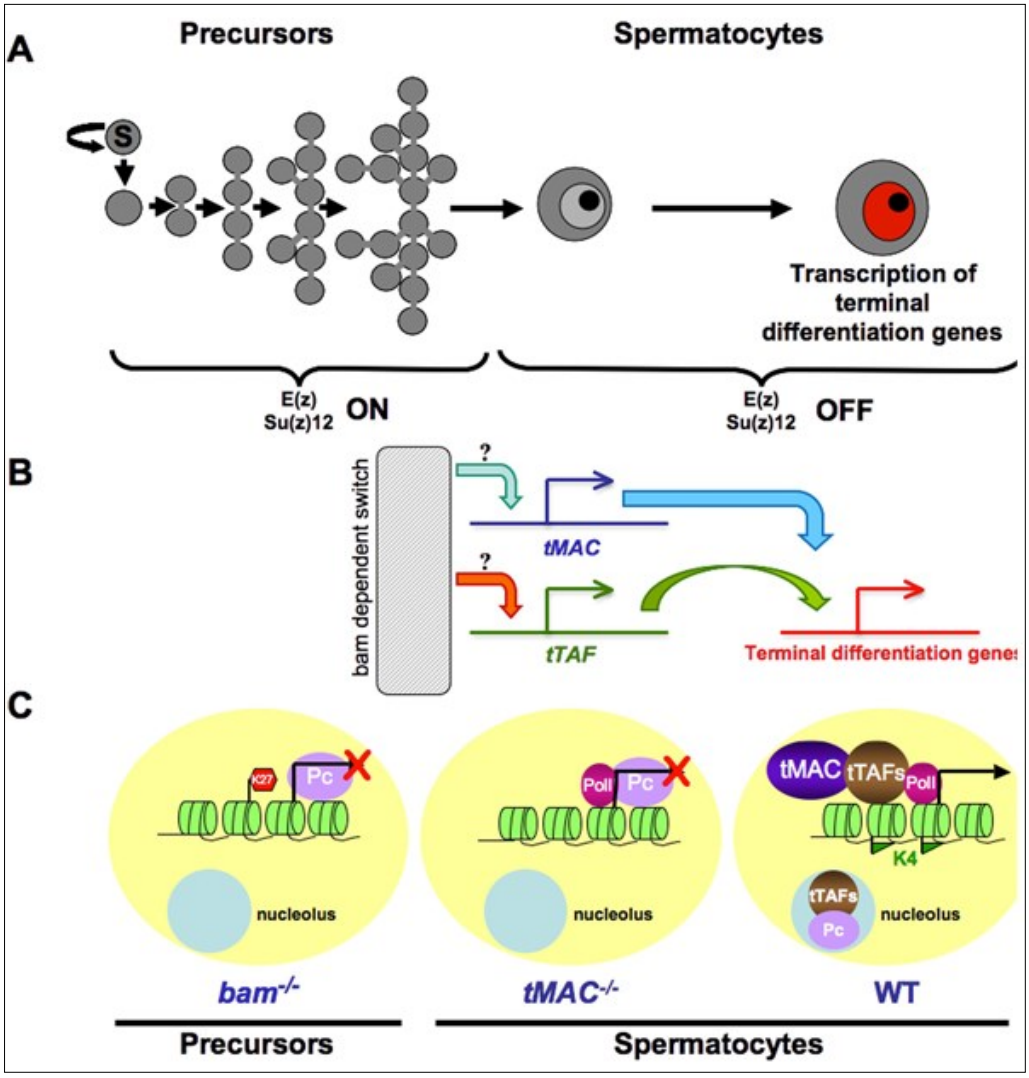

Figure 1. Model for developmental the transition of *Drosophila* germ cells through regulation of PcG activity. A) PRC2 activity is ON in precursor cell, but OFF in differentiating cells. B) After the switch from spermatogonia to spermatocytes, tMAC and tTAF activation counters PRC1 activity to turn differentiation genes. C) tMAC and tTAF work cooperatively to remove PcG repressive function and activate transcription. But in tMAC mutant, PRC1 (PC) still binds to genes' promoter to repress transcription.

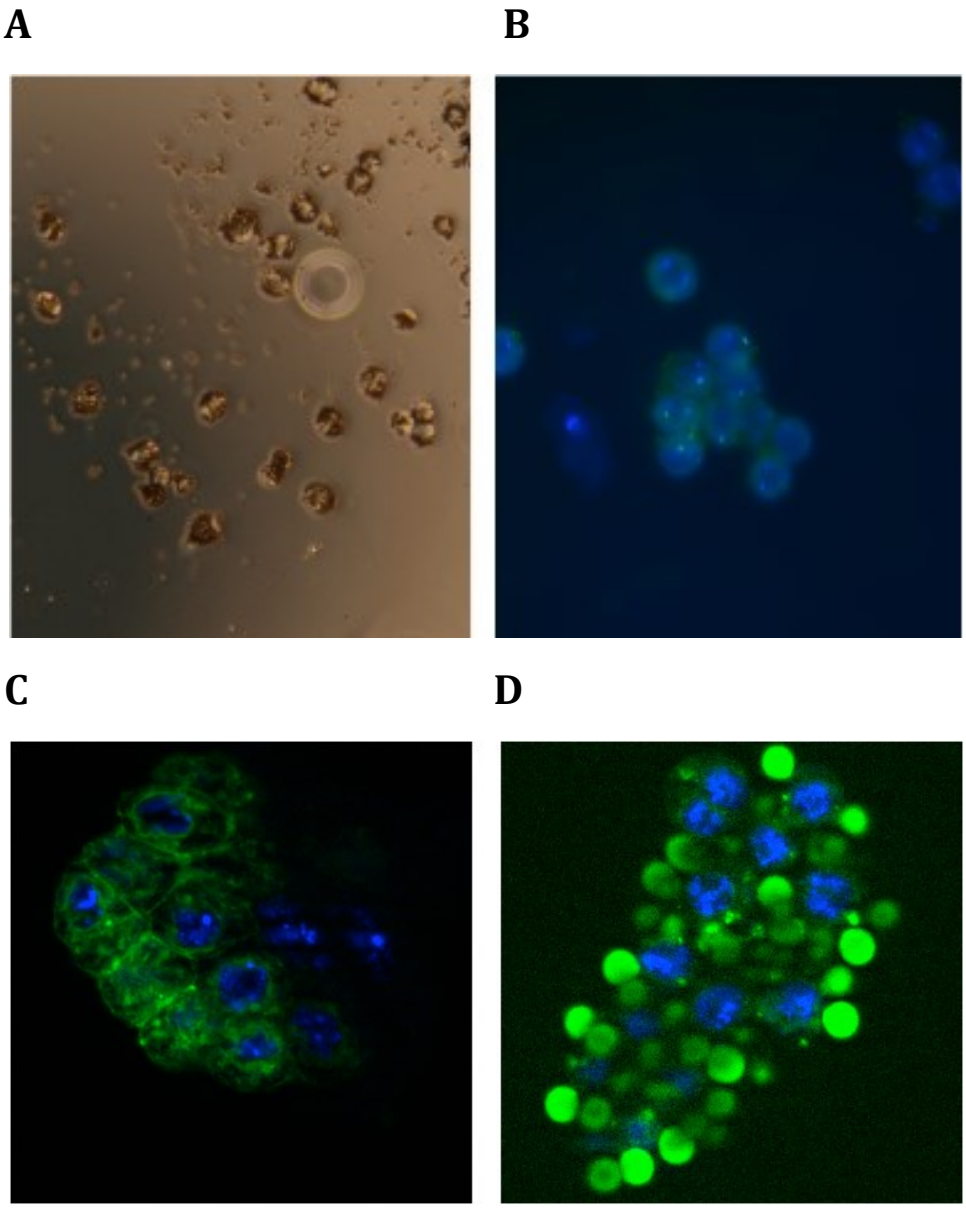

Figure 4-2. Techniques for purifying spermatogonia and spermatocyte. Using transgene with stage-specific promoter express CD8 membrane protein fused to GFP enables us to isolate spermatocytes using CD8 antibody conjugated to magnetic beads. A) Germ cells with magnetic anti-CD8 beads bound B) Germ cells express CD8-GFP at membrane. C) *bam* mutant spermatogonial cyst with bam-Gal4 activating UAS-CD8-GFP. D) Purified *bam* mutant with anti-CD8 magnetic beads.

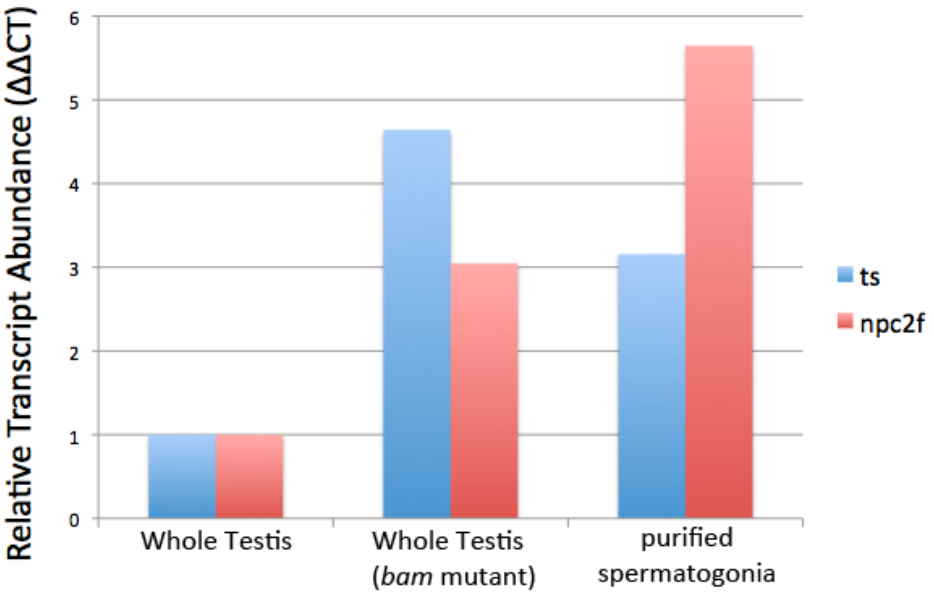

	8-cell cyst	16-cell cyst	spermatocyte
ts	135	165	3
npc2f	81	27	4

Figure 4-3. qRT-PCR validation for purified spermatogonia sample. Biological sample of whole testis, whole *bam* mutant testis (no spermatocytes) and purified spermatogonia are indicated in the X-axis. Y-axis indicates relative abundance determined by qPCR (ddCT). Values are normalized around whole testis sample as 1. Transcript of putative genes *ts* and *npc2f* are enriched in spermatogonial cysts (values indicated in table are in RPKM).

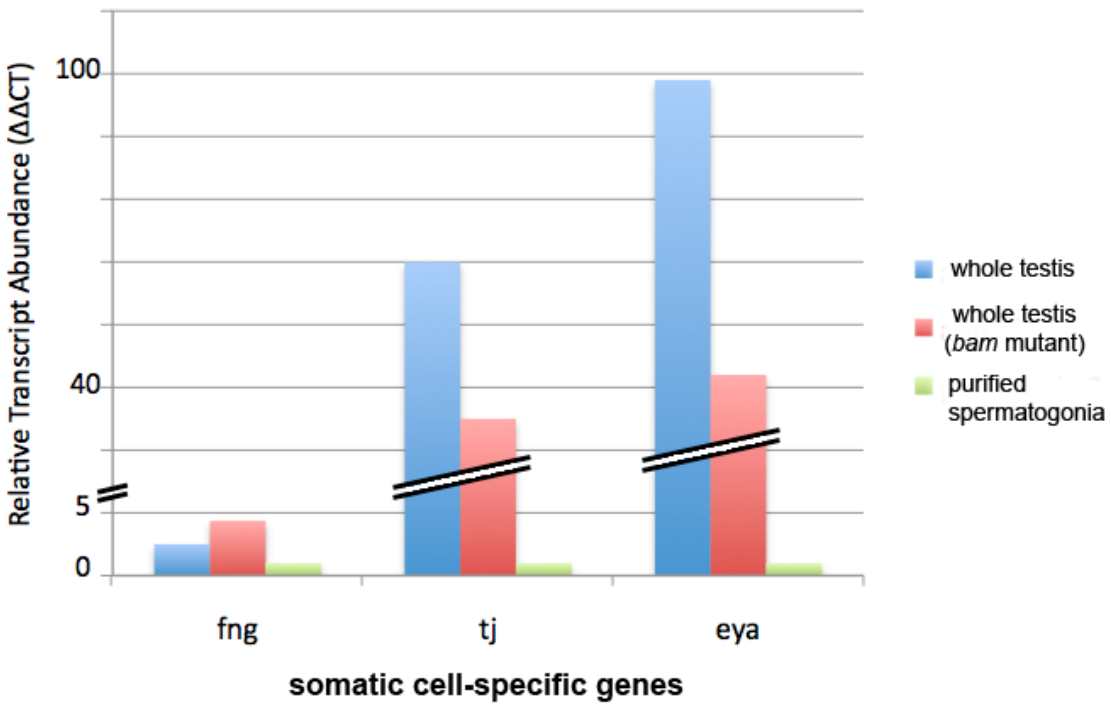

Figure 4-4. qRT-PCR validation for purified spermatogonia sample indicates no somatic cell contamination. Biological sample of whole testis (blue), whole *bam* mutant testis (no spermatocytes, red) and purified spermatogonia (green). X-axis indicates somatic cell-specific genes *fringe (fng*), *traffic jam* (*tj)* and *eyes absent* (*eya*). Y-axis indicates relative abundance determined by qPCR (ddCT). Values are normalized around purified spermatogonia sample as 1.

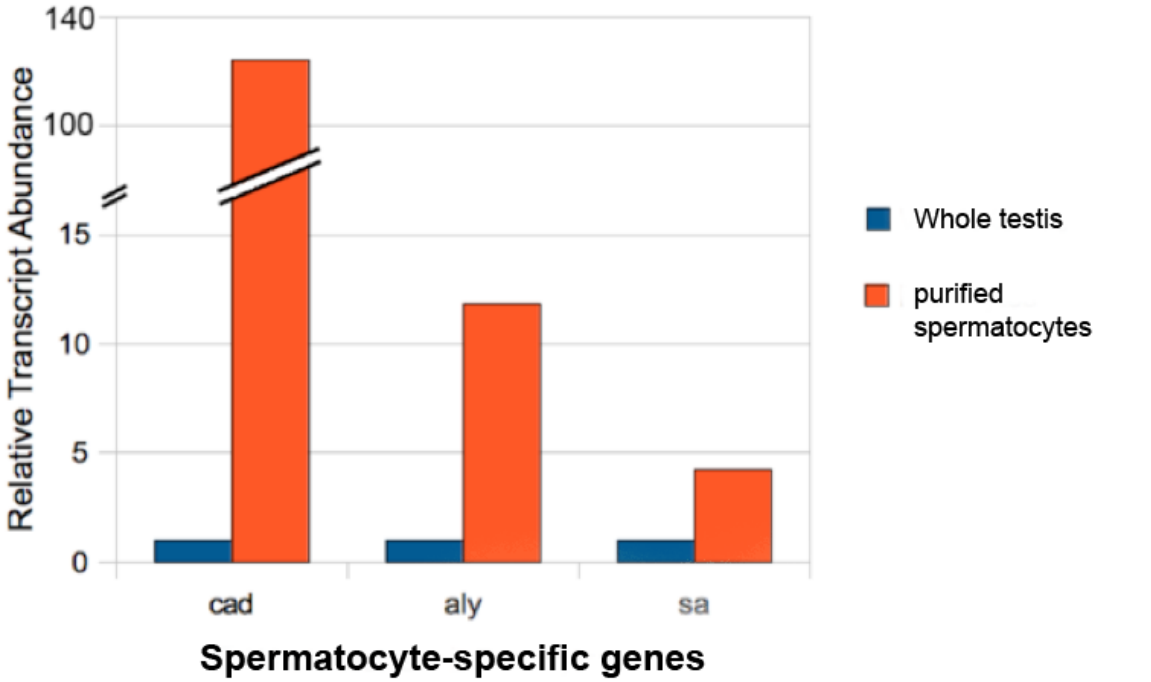

	8-cell cyst	16-cell cyst	spermatocyte
cad	0	0	29.08
aly	0	0	134.54
sa	3.63	0	161.38

Figure 4-5. qRT-PCR validation for purified spermatocyte sample show enrichment spermatocyte-specific genes. Biological sample of whole testis and purified spermatocyte are indicated in the X-axis. Spermatocyte enriched genes *caudal* (*cad*), *always early* (*aly*) and *spermatocyte arrest* (*sa*) are also indicated on the X-axis. Y-axis indicates relative abundance determined by qPCR (ddCT). Values are normalized around whole testis sample as 1. Transcript of putative genes *ts* and *npc2f* are enriched in spermatogonial cysts (values indicated in table are in RPKM). Transcript of putative genes *cad, aly* and *sa* are enriched in spermatogonial cysts (values indicated in table are in RPKM).

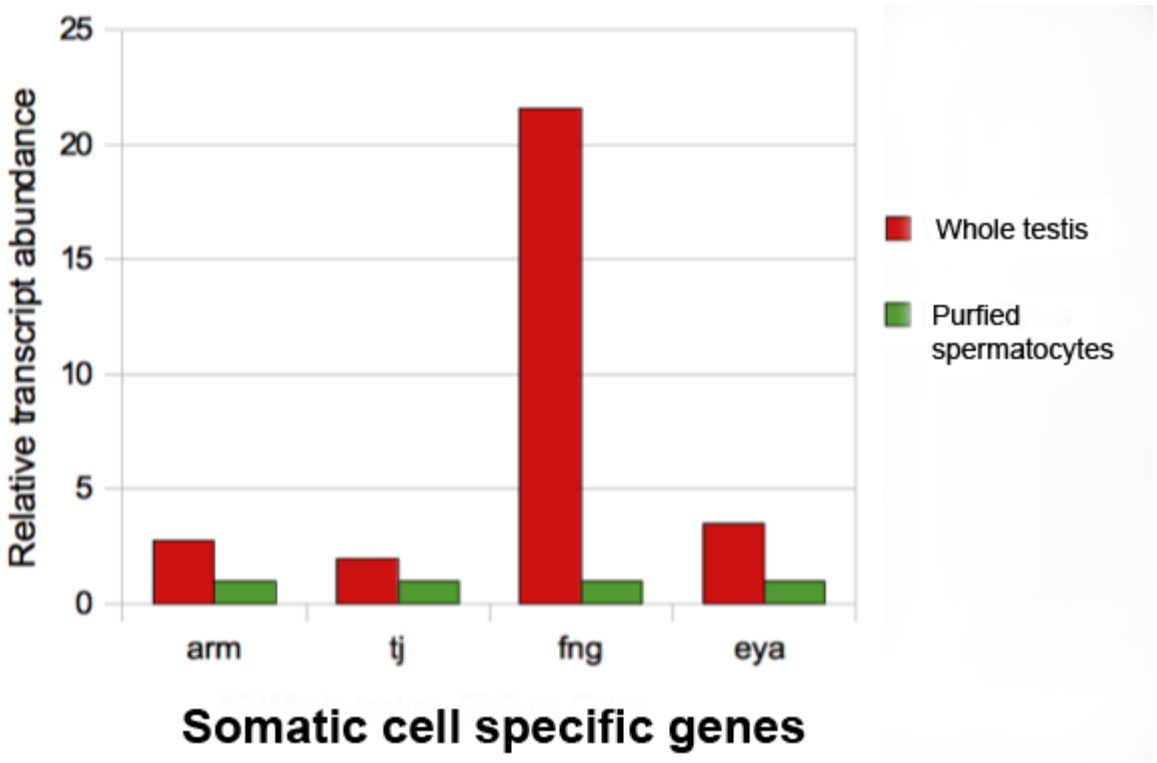

Figure 4-6. qRT-PCR validation for purified spermatocyte sample show depletion of somatic-specific genes. Biological sample of whole testis and purified spermatocytes are indicated in the X-axis. Somatic enriched genes *armadillo* (*arm*), *traffic jam* (*tj) fringe (fng)* and *eyes absent* (*eya*) are also indicated on the X-axis. Y-axis indicates relative abundance determined by qPCR (ddCT). Values are normalized around purified spermatocyte sample as 1.

A

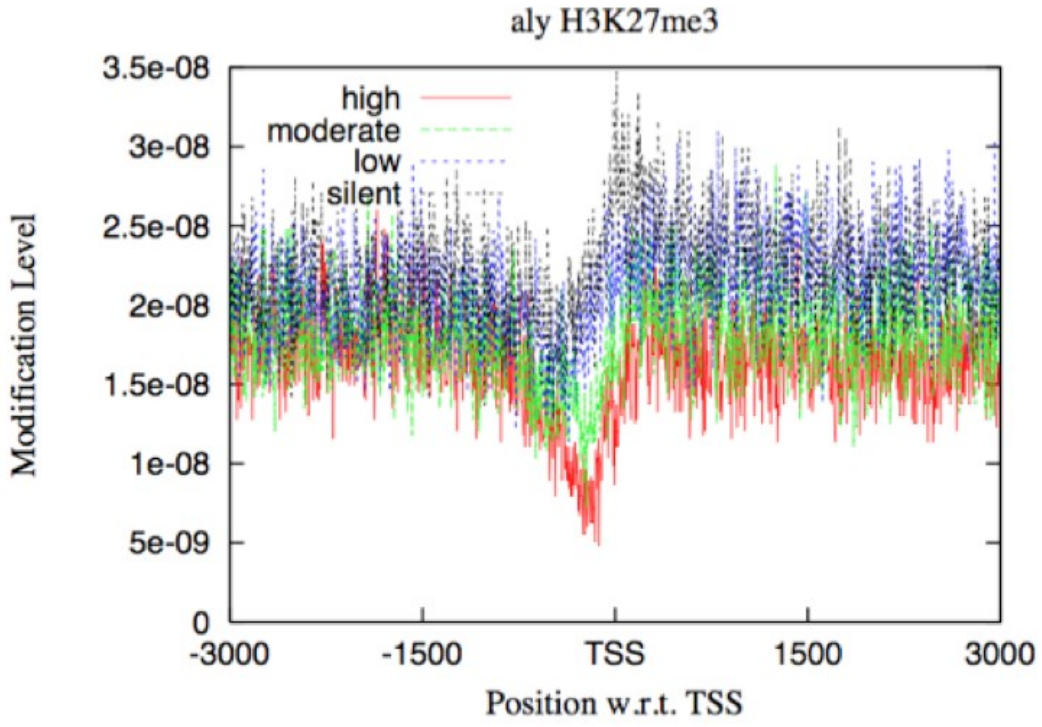
aly H3K27me3
Modification Level
3.5e-08
3e-08
2.5e-08
2e-08
1.5e-08
1e-08
5e-09
0
high
moderate
low
silent
-3000
-1500
TSS
1500
3000
Position w.r.t. TSS

B

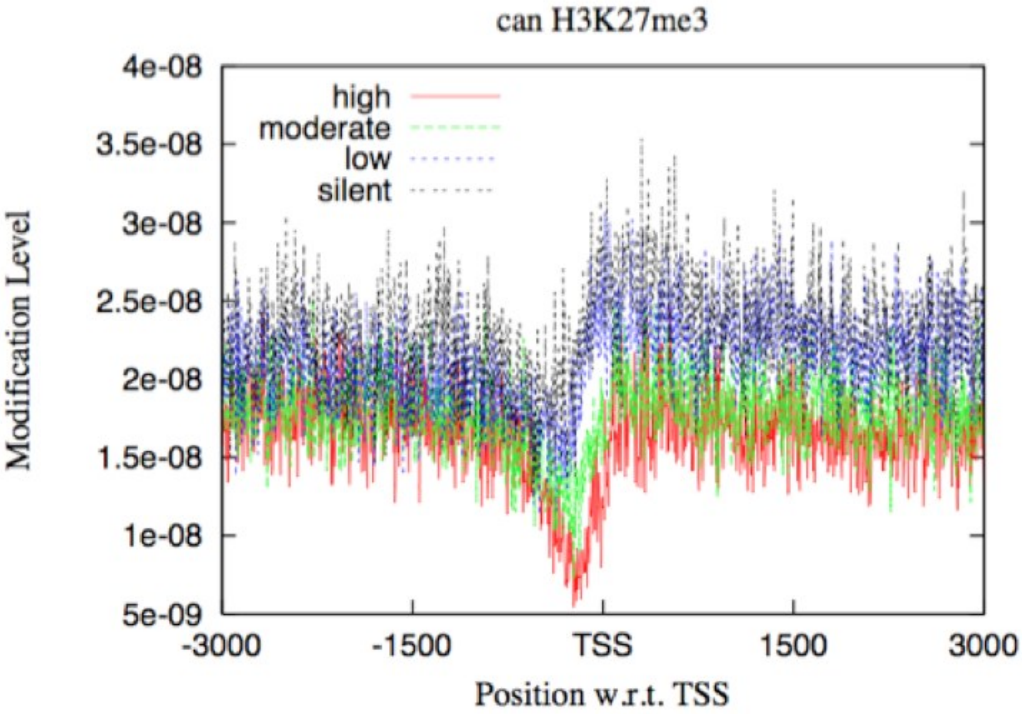
can H3K27me3
Modification Level
4e-08
3.5e-08
3e-08
2.5e-08
2e-08
1.5e-08
1e-08
5e-09
high
moderate
low
silent
-3000
-1500
TSS
1500
3000
Position w.r.t. TSS

C

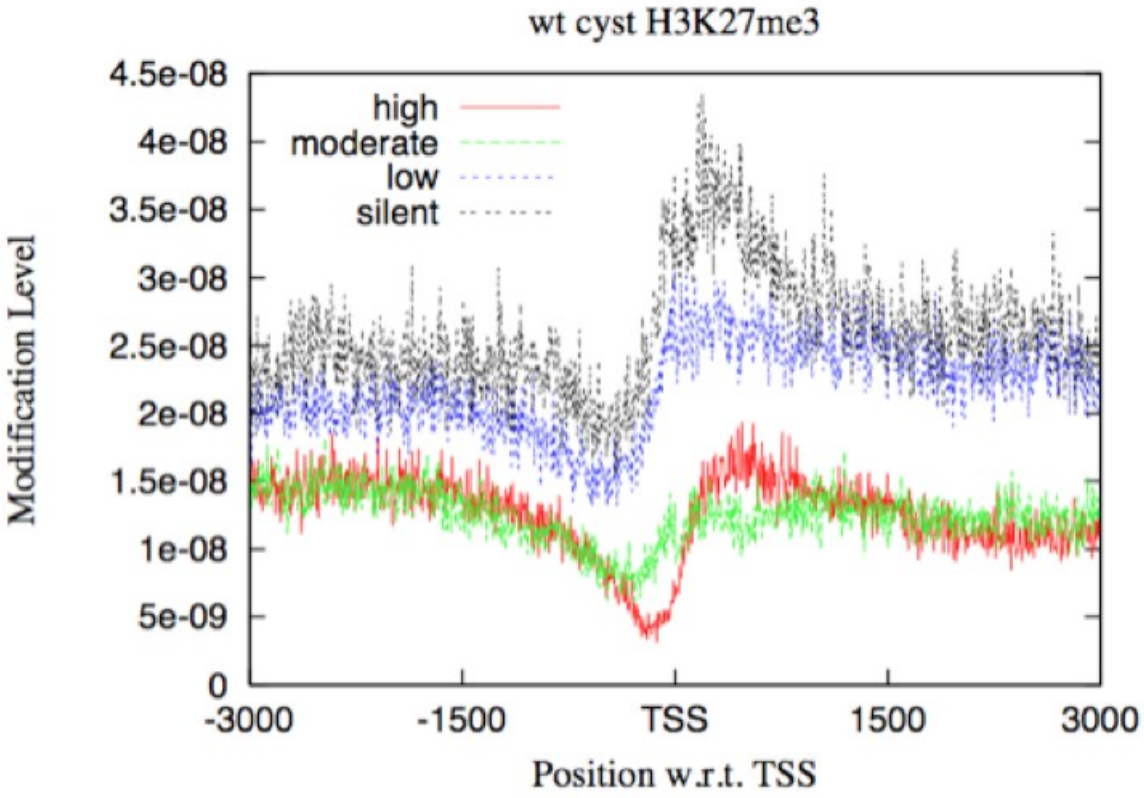

Figure 4-7. Validation of H3K27me3 ChIP for purified spermatocytes.

Enrichment of H3K27me3 ChIP for A) tMAC *(aly*) B) tTAF (*can*) mutant spermatocytes C) wildtype spermatocytes. ChIP-seq is validated by alignment of 4 classes of genes (High, Moderate, Low and Silent expression) at their transcription start site (TSS). The average H3K27me3 enrichment for each class of genes is plotted on the y-axis to reveal chromatin profile.

A

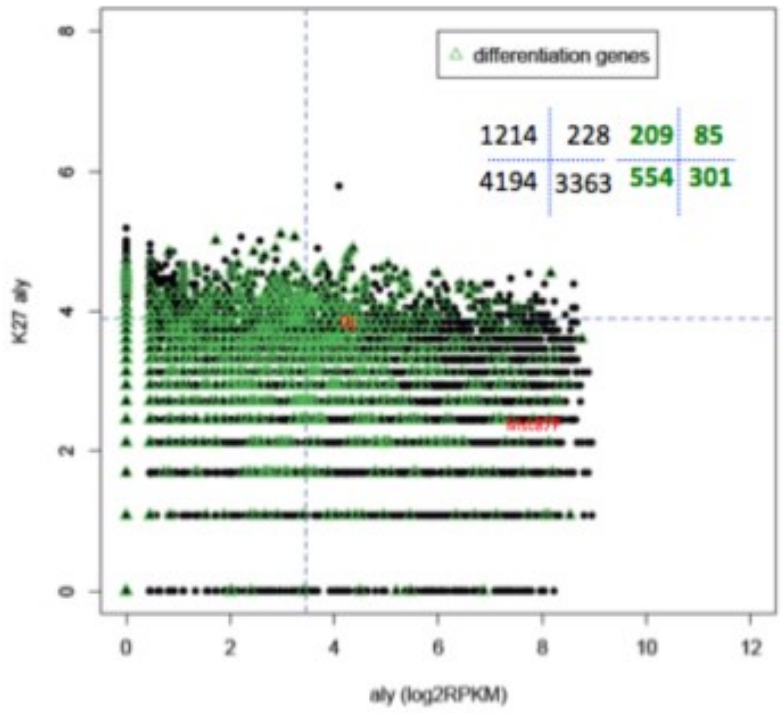
differentiation genes
1214
228
209
85
4194
3363
554
301
K27 aly
aly (log2RPKM)
0
2
4
6
8
10
12

B

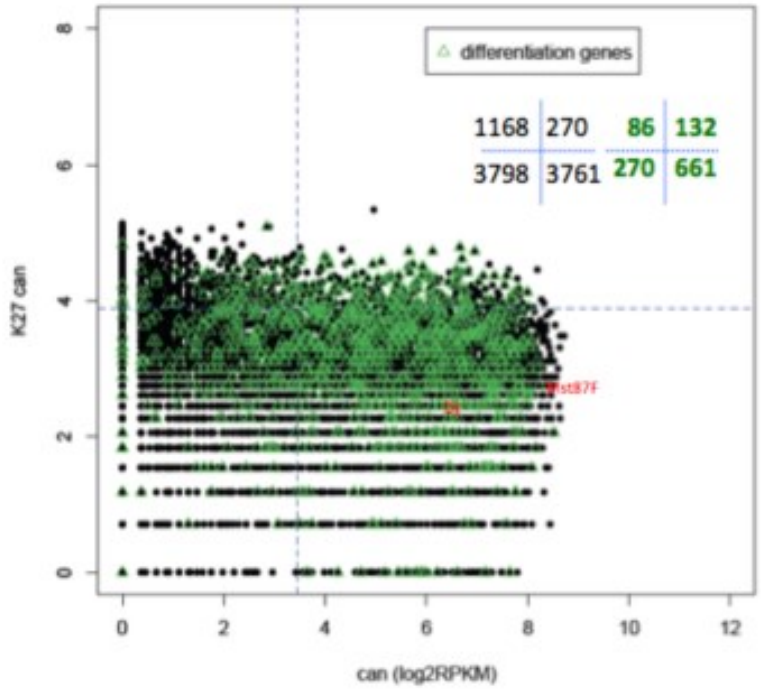
differentiation genes
1168
270
86
132
3798
3761
270
661
K27 can
can (log2RPKM)
0
2
4
6
8
10
12

C

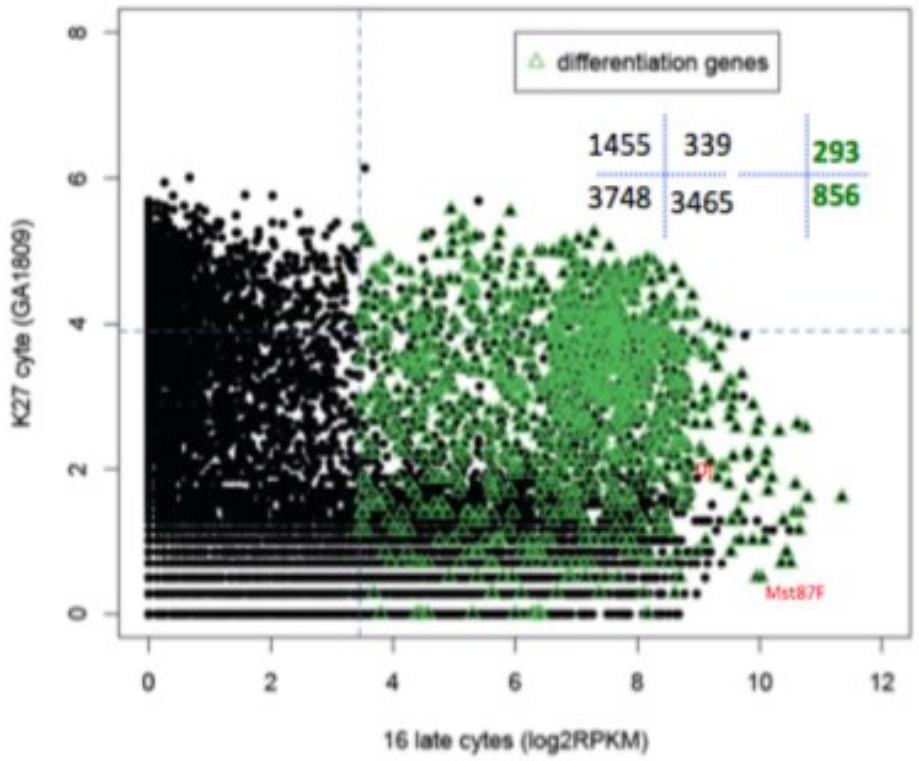

Figure 4-8. ChIP of H3K27me3 modified histones vs. gene expression (RNA-seq of single 16-cell cysts) for tMAC, tTAF and wildtype spermatocytes

H3K27me3 enrichment for **A)** tMAC (aly), **B)** tTAF (can) and **C)** wildtype are plotted against gene expression data. Each gene is represented by one point. H3K27me3 ChIP (y-axis) is plotted against corresponding gene expression (x-axis). Differentiation genes are marked in green. Threshold for each quadrant is determined by $P<0.05$. Expression and chromatin profiles of tMAC and tTAF indicate two desistance stages where tTAF mutant is molecularly closer to differentiating spermatocytes than early spermatocytes. Putative terminal differentiation genes *Dj and MST87F* are labeled in red.

A

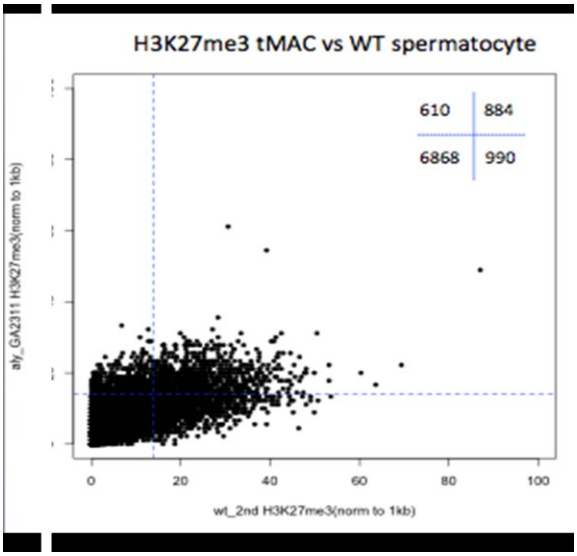

B

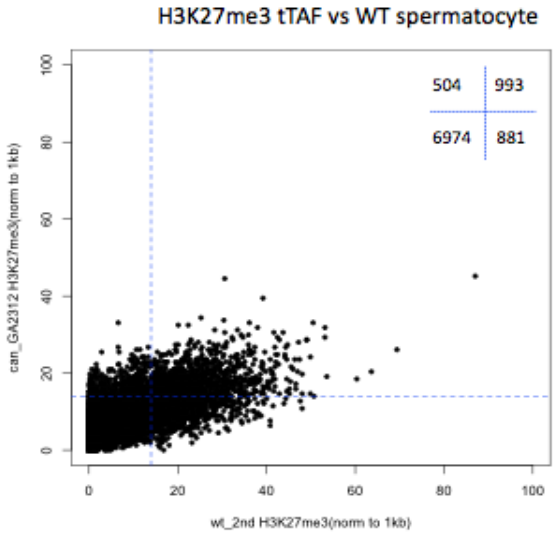

Figure 4-9. Comparison of H3K27me3 ChIP profiles in early versus late stages of spermatocyte development. Plot of H3K27me3 ChIP enrichment for A) tMAC (y-axis) vs. wildtype spermatocyte (x-axis) and B) tTAF (y-axis) vs. wildtype spermatocyte (x-axis).

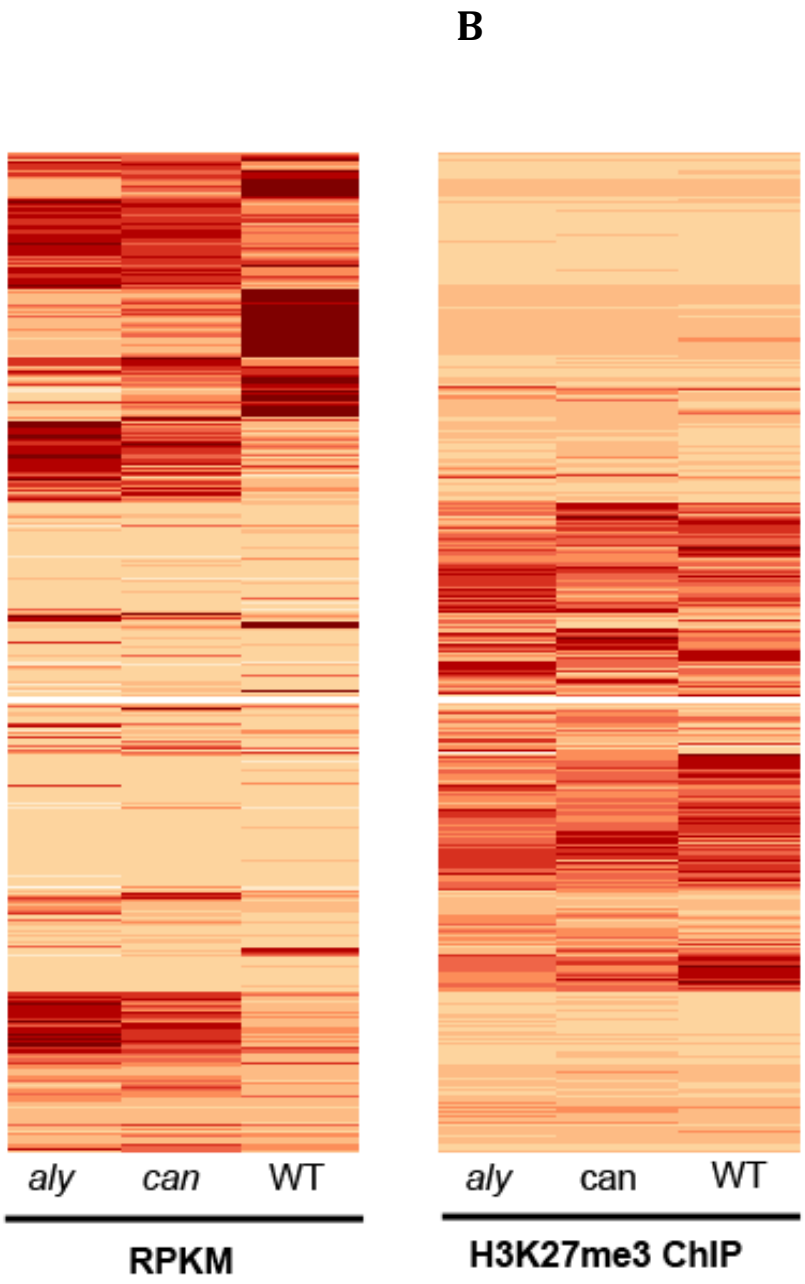

Figure 4-10. Cluster analysis of both gene expression and H3K27me3 ChIP enrichment in spermatocyte. Heat map of gene expression (RPKM) and H3K27me3 ChIP-seq for each genotype**.** Darker red regions represent high RPKM and high H3K27me3 ChIP enrichment.

A

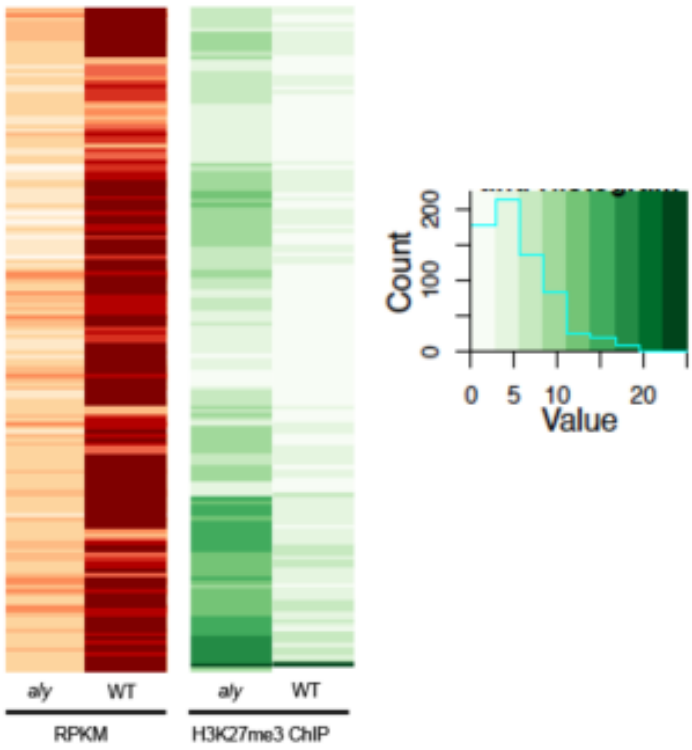
aly
WT
RPKM
aly
WT
H3K27me3 ChIP
Count
0
100
200
0
5
10
20
Value

B

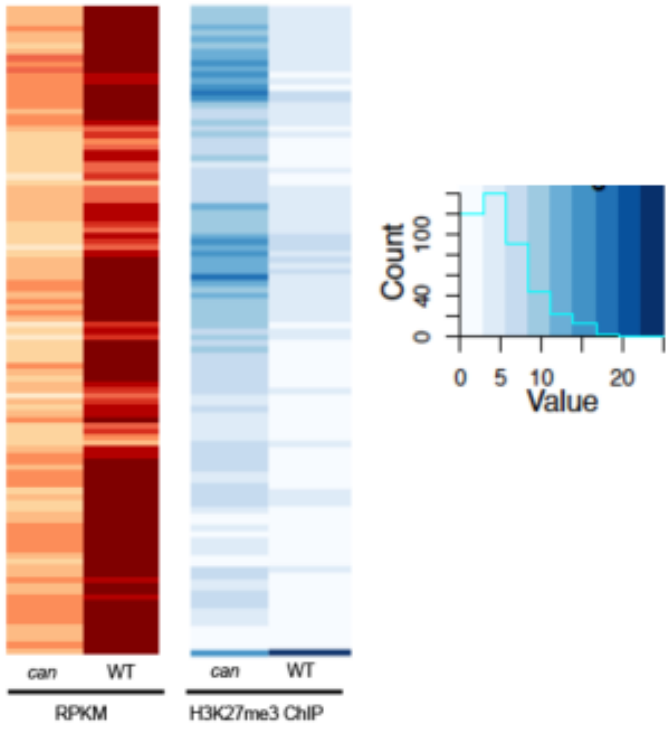
can
WT
RPKM
can
WT
H3K27me3 ChIP
Count
0
40
100
0
5
10
20
Value

Figure 4-11. Selected gene cluster of genes potentially regulated by tMAC and tTAF through antagonism of PRC2. A) gene cluster with enriched expression low in tMAC mutant, high in wildtype mutant, H3K27me3 enriched in tMAC mutant and low in wildtype B) gene cluster with enriched expression low in tTAF mutant, high in wildtype mutant, H3K27me3 enriched in tTAF mutant and low in wildtype.

REFERENCES:

Ahmad K, Henikoff S (2002a) Histone H3 variants specify modes of chromatin assembly. Proc Natl Acad Sci U S A 99(Suppl 4):16477–16484

Ahmad K, Henikoff S (2002b) The histone variant H3.3 marks active chromatin by replication-independent nucleosome assembly. Mol Cell 9:1191–1200

Ai X, Parthun MR (2004) The nuclear Hat1p/Hat2p complex: a molecular link between type B histone acetyltransferases and chromatin assembly. Mol Cell 14:195–205

Akkers RC, van Heeringen SJ, Jacobi UG, Janssen-Megens EM, Francoijs KJ, Stunnenberg HG, Veenstra GJ (2009) A hierarchy of H3K4me3 and H3K27me3 acquisition in spatial gene regulation in Xenopus embryos. Dev Cell, 17:425-434.

Annunziato AT, Schindler RK, Riggs MG, Seale RL (1982) Association of newly synthesized histones with replicating and nonreplicating regions of chromatin. J Biol Chem 257:8507–8515

Armakolas A, Klar AJ (2006) Cell type regulates selective segregation ofmouse chromosome 7 DNA strands inmitosis. Science 311:1146–1149

Armakolas A, Klar AJ (2007) Left-right dynein motor implicated in selective chromatid segregation in mouse cells. Science 315:100–101

Bannister AJ, Kouzarides T (2011) Regulation of chromatin by histone modifications. Cell Res 21:381–395

Bayne EH, White SA, Kagansky A, Bijos DA, Sanchez-Pulido L, Hoe KL, Kim DU, Park HO, Ponting CP, Rappsilber J, Allshire RC (2010) Stc1: a critical link between RNAi and chromatin modification required for heterochromatin integrity. Cell 140:666–677

Beall EL, Lewis PW, Bell M, Rocha M, Jones DL, and Botchan MR (2007) Discovery of tMAC: a Drosophila testis-specific meiotic arrest complex paralogous to Myb-Muv B. Genes Dev 21(8): 904-919

Berger SL (2007) The complex language of chromatin regulation during transcription. Nature 447:407–412

Bergmann JH, Rodriguez MG, Martins NM, Kimura H, Kelly DA, Masumoto H, Larionov V, Jansen LE, Earnshaw WC (2011) Epigenetic engineering shows H3K4me2 is required for HJURP targeting and CENP-A assembly on a synthetic human kinetochore. EMBO J 30:328–340

Bernstein BE, Mikkelsen TS, Xie X, Kamal M, Huebert DJ, Cuff J, Fry B, Meissner A, Wernig M, Plath K, Jaenisch R, Wagschal A, Feil R, Schreiber SL, and Lander ES (2006) A bivalent chromatin structure marks key developmental genes in embryonic stem cells. Cell 125(2): 315-326.

Bernstein E, Allis CD (2005) RNA meets chromatin. Genes Dev 19:1635–1655

Betschinger J, Knoblich JA (2004) Dare to be different: asymmetric cell division in Drosophila, C. elegans and vertebrates. Curr Biol 14:R674–685

Betzig E, Patterson GH, Sougrat R, Lindwasser OW, Olenych S, Bonifacino JS, Davidson MW, Lippincott-Schwartz J, Hess HF. Imaging intracellular fluorescent proteins at nanometer resolution. Science, 2006. 313(5793): p. 1642-5

Blower MD, Sullivan BA, Karpen GH (2002) Conserved organization of centromeric chromatin in flies and humans. Dev Cell 2:319–330

Bonasio R, Tu S, Reinberg D (2010) Molecular signals of epigenetic states. Science 330:612–616

Borsani G, Tonlorenzi R, Simmler MC, Dandolo L, Arnaud D, Capra V, Grompe M, Pizzuti A, Muzny D, Lawrence C, Willard HF, Avner P, Ballabio A (1991) Characterization of a murine gene expressed from the inactive X chromosome. Nature 351:325–329

Boyer LA, Plath K, Zeitlinger J, Brambrink T, Medeiros LA, Lee TI, Levine SS, Wernig M, Tajonar A, Ray MK, Bell GW, Otte AP, Vidal M, Gifford DK, Young RA, and Jaenisch R (2006). Polycomb complexes repress developmental regulators in murine embryonic stem cells. *Nature* 441(7091): 349-353

Buszczak M, Spradling AC (2006) Searching chromatin for stem cell identity. Cell 125(2):233-6

Byrd KN, Shearn A (2003) ASH1, a Drosophila trithorax group protein, is required for methylation of lysine 4 residues on histone H3. Proc Natl Acad Sci U S A, 100:11535-11540

Cairns J (1975) Mutation selection and the natural history of cancer. Nature 255:197–200

Cao R, Wang L, Wang, H, Xia L, Erdjument-Bromage H, Tempst P, Jones RS, and Zhang, Y (2002) Role of histone H3 lysine 27 methylation in Polycomb-group silencing. *Science* 298(5595): 1039-1043

Chen CC, Carson JJ, Feser J, Tamburini B, Zabaronick S, Linger J, Tyler JK (2008) Acetylated lysine 56 on histone H3 drives chromatin assembly after repair and signals for the completion of repair. Cell 134:231–243

Chen X, Lu C, Morillo J, Eun S and Fuller MT (2011) Sequential changes at differentiation gene promoters as they become active in a stem cell lineage. *Development* 138: 2441-2450

Chen X, Hiller M, Sancak Y, and Fuller MT (2005) Tissue-specific TAFs counteract Polycomb to turn on terminal differentiation. Science 310(5749): 869-872

Cheng J, Turkel N, Hemati N, Fuller MT, Hunt AJ, Yamashita YM (2008) Centrosome misorientation reduces stem cell division during ageing. Nature 456:599–604

Chepelev I, Chen X (2013) Alternative splicing switching in stem cell lineages. Front Biol 8:50–59

Clarke MF, Fuller M (2006) Stem cells and cancer: two faces of eve. *Cell* 124(6) 1111-1115

Clevers H (2005) Stem cells, asymmetric division and cancer. Nat Genet 37:1027–1028

Conboy MJ, Karasov AO, Rando TA (2007) High incidence of non-random template strand segregation and asymmetric fate determination in dividing stem cells and their progeny. PLoS Biol 5:e102

Corpet A, Almouzni G (2009) Making copies of chromatin: the challenge of nucleosomal organization and epigenetic information. Trends Cell Biol 19:29–41

Cseresnyes, Z., U. Schwarz, and C.M. Green, Analysis of replication factories in human cells by super-resolution light microscopy. BMC Cell Biol, 2009. 10: p. 88.

Cui K, Zang C, Roh TY, Schones DE, Childs RW, Peng W, Zhao K (2009) Chromatin signatures in multipotent human hematopoietic stem cells indicate the fate of bivalent genes during differentiation. Cell Stem Cell, 4:80-93

De Koning L, Corpet A, Haber JE, Almouzni G (2007) Histone chaperones: an escort network regulating histone traffic. Nat Struct Mol Biol 14:997–1007

Deal RB, Henikoff JG, Henikoff S (2010) Genome-wide kinetics of nucleosome turnover determined by metabolic labeling of histones. Science 328:1161–1164

Dellino GI, Schwartz YB, Farkas G, McCabe D, Elgin SC, and Pirrotta V (2004)

Polycomb silencing blocks transcription initiation. Molecular cell 13(6): 887-893.

Dion MF, Kaplan T, Kim M, Buratowski S, Friedman N, Rando OJ (2007) Dynamics of replication-independent histone turnover in budding yeast. Science 315:1405–1408

Drane P, Ouararhni K, Depaux A, Shuaib M, Hamiche A (2010) The death-associated protein DAXX is a novel histone chaperone involved in the replication-independent deposition of H3.3. Genes Dev 24:1253–1265

Dynlacht BD, Hoey T, and Tjian R (1991) Isolation of coactivators associated with the TATA-binding protein that mediate transcriptional activation. *Cell* 66: 563–576

Eickbush TH, and Moudrianakis EN (1978) The histone core complex: An octamer assembled by two sets of protein-protein interactions. Biochemistry 17, 4955–4964

Eun SH, Gan Q, Chen X (2010) Epigenetic regulation of germ cell differentiation. Curr Opin Cell Biol 22:737–743

Falconer E, Chavez EA, Henderson A, Poon SS, McKinney S, Brown L, Huntsman DG, Lansdorp PM (2010) Identification of sister chromatids by DNA template strand sequences. Nature 463:93–97

Fei JF, Huttner WB (2009) Nonselective sister chromatid segregation in mouse embryonic neocortical precursor cells. Cereb Cortex 19(Suppl 1):i49–54

Feinberg AP, Ohlsson R, Henikoff S (2006) The epigenetic progenitor origin of human cancer. Nat Rev Genet 7:21–33

Ferguson-Smith AC (2011) Genomic imprinting: the emergence of an epigenetic paradigm. Nat Rev Genet 12:565–575

Fischle W, Tseng BS, Dormann HL, Ueberheide BM, Garcia BA, Shabanowitz J, Hunt DF, Funabiki H, Allis CD (2005) Regulation of HP1-chromatin binding by histone H3 methylation and phosphorylation. Nature 438:1116–1122

Fischle W, Wang Y, Allis CD (2003) Binary switches and modification cassettes in histone biology and beyond. Nature 425:475–479

Fischle W, Wang Y, Jacobs SA, Kim Y, Allis CD, and Khorasanizadeh S (2003) Molecular basis for the discrimination of repressive methyl-lysine marks in histone H3 by Polycomb and HP1 chromodomains. Genes & development 17(15): 1870-1881

Francis NJ (2009a). Does maintenance of polycomb group proteins through DNA replication contribute to epigenetic inheritance? Epigenetics 4:370–373

Francis NJ (2009b). Mechanisms of epigenetic inheritance: copying of polycomb repressed chromatin. Cell Cycle 8:3513–3518

Francis NJ, Follmer NE, Simon MD, Aghia G, Butler JD (2009) Polycomb proteins remain bound to chromatin and DNA during DNA replication in vitro. Cell 137:110–122

Francis NJ, Kingston RE, and Woodcock CL (2004) Chromatin compaction by a polycomb group protein complex. Science 306(5701): 1574-1577

Fredriksson S, Gullberg M, Jarvius J, Olsson C, Pietras K, Gústafsdóttir SM, Ostman A, Landegren U. (2002) Protein detection using proximity-dependent DNA ligation assays. Nat Biotechnol. 2002 May;20(5):473-7

Fuller MT, Spradling AC (2007) Male and female Drosophila germline stem cells: two versions of immortality. Science 316:402–404

Gan Q, Chepelev I, Wei G, Tarayrah L, Cui K, Zhao K, Chen X (2010) Dynamic regulation of alternative splicing and chromatin structure in Drosophila gonads revealed by RNA-seq. *Cell Research* (Epub)

Gan Q,Schones D, Eun SH, Wei G, Cui K, Zhao K Chen X (2010) Monovalent and unpoised status of most genes in undifferentiated cell-enriched Drosophila testis. Genome Biology 11(4) R42

Gasser R, Koller T, Sogo JM (1996) The stability of nucleosomes at the replication fork. J Mol Biol 258:224–239

Goldberg AD, Banaszynski LA, Noh KM, Lewis PW, Elsaesser SJ, Stadler S, Dewell S, Law M, Guo X, Li X, Wen D, Chapgier A, DeKelver RC, Miller JC, Lee YL, Boydston EA, Holmes MC, Gregory PD, Greally JM, Rafii S, Yang C, Scambler PJ, Garrick D, Gibbons RJ, Higgs DR, Cristea IM, Urnov FD, Zheng D, Allis CD (2010) Distinct factors control histone variant H3.3 localization at specific genomic regions. Cell 140:678–691

Gruss, C., Wu, J., Koller, T., and Sogo, J. M. (1993). Disruption of the nucleosomes at the replication fork. EMBO J. 12, 4533–4545

Guenther MG, Levine SS, Boyer LA, Jaenisch R, and Young, RA 2007. A chromatin landmark and transcription initiation at most promoters in human cells. Cell 130(1): 77-88

Guilbaud G, Rappailles A, Baker A, Chen CL, Arneodo A, Goldar A, D'Aubenton-Carafa Y, Thermes C, Audit B, Hyrien O (2011) Evidence for sequential and increasing activation of replication origins along replication timing gradients in the human

genome. PLoS Comput Biol 7:e1002322

Hansen KH, Helin K (2009) Epigenetic inheritance through self-recruitment of the polycomb repressive complex 2. Epigenetics 4:133–138

Henikoff S, Furuyama T, Ahmad K (2004a) Histone variants, nucleosome assembly and epigenetic inheritance. Trends Genet 20:320–326

Henikoff S, McKittrick E, Ahmad K (2004b) Epigenetics, histone H3 variants, and the inheritance of chromatin states. Cold Spring Harb Symp Quant Biol 69:235–243

Hiller MA, Lin TY, Wood C, and Fuller MT (2001) Developmental regulation of transcription by a tissue-specific TAF homolog. Genes Dev 15(8): 1021-1030

Hiller M, Chen X, Pringle MJ, Suchorolski M, Sancak Y, Viswanathan S, Bolival B, Lin TY, Marino S, and Fuller MT (2004) Testis-specific TAF homologs collaborate to control a tissuespecific transcription program. Development 131(21): 5297-5308

Hung MS, Karthikeyan N, Huang B, Koo HC, Kiger J, Shen CJ (1999) Drosophila proteins related to vertebrate DNA (5-cytosine) methyltransferases. Proc Natl Acad Sci USA 96:11940–11945

Hunter T, Pines J. (1994) Cyclins and cancer. II: Cyclin D and CDK inhibitors come of age. Cell:79(4):573-82

Inaba M, Yamashita YM (2012) Asymmetric stem cell division: precision for robustness. Cell Stem Cell 11:461–469

Inaba M, Yuan H, Salzmann V, Fuller MT, Yamashita YM (2010) E-cadherin is required for centrosome and spindle orientationin Drosophila male germline stem cells. PLoS One 5:e12473

Irvine DV, Zaratiegui M, Tolia NH, Goto DB, Chitwood DH, Vaughn MW, Joshua-Tor L, Martienssen RA (2006) Argonaute slicing is required for heterochromatic silencing and spreading. Science 313:1134–1137

Jackson V, Chalkley R (1981a) A new method for the isolation of replicative chromatin: selective deposition of histone on both new and old DNA. Cell 23:121–134

Jackson V, Chalkley R (1981b) A reevaluation of new histone deposition on replicating chromatin. J Biol Chem 256:5095–5103

Jackson V, Shires A, Tanphaichitr N, Chalkley R (1976) Modifications to histones immediately after synthesis. J Mol Biol 104:471–483

Jackson V (1987) Deposition of newly synthesized histones: New histones H2A and H2B do not deposit in the same nucleosome with new histones H3 and H4. Biochemistry 26, 2315–2325

Jackson V (1990) In vivo studies on the dynamics of histone-DNA interaction: Evidence for nucleosome dissolution during replication and transcription and a low level of dissolution independent of both. Biochemistry 29, 719–731

Jacobs JJ, van Lohuizen M (2002) Polycomb repression: from cellular memory to cellular proliferation and cancer. Biochim Biophys Acta 1602:151–161

Jaenisch R, Young R (2008) Stem cells, the molecular circuitry of pluripotency and nuclear reprogramming. Cell 132:567–582

Jenuwein T, Allis CD (2001) Translating the histone code. Science 293:1074–1080

Kamakaka RT, Biggins S (2005) Histone variants: deviants? Genes Dev 19:295–310

Kapoor TM, Lampson MA, Hergert P, Cameron L, Cimini D, Salmon ED, McEwen BF, Khodjakov A (2006) Chromosomes can congress to the metaphase plate before biorientation. Science 311:388–391

Karpowicz P, Morshead C, Kam A, Jervis E, Ramunas J, Cheng V, van der Kooy D (2005) Support for the immortal strand hypothesis: neural stem cells partition DNA asymmetrically in vitro. J Cell Biol 170:721–732

Karpowicz P, Pellikka M, Chea E, Godt D, Tepass U, van der Kooy D (2009) The germline stem cells of Drosophila melanogaster partition DNA non-randomly. Eur J Cell Biol 88:397–408

Kiel MJ, He S, Ashkenazi R, Gentry SN, Teta M, Kushner JA, Jackson TL, Morrison SJ (2007) Haematopoietic stem cells do not asymmetrically segregate chromosomes or retain BrdU. Nature 449:238–242

Kiger AA, Jones DL, Schulz C, Rogers MB, Fuller MT (2001) Stem cell self-renewal specified by JAK-STAT activation in response to a support cell cue. Science 294:2542–2545

Klar AJ (1994) A model for specification of the left-right axis in vertebrates. Trends Genet 10:392–396

Klar AJ (2007) Lessons learned from studies of fission yeast mating-type switching and silencing. Annu Rev Genet 41:213–236

Knoblich JA (2008) Mechanisms of asymmetric stem cell division. Cell 132:583–597

Konev AY, Tribus M, Park SY, Podhraski V, Lim CY, Emelyanov AV, Vershilova E, Pirrotta V, Kadonaga JT, Lusser A, Fyodorov DV (2007) CHD1 motor protein is required for deposition of histone variant H3.3 into chromatin in vivo. Science 317:1087–1090

Kouzarides T (2007) Chromatin modifications and their function. Cell 128(4):693-705

Kouskouti A, Talianidis I (2005) Histone modifications defining active genes persist after transcriptional and mitotic inactivation. EMBO J 24:347–357

Lansdorp PM (2007) Immortal strands? Give me a break. Cell 129:1244–1247

Leatherman JL, Dinardo S (2008) Zfh-1 controls somatic stem cell self-renewal in the Drosophila testis and nonautonomously influences germline stem cell self-renewal. Cell Stem Cell 3:44–54

Leatherman JL, Dinardo S (2010) Germline self-renewal requires cyst stem cells and stat regulates niche adhesion in Drosophila testes. Nat Cell Biol 12:806–811

Lengsfeld BM, Berry KN, Ghosh S, Takahashi M, FrancisNJ (2012) A polycomb complex remains bound through DNA replication in the absence of other eukaryotic proteins. Sci Rep 2:661

Leonhardt H, Page AW, Weier HU, Bestor TH (1992) A targeting sequence directs DNA methyltransferase to sites of DNA replication in mammalian nuclei. Cell 71(5): p. 865-73

Leonhardt H, Rahn HP, Weinzierl P, Sporbert A, Cremer T, Zink D, Cardoso MC (2000) Dynamics of DNA replication factories in living cells. J Cell Biol 149(2): p. 271-80

Lew DJ, Burke DJ, Dutta A (2008) The immortal strand hypothesis: how could it work? Cell 133:21–23

Li Q, Zhou H, Wurtele H, Davies B, Horazdovsky B, Verreault A, Zhang Z (2008) Acetylation of histone H3 lysine 56 regulates replication-coupled nucleosome assembly. Cell 134:244–255

Lim C, Tarayrah L, Chen X (2012) Transcriptional regulation during Drosophila spermatogenesis. Spermatogenesis 2:158–166

Lin TY, Viswanathan S, Wood C, Wilson PG, Wolf N, and Fuller MT (1996) Coordinate developmental control of the meiotic cell cycle and spermatid differentiation in Drosophila males. Development 122(4): 1331-1341

Lo SM, Follmer NE, Lengsfeld BM, Madamba EV, Seong S, Grau DJ, Francis NJ (2012) A bridging model for persistence of a polycomb group protein complex through DNA replication in vitro. Mol Cell 46:784–796

Losick VP, Morris LX, Fox DT, Spradling A (2011) Drosophila stem cell niches: a decade of discovery suggests a unified view of stem cell regulation. Dev Cell 21:159–171

Lyko F, Ramsahoye BH, Jaenisch R (2000a) DNA methylation in Drosophila melanogaster. Nature 408:538–540

Lyko F, Whittaker AJ, Orr-Weaver TL, Jaenisch R (2000b) The putative Drosophila methyltransferase gene dDnmt2 is contained in a transposon-like element and is expressed specifically in ovaries. Mech Dev 95:215–217

Malik HS, Henikoff S (2009) Major evolutionary transitions in centromere complexity. Cell 138:1067–1082

Mardis ER (2007) ChIP-seq: welcome to the new frontier. Nature 4(8) 613-4

Martin C, Zhang Y (2007) Mechanisms of epigenetic inheritance. Curr Opin Cell Biol 19:266–272

Masumoto H, Hawke D, Kobayashi R, Verreault A (2005) A role for cell-cycle-regulated histone H3 lysine 56 acetylation in the DNA damage response. Nature 436:294–298

McNairn AJ, Gilbert DM (2003) Epigenomic replication: linking epigenetics to DNA replication. BioEssays 25:647–656

Mellone BG, Grive KJ, Shteyn V, Bowers SR, Oderberg I, Karpen GH (2011) Assembly of Drosophila centromeric chromatin proteins during mitosis. PLoS Genet 7: e1002068

Merok JR, Lansita JA, Tunstead JR, Sherley JL (2002) Cosegregation of chromosomes containing immortal DNA strands in cells that cycle with asymmetric stem cell kinetics. Cancer Res 62:6791–6795

Milne TA, Briggs SD, Brock HW, Martin ME, Gibbs D, Allis CD, and Hess JL (2002) MLL targets SET domain methyltransferase activity to Hox gene promoters. Mol Cell 10(5): 1107-1117

Min J, Zhang Y, Xu RM (2003) Structural basis for specific binding of polycomb chromodomain to histone H3 methylated at Lys 27. Genes Dev 17:1823–1828

Mito Y, Henikoff JG, Henikoff S (2007) Histone replacement marks the boundaries of cis-regulatory domains. Science 315:1408–1411

Moggs JG, Grandi P, Quivy JP, Jonsson ZO, Hubscher U, Becker PB, Almouzni G (2000) A CAF-1-PCNA-mediated chromatin assembly pathway triggered by sensing DNA damage. Mol Cell Biol 20:1206–1218

Morrison SJ, Kimble J (2006) Asymmetric and symmetric stemcell divisions in development and cancer. Nature 441:1068–1074

Morrison SJ, Spradling AC (2008) Stem cells and niches: mechanisms that promote stem cell maintenance throughout life. Cell 132:598–611

Mostoslavsky R, Alt FW, Rajewsky K (2004) The lingering enigma of the allelic exclusion mechanism. Cell 118:539–544

Motamedi MR, Verdel A, Colmenares SU, Gerber SA, Gygi SP, Moazed D (2004) Two RNAi complexes, RITS and RDRC, physically interact and localize to noncoding centromeric RNAs. Cell 119:789–802

Murti, K.G., et al., Dynamics of human replication protein A subunit distribution and partitioning in the cell cycle. Exp Cell Res, 1996. 223(2): p. 279-89.

Muse GW, Gilchrist DA, Nechaev S, Shah R, Parker JS, Grissom SF, Zeitlinger J, Adelman K (2007) RNA polymerase is poised for activation across the genome. Nat Genet 39:1507-1511

Nakano S, Stillman B, Horvitz HR (2011) Replication-coupled chromatin assembly generates a neuronal bilateral asymmetry in C. elegans. Cell 147:1525–1536

Pastrana, E. (2013) Bessel beam beyond the limit. Nature Methods 10, 102–103

Petruk S, Sedkov Y, Johnston DM, Hodgson JW, Black KL, Kovermann SK, Beck S, Canaani E, Brock HW, Mazo A (2012) TrxG and PcG proteins but not methylated histones remain associated with DNA through replication. Cell 150:922–933

Pine SR, Ryan BM, Varticovski L, Robles AI, Harris CC (2010) Microenvironmental modulation of asymmetric cell division in human lung cancer cells. Proc Natl Acad Sci USA 107:2195–2200

Planchon TA, Gao L, Milkie DE, Davidson MW, Galbraith JA, Galbraith CG, Betzig E. (2011) Rapid three-dimensional isotropic imaging of living cells using Bessel beam plane illumination. (Nature Methods 8(5):417-23

Potten CS, Owen G, Booth D (2002) Intestinal stem cells protect their genome by selective segregation of template DNA strands. J Cell Sci 115:2381–2388

Quyn AJ, Appleton PL, Carey FA, Steele RJ, Barker N, Clevers H, Ridgway RA, Sansom OJ, Nathke IS (2010) Spindle orientation bias in gut epithelial stem cell compartments is lost in precancerous tissue. Cell Stem Cell 6:175–181

Pugh BF and Tjian R (1990) Mechanism of transcriptional activation by Sp1: Evidence for coactivators. Cell 61: 1187–1197

Rando TA (2006) Stem cells, ageing and the quest for immortality. Nature 441:1080–1086

Rando TA (2007) The immortal strand hypothesis: segregation and reconstruction. Cell 129:1239–1243

Ray-Gallet D, Quivy JP, Scamps C, Martini EM, Lipinski M, Almouzni G (2002) HIRA is critical for a nucleosome assembly pathway independent of DNA synthesis. Mol Cell 9:1091–1100

Rebollo E, Sampaio P, Januschke J, Llamazares S, Varmark H, Gonzalez C (2007) Functionally unequal centrosomes drive spindle orientation in asymmetrically dividing Drosophila neural stem cells. Dev Cell 12:467–474

Recht J, Tsubota T, Tanny JC, Diaz RL, Berger JM, Zhang X, Garcia BA, Shabanowitz J, Burlingame AL, Hunt DF, Kaufman PD, Allis CD (2006) Histone chaperone Asf1 is required for histone H3 lysine 56 acetylation, a modification associated with S phase in mitosis and meiosis. Proc Natl Acad Sci U S A 103:6988–6993

Richards EJ, Elgin SC (2002) Epigenetic codes for heterochromatin formation and silencing: rounding up the usual suspects. Cell 108:489–500 Ringrose L, Paro R (2004) Epigenetic regulation of cellular memory by the polycomb and trithorax group proteins. Annu Rev Genet 38:413–443

Ringrose L, Paro R (2004) Epigenetic regulation of cellular memory by the Polycomb and Trithorax group proteins. Annu Rev Genet. 38:413-43.

Rinn JL, Chang HY (2012) Genome regulation by long noncoding RNAs. Annu Rev Biochem 81:145–166

Rocheteau P, Gayraud-Morel B, Siegl-Cachedenier I, Blasco MA, Tajbakhsh S (2012) A subpopulation of adult skeletal muscle stem cells retains all template DNA strands after cell division. Cell 148:112–125

Rossi DJ, Jamieson CH, Weissman IL (2008) Stems cells and the pathways to aging and cancer. Cell 132:681–696

Roth TM, Chiang CY, Inaba M, Yuan H, Salzmann V, Roth CE, Yamashita YM (2012)

Centrosome misorientation mediates slowing of the cell cycle under limited nutrient conditions in Drosophila male germline stem cells. Mol Biol Cell 23:1524–1532

Ruiz-Carrillo A, Wangh LJ, Allfrey VG (1975) Processing of newly synthesized histone molecules. Science 190:117–128

Russev G, Hancock R (1981) Formation of hybrid nucleosomes containing new and old histones. Nucleic Acids Res 9:4129–4137

Saha A,Wittmeyer J, Cairns BR (2006) Chromatin remodelling: the industrial revolution of DNA around histones. Nat Rev Mol Cell Biol 7:437–447

Schones DE, Cui K, Cuddapah S, Roh TY, Barski A, Wang Z, Wei G, Zhao K (2008) Dynamic regulation of nucleosome positioning in the human genome. Cell 132:887-898

Schreiber SL, Bernstein BE (2002) Signaling network model of chromatin. Cell 111:771–778

Schuh M, Lehner CF, Heidmann S (2007) Incorporation of Drosophila CID/CENP-A and CENP-C into centromeres during early embryonic anaphase. Curr Biol 17:237–243

Schwartz BE, Ahmad K (2005) Transcriptional activation triggers deposition and removal of the histone variant H3.3. Genes Dev 19:804–814

Schwartz YB, Kahn TG, Stenberg P, Ohno K, Bourgon R, Pirrotta V (2010) Alternative epigenetic chromatin states of polycomb target genes. PLoS Genet, 6:e1000805

Seale RL (1975) Assembly of DNA and protein during replication in HeLa cells. Nature 255:247–249

Sheng XR, Matunis E (2011) Live imaging of the Drosophila spermatogonial stem cell niche reveals novel mechanisms regulating germline stem cell output. Development 138:3367–3376

Shibahara K, Stillman B (1999) Replication-dependent marking of DNA by PCNA facilitates CAF-1-coupled inheritance of chromatin. Cell 96:575–585

Shinin V, Gayraud-Morel B, Gomes D, Tajbakhsh S (2006) Asymmetric division and cosegregation of template DNA strands in adult muscle satellite cells. Nat Cell Biol 8:677– 687

Skora AD, Spradling AC (2010) Epigenetic stability increases extensively during Drosophila follicle stem cell differentiation. Proc Natl Acad Sci U S A 107:7389–7394

Smith DJ, Whitehouse I (2012) Intrinsic coupling of laggingstrand synthesis to chromatin assembly. Nature 483:434–438

Smith GH (2005) Label-retaining epithelial cells in mouse mammary gland divide asymmetrically and retain their template DNA strands. Development 132:681–687

Sotiropoulou PA, Candi A, Blanpain C (2008) The majority of multipotent epidermal stem cells do not protect their genome by asymmetrical chromosome segregation. Stem Cells 26:2964–2973

Stock JK, Giadrossi S, Casanova M, Brookes E, Vidal M, Koseki H, Brockdorff N, Fisher AG, and Pombo A (2007) Ring1-mediated ubiquitination of H2A restrains poised RNA polymerase II at bivalent genes in mouse ES cells. Nat Cell Biol 9(12): 1428-1435

Sullivan BA, Karpen GH (2004) Centromeric chromatin exhibits a histonemodification pattern that is distinct from both euchromatin and heterochromatin. Nat Struct Mol Biol 11:1076–1083

Szenker E, Ray-Gallet D, Almouzni G (2011) The double face of the histone variant H3.3. Cell Res 21:421–434

Tagami H, Ray-Gallet D, Almouzni G, Nakatani Y (2004) Histone H3.1 and H3.3 complexes mediate nucleosome assembly pathways dependent or independent of DNA synthesis. Cell 116(1):51-61

Tajbakhsh S, Gonzalez C (2009) Biased segregation of DNA and centrosomes: moving together or drifting apart? Nat Rev Mol Cell Biol 10:804–810

Thorpe PH, Bruno J, Rothstein R (2009) Kinetochore asymmetry defines a single yeast lineage. Proc Natl Acad Sci U S A 106:6673–6678

Toledano H, D'Alterio C, Czech B, Levine E, Jones DL (2012) The let-7-Imp axis regulates ageing of the Drosophila testis stem-cell niche. Nature 485:605–610

Tran V, Lim C, Xie J, Chen X (2012) Asymmetric division of Drosophila male germline stem cell shows asymmetric histone distribution. Science 338:679–682 *(Excerpts from the text in this publication are used for this thesis.)*

Tran, V., L. Feng, and X. Chen, Asymmetric distribution of histones during Drosophila male germline stem cell asymmetric divisions. Chromosome Res, 2013. **21**(3): p. 255-69. *(Excerpts from the text in this publication are used for this thesis.)*

Tulina N, Matunis E (2001) Control of stem cell self-renewal in Drosophila spermatogenesis by JAK-STAT signaling. Science 294:2546–2549

Turner BM (2002) Cellular memory and the histone code. Cell 111:285–291

Vagnarelli P, Ribeiro SA, Earnshaw WC (2008) Centromeres: old tales and new tools. FEBS Lett 582:1950–1959

Valls E, Sanchez-Molina S, Martinez-Balbas MA (2005) Role of histone modifications in marking and activating genes through mitosis. J Biol Chem 280:42592–42600

Verdaasdonk JS, Bloom K (2011) Centromeres: unique chromatin structures that drive chromosome segregation. Nat Rev Mol Cell Biol 12:320–332

Verreault A, Kaufman PD, Kobayashi R, Stillman B (1996) Nucleosome assembly by a complex of CAF-1 and acetylated histones H3/H4. Cell 87:95–104

Verzijlbergen KF, Menendez-Benito V, van Welsem T, van Deventer SJ, Lindstrom DL, Ovaa H, Neefjes J, Gottschling DE, van Leeuwen F (2010) Recombinationinduced tag exchange to track old and new proteins. Proc Natl Acad Sci U S A 107:64–68

Waghmare SK, Bansal R, Lee J, Zhang YV, McDermitt DJ, Tumbar T (2008) Quantitative proliferation dynamics and random chromosome segregation of hair follicle stem cells. EMBO J 27:1309–1320

Wang X, Tsai JW, Imai JH, Lian WN, Vallee RB, Shi SH (2009) Asymmetric centrosome inheritance maintains neural progenitors in the neocortex. Nature 461:947–955

Wang H, Wang L, Erdjument-Bromage, H, Vidal M, Tempst P , Jones RS, and Zhang Y (2004) Role of histone H2A ubiquitination in Polycomb silencing. Nature 431(7010): 873-878

Wang Z, Gerstein M, Snyder M (2009) RNA-Seq: a revolutionary tool for transcriptomics. Nat Rev Genet 10:57-63.

White MA, Eykelenboom JK, Lopez-Vernaza MA, Wilson E, Leach DR (2008) Non-random segregation of sister chromosomes in Escherichia coli. Nature 455:1248–1250

White-Cooper H, Leroy D, MacQueen A, and Fuller MT (2000) Transcription of meiotic cell cycle and terminal differentiation genes depends on a conserved chromatin associated protein, whose nuclear localisation is regulated. Development 127(24): 5463-5473

White-Cooper H, Schafer MA, Alphey LS, and Fuller MT (1998) Transcriptional and posttranscriptional control mechanisms coordinate the onset of spermatid differentiation with meiosis I in Drosophila. Development 125(1): 125-134

Xia L, Jia S, Huang S, Wang H, Zhu Y, Mu Y, Kan L, Zheng W, Wu D, Li X, Sun Q, Meng A, Chen D (2010) The Fused/Smurf complex controls the fate of Drosophila germline stem cells by generating a gradient BMP response. Cell 143(6):978-90

Xu M, Long C, Chen X, Huang C, Chen S, Zhu B (2010) Partitioning of histone H3-H4 tetramers during DNA replication-dependent chromatin assembly. Science 328:94–98

Yadlapalli S, Cheng J, Yamashita YM (2011a) Drosophila male germline stem cells do not asymmetrically segregate chromosome strands. J Cell Sci 124:933–939

Yadlapalli S, Cheng J, Yamashita YM (2011b) Overlooked areas need attention for sound evaluation of DNA strand inheritance patterns in Drosophila male germline stem cells. J Cell Sci 124:4138–4139

Yadlapalli S, Yamashita YM (2013) Chromosome-specific nonrandom sister chromatid segregation during stem cell division. Nature. doi:10.1038/nature12106

Yamashita YM (2013) Non-random sister chromatid segregation of sex chromosomes in Drosophila male germline stem cells. Chromosome Research,
Yamashita YM, Fuller MT (2005) Asymmetric stem cell division and function of the niche in the Drosophila male germ line. Int J Hematol 82:377–380

Yamashita YM, Fuller MT, Jones DL (2005) Signaling in stem cell niches: lessons from the Drosophila germline. J Cell Sci 118:665–672

Yamashita YM, Jones DL, Fuller MT (2003) Orientation of asymmetric stem cell division by the APC tumor suppressor and centrosome. Science 301:1547–1550

Yamashita YM, Mahowald AP, Perlin JR, Fuller MT (2007) Asymmetric inheritance of mother versus daughter centrosome in stem cell division. Science 315:518–521

Yuan H, Chiang CY, Cheng J, Salzmann V, Yamashita YM (2012a) Regulation of cyclin A localization downstream of Par-1 function is critical for the centrosome orientation checkpoint in Drosophila male germline stem cells. Dev Biol 361:57–67

Yuan W, Wu T, Fu H, Dai C, Wu H, Liu N, Li X, Xu M, Zhang Z, Niu T, Han Z, Chai J, Zhou XJ, Gao S, Zhu B (2012b) Dense chromatin activates polycomb repressive complex 2 to regulate H3 lysine 27 methylation. Science 337:971–975

Zeitlinger J, Stark A, Kellis M, Hong JW, Nechaev S, Adelman K, Levine M, and Young, RA (2007) RNA polymerase stalling at developmental control genes in the Drosophila melanogaster embryo. Nat Genet 39(12): 1512-1516

Zhao J, Sun BK, Erwin JA, Song JJ, Lee JT (2008) Polycomb proteins targeted by a short repeat RNA to the mouse X chromosome. Science 322:750–756

Zhou Q, Lieberman PM, Boyer TG, and Berk AJ (1992) Holo-TFIID supports transcriptional stimulation by diverse activators and from a TATA-less promoter. Genes & Dev. 6: 1964–1974

Zhu B, Reinberg D (2011) Epigenetic inheritance: uncontested? Cell Res 21:435–441

Vuong Tran

3601 Greenway, #503
Baltimore, MD 21218
(360) 888-9377
vuongkhaitran@gmail.com

Johns Hopkins University
Department of Biology
3400 N. Charles St.
Baltimore, MD 21218

Research Experience

2003 – 2006	Laboratory Assistant, Fred Hutchinson Cancer Research Center, Dr. Bruce Edgar
2006 – 2008	Research Technician, Fred Hutchinson Cancer Research Center, Dr. Bruce Edgar
2008 – present	Pre-doctoral Fellow, Johns Hopkins University, Dr. Xin Chen

Teaching Experience

2009	Laboratory Teaching Assistant for Genetics, Johns Hopkins University
20010 – 2011	Laboratory Teaching Assistant for Developmental Biology, Johns Hopkins University
2012 – present	Mentoring multiple rotation students in the Chen Lab, Johns Hopkins University

Professional Membership

2009 – present	Genetic Society of America

Honors

2012	Selected Talk for the Cell, Molecular, Developmental Biology Departmental Retreat

Publications

1. Shibutani, S. T., de la Cruz, A. F. A., Turbyfill III, W. J., **Tran, V.**, Reis, T., Edgar, B. A., Duronio, R. J. (2008) Intrinsic negative cell cycle regulation provided by PIP box- and Cul4Cdt2-mediated destruction of E2f1 during S phase. Dev. Cell 15, 890-900. PMCID: PMC2644461

2. Zielke, N.*, Kim, K. J.*, **Tran, V.***, Shibutani, S. T., Bravo, M-J., Nagarajan, van Straaten, M. S., Woods, B., von Dassow, G., Rottig, C., Lehner, C. F., Grewal, S., Duronio, R. J., and Edgar, B. A. (2011) Control of *Drosophila* endocycles by E2F

and CRL4^{Cdt2}. Nature 480(7375):123-7 PMCID: PMC3330263 (* indicating authors of equal contribution.)

3. **Tran, V.**, Gan, Q., Chen, X. (2012) Chromatin Immunoprecipitation (ChIP) using *Drosophila* tissue. J. Vis. Exp. (61), e3745, doi:10.3791/3745.

4. **Tran, V.*,** Lim, C.*, Xie, J. and Chen, X. (2012) Asymmetric division of *Drosophila* male germline stem cell shows asymmetric histone distribution. Science, 338(6107): 679-682, PMCID: PMC3532436 (* indicating authors of equal contribution). Featured in Faculty of 1000 Biology.

5. **Tran,V.*,** Feng, L.J.* and Chen, X. (2013) Asymmetric distribution of histones during Drosophila male germline stem cell asymmetric divisions. Invited review to Chromosome Research, 21:255-269. PMCID: PMC23681658 (* indicates authors of equal contribution)